UNIVERSITÀ
DI PAVIA

PhD in Biomedical Sciences- XXXII cycle

Dipartimento di Biologia e Biotecnologie "L. Spallanzani"

STUDY OF HUMAN AND ANIMAL ERYTHROCYTES: MARKERS OF AGING AND CLINICAL DISORDERS

PhD Student: Anjali Gaur

Tutor: Prof. Vittorio Bellotti

Anno Accademico 2016-2019

This project has received funding from the European Union's Horizon 2020 research and innovation programme under grant agreement No *675115 — RELEVANCE — H2020-MSCA-ITN-2015/H2020-MSCA-ITN-2015*.

Anjali Gaur ESR 15

RELEVANCE (Regulation of red cell life-span, erythropoiesis, survival, senescence and clearance) is an Innovative Training Network of the Marie Skłodowska-Curie actions and part of the European Union's Horizon 2020. It is a consortium of thirteen European partners academic research centers, diagnostic labs, blood supply centers, and small companies. Fifteen early stage researchers (ESRs) were trained in interactive and multidisciplinary work during this three-year project. The aim of the RELEVANCE project was to improve prognostic, diagnostic and therapeutic approaches of disorders of red blood cells and to gain deeper knowledge of the production, function, and clearance of RBCs. Topics and partners are combined into five work packages [1].

Experimental work was carried out in three different laboratories (partner institutes):

1. University of Pavia, Italy
2. University Zürich, Switzerland
3. Sanquin Blood Supply, Netherlands

Acknowledgements

I would like to thank all the following people for their tremendous help and support during my PhD. I am especially grateful to both the host institutes of RELEVANCE consortium for their warm hospitality and help during my secondments.

University of Pavia, Italy

Prof. Vittorio Belloti

Dr. Osera Cecilia

Prof. Enrica Tira

Prof. Giampaolo Minetti

Prof. Alessandra Albertini

Prof. Marco Biggiogera

Dr. Sofia Giorgetti

Borana Qalliu MSc

Institute of Veterinary Physiology, University of Zurich, Switzerland

Dr. Anna Bogdanova

Dr. Nikolai Bogganov

Dr. Elena Seiler

Dr. Asya Makhro

Ankie van Cromvoirt MSc

Nynke Moelijker MSc

Sanquin, Amsterdam, Netherlands

Dr. Robin Van Bruggen

Dr. Marieke Von Lindern

Boukje Beuger MSc

Thomas Klei MSc

Paul Verkuijlen BSc

Martijn Veldthuis BSc

Laboratories of Biochemistry and Molecular Biology, University of Parma

Prof. Andrea Mozzarelli

Dr. Serena Faggiano

Servizio Immunoematologia

e Medicina Trasfusionale (S.I.M.T.)

Table of Contents

List of Figures & Tables

Figures

Tables

Chapter 1. Introduction

Blood

Blood is a kind of connective tissue, and its primary purpose is to transport and distribute oxygen, nutrients, waste products and hormones around the body. Together, the heart, blood and blood vessels make up the circulatory system. Blood also regulates body temperature, pH levels and volume of fluids in the body. It prevents infection as well as the loss of blood.

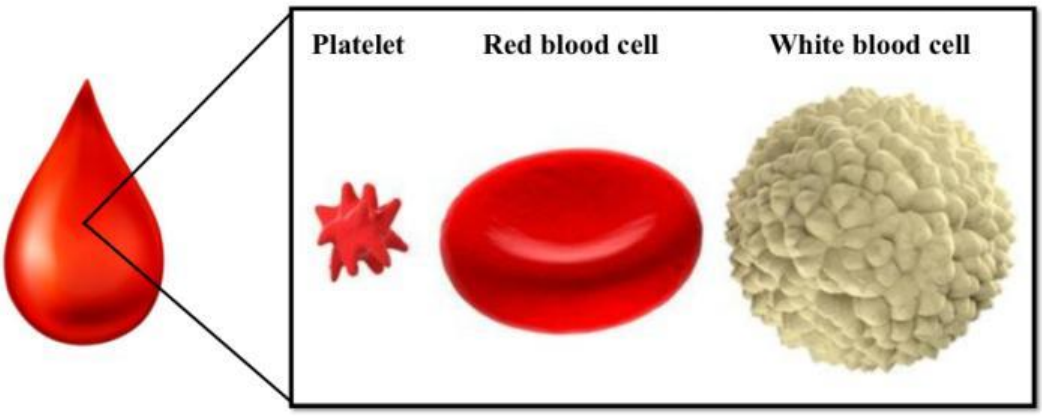

Figure 1. *Blood components. Red blood cells transport oxygen, and white blood cells protect the body against invading microbes and platelets form a plug at the site of a cut to stop bleeding.*

Red Blood Cells

The red blood cell (RBC), also known as ‘erythrocyte’ (from Greek erythros for "red" and kytos for "hollow vessel", with -cyte translated as "cell" in modern usage) is a distinctive cell as it has evolved as a specialized oxygen carrier [4]. The structure and shape of an erythrocyte are tightly related to its function. Erythrocytes have an exceptionally flexible membrane, which allows these cells to pass through capillaries that are narrower than the cells themselves. RBCs live for an average of approximately 120 days in humans [5]. At the end of the lifespan, old RBCs get cleared in the spleen. RBCs are lacking organelles as well as a nucleus, and they are therefore incapable of undergoing apoptosis. The metabolism of an RBC comprises only anaerobic glycolysis and pentose phosphate pathway (PPP) [6].

The basics of erythrocytes can be divided into the following major topics:

1. Production
2. Function and metabolism
3. Immune adherence clearance
4. Aging and removal

Erythrocyte production

Erythrocyte production (erythropoiesis) takes place in the bone marrow and comprises of numerous developmental phases: hematopoietic stem cell, burst-forming unit-erythroid (BFU-E), colony-forming unit-erythroid (CFU-E), proerythroblast, basophilic erythroblast, polychromatic erythroblast, orthochromatic erythroblast, reticulocyte and eventually mature erythrocyte. Only reticulocytes and erythrocytes are found in circulation [7].

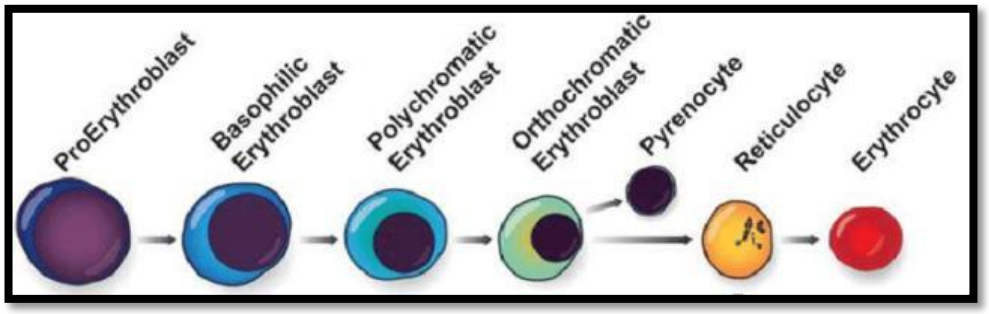

Figure 2. *Stages of erythropoiesis [8]. The production of erythrocytes consists of distinctive phases.*

Erythropoiesis is regulated by a negative feedback loop where levels of oxygen control levels of erythropoietin (EPO) in plasma. EPO is synthesized in the liver in the womb, while in adults, main the site of EPO production is in the kidney by peritubular cells. EPO production is stimulated by hypoxia [9]. There are, however, reports that suggest EPO synthesis in non-renal tissues such as liver in anephric individual [10]. With several growth factors participating in erythropoiesis regulation, EPO has been recognized as the master regulator [11]. Terminal erythropoiesis takes place in erythroblastic island, first described as a specialized microenvironment by Bessis in 1958 [12]. Macrophages play two significant roles in erythroid development: as a provider of iron necessary for heme synthesis, and by phagocytosing the expelled nuclei in the final erythroid differentiation. The latter is facilitated by an interaction via a phosphatidylserine (PS) receptor on the macrophage and PS-exposing nuclei [13].

Erythrocyte function and metabolism

Transporting oxygen (O_2) around the body is the main function of erythrocytes. Upon inhalation, oxygen reaches the lungs and is transferred to blood via passive diffusion across the alveoli according to concentration gradients. Erythrocytes are packed with haemoglobin (Hb) which binds oxygen in the lungs forming Oxy-Hb. Oxygen is delivered to tissues by circulating erythrocytes, leaving Hb in a deoxygenated form [14]. Cellular respiration produces carbon dioxide (CO_2), which is converted to bicarbonate (HCO_3^-) by enzyme carbonic anhydrase found in erythrocytes. 20% of CO_2 binds to Hb in erythrocytes and get delivered to the lungs, where it diffuses through the alveoli and exhaled.

Pentose Phosphate Pathway (PPP) as well as Glycolysis takes place in erythrocytes. Glycolytic pathway of erythrocytes is essential for energy metabolism as they lack mitochondria and a nucleus [15]. Since erythrocytes contain no mitochondria, there is no respiratory chain, no citric acid cycle and no oxidation of fatty acids or ketone bodies. Glucose, therefore, is the main source erythrocytes heavily dependent upon for energy. Glucose is broken down into lactate by anaerobic glycolysis, which is the only pathway that supplies the red blood cells with ATP.

Immune adherence clearance of erythrocytes

Erythrocytes play an important role as modulators of the immune system. The process is called immune adherence clearance (IAC). Erythrocytes express the immune receptor complement factor 1 (CR1), also known as CD35. Erythrocytes bind complement-opsonized pathogens via CR1 in circulation and deliver them to the spleen where they are phagocytosed by spleen macrophages leaving the erythrocyte intact [16].

Erythrocyte aging and removal

Erythrocyte aging process is of special scientific and clinical significance. A series of time-dependent, unidirectional but not-necessarily linear molecular events are involved in erythrocyte aging leading to clearance [17]. A range of physical and metabolic damages occur in erythrocytes as they age. These damages include membrane vesiculation modification of haemoglobin as well as failure of antioxidant defenses and cellular homeostasis [18]. Several age markers have been identified in the past such as increase in erythrocyte density, nonenzymatic glycation of haemoglobin and deamidation of protein 4.1b to 4.1a [19-22]. Since mature erythrocytes are incapable of synthesizing new proteins, the markers of aging are derived from modifications of pre-existing molecules. The phenotypes of erythrocyte aging are classified as changes in cell shape, drop in metabolic activity, oxidative injury, membrane remodeling, removal markers exposure on the cell surface as well as micro-vesiculation. The spleen is a lymphoid organ which serves many functions such as filtration of blood, iron recycling and pathogen clearance. The spleen consists of white pulp, red pulp and marginal zone. Macrophages and erythroid cells are in constant interplay and their interactions are essential not only during erythropoiesis but also during aging and clearance [23]. Macrophages present in the red pulp of the spleen are responsible for clearing old and damaged erythrocytes. Removal signals on erythrocytes include Band 3 clustering and phosphatidylserine (PS) exposure. Erythrocyte destruction is controlled by antagonist effects of PS & CD47 on phagocytic activity of macrophages [24].

Chapter 1.1. Protein 4.1

The erythrocyte membrane skeleton (MS) has been characterized in the past, and its general role is to maintain the shape and mechanical properties of RBCs. Protein 4.1 is located in the membrane skeleton and interacts mainly with spectrin, actin, and protein p55 [25].

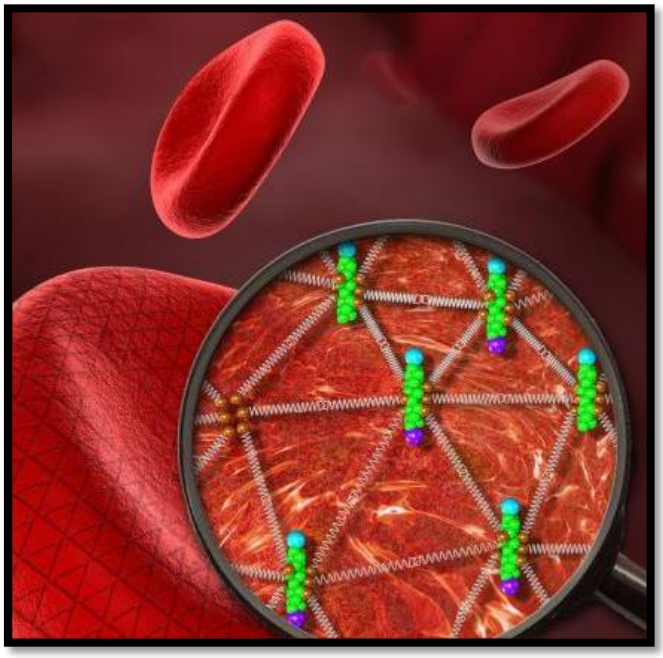

Figure 3. *Two-dimensional triangular protein meshwork underlying erythrocyte membrane skeleton [26].*

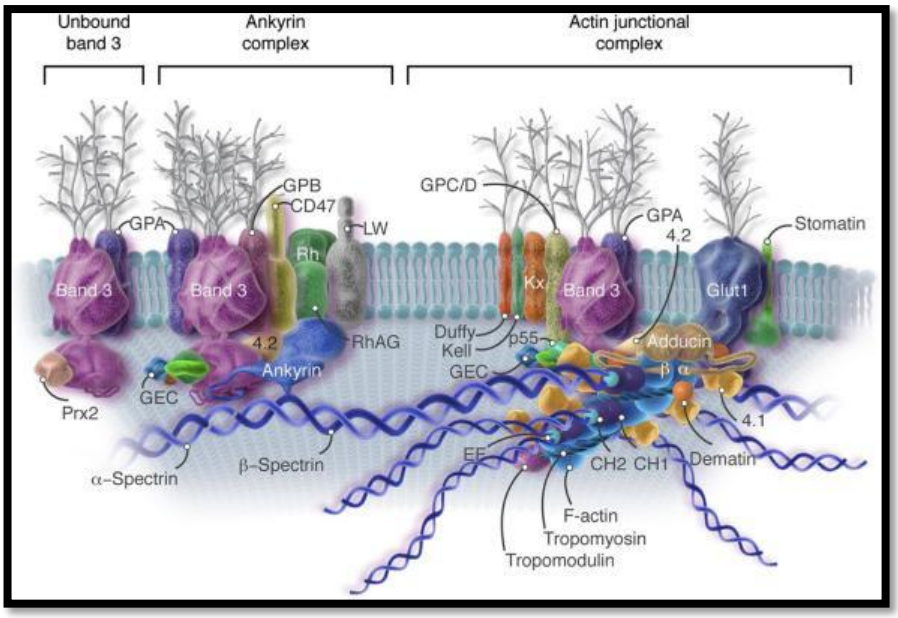

Figure 4. *Erythrocyte membrane skeleton anatomy [27].*

The major function of protein 4.1 is stabilizing cell shape and providing deformability and mechanical stability to the cell [28]. Protein 4.1 exists as two polypeptides: bands 4.1a and 4.1b are proteins of

80,000 and 78,000 molecular weight respectively. There is a close relation between the primary structure and the function of the two polypeptides [29]. There are around 100,000 copies of each form present per erythrocyte ghost (erythrocyte membrane) [30]. Several approaches have been tried and tested to study protein 4.1 molecular structure. Both the isomers were cleaved selectively by using chemicals and proteolysis, which showed identical susceptible sites present on both a and b components of the protein [29]. Through the interactions with other proteins in the membrane skeleton, protein 4.1 is known to play an essential role in the mechanical stability as well as deformability of RBCs. The important role of protein 4.1 was confirmed by a study that showed protein 4.1 deficiency resulted in membrane instability [31]. The stability was able to be restored to normal by reincorporating purified forms of protein 4.1 into the deficient cell membranes [32]. This study therefore had a direct evidence of the important role of protein 4.1 in maintaining the membrane stability. Past observations suggest that protein 4.1a ratio to protein 4.1b increases with erythrocyte aging [2]. One of the studies supporting the proposal of protein 4.1 as an internal marker was done with seven transient erythroblastopenia patients. 4.1 protein present in erythrocytes was mainly in the 'a' form upon diagnosis. Whereas, after recovery 4.1b was more predominant form present, resulting in a normal 4.1a/4.1b ratio. Constructed on these evidences, studies have been designed to find out more about the conversion of protein 4.1b to 4.1a.

In most mammalian RBCs including human, protein 4.1 consists of a doublet of polypeptides, suggesting that post-translational modification of protein 4.1b to 4.1a is a common phenomenon in mammalian RBCs.

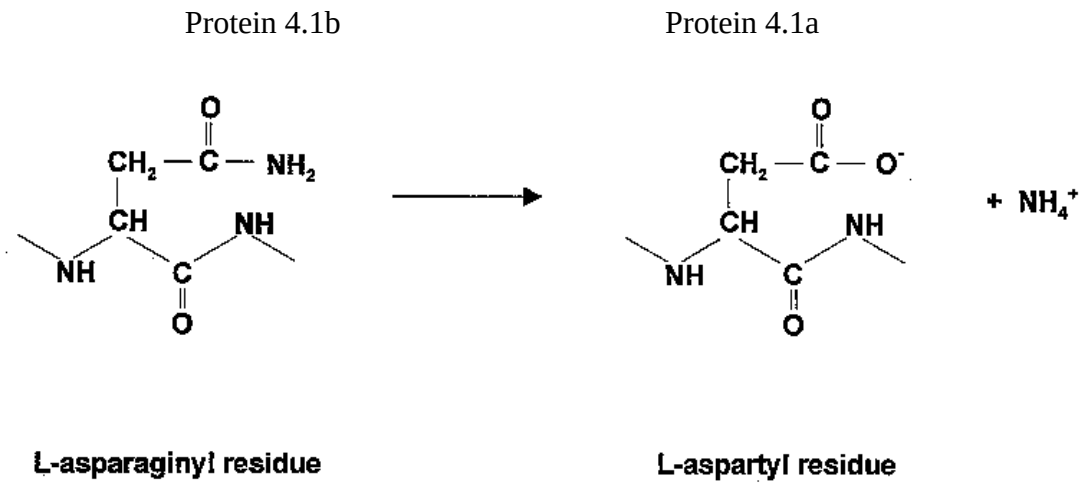

Figure 5. *Deamidation process of protein 4.1b to 4.1a [33].*

The post-translation modification has been demonstrated to be a non-enzymatic deamidation process, which takes place at two asparaginyl residues of protein 4.1b. The deamidation at the 502nd asparaginyl residue occurs slowly changing it to aspartate and is the reason for the conversion of protein 4.1b to 4.1a. This deamidation process is believed to result in conformational changes in protein 4.1 resulting in the apparent difference in molecular weight.

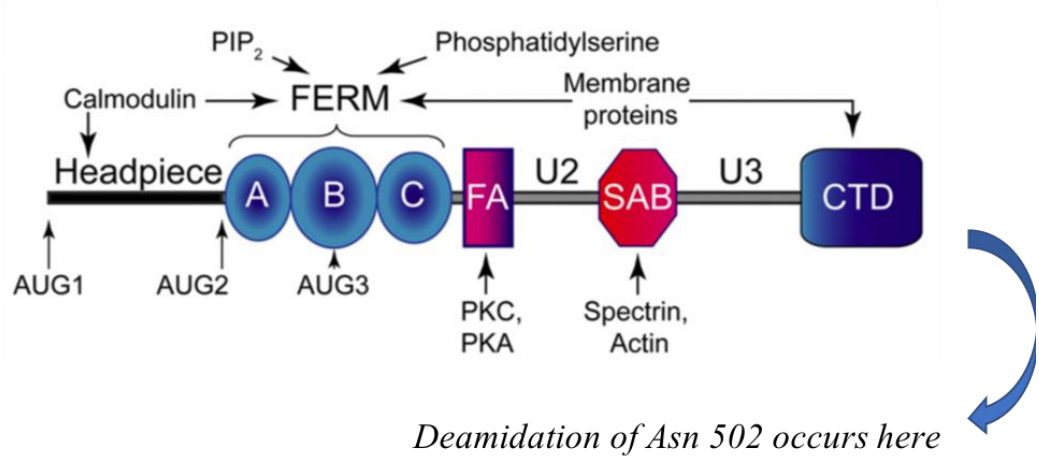

Figure 6. *Spontaneous deamidation of asparaginyl residues [34].*

C-terminal domain (CTD) is a sequence domain unique to protein 4.1. This domain is linked with protein-protein interactions. The first description of CTD was a 22/24 kDa domain and it was observed by chymotryptic digestion of protein 4.1 of erythrocytes [29, 35]. This fragment however is not stable and gets processed resulting in a stable 15 kDa fragment by chymotrypsin. This 15 kDa fragment is what represents the CTD of protein 4.1 and is derived from residues ranging from 709-858.

Neocytolysis

"Neocytolysis" theory says that EPO does not only produce RBCs, but also protects young RBCs (neocytes). A sudden decrease in plasma EPO results in selective clearance of neocytes. Mild anaemia was observed in astronauts during the first week in space. Microgravity increases haematocrit in the central organs of the body stopping EPO production. The neocytolysis theory first proposed that EPO decline stops erythropoiesis, and triggers the clearance of neocytes produced before launch. The same may occur during rapid RBC mass reduction like in people descending from high altitude where the RBC mass increased as an adaptation to hypoxia. After return to sea level, EPO drops and the organism reduces RBC mass by clearing the excess faster than the normal rate (0.8% per day in

humans), selectively clearing neocytes. Neocytolysis has not been validated so far and it has recently been critically reviewed [36].

Erythrocyte membrane skeleton defects in clinical disorders

Elucidating and understanding the functions of erythrocyte membrane skeleton components and their interaction with neighboring membrane proteins as well as lipids has been a remarkable achievement in modern hematology and biochemistry. Characterization and classification of molecular defects of the membrane skeleton changing the cell shape and stability leading to clinical disorders have been studied in the past years. Many of these defects are mainly structural or functional disorders of skeletal proteins, expressed clinically as misshapen red cells with or without shortened survival. Disorders that fall into this group are hereditary spherocytosis (HS), hereditary elliptocytosis (HE) [37]. It is known that probably all patients with HS or HE have a defective MS although an explanation at the molecular level is not always apparent.

Two types of defects are observed in these patients: 1) complete or partial deficiency of a skeletal protein, or 2) defective interactions amongst skeletal proteins. The hereditary membrane skeleton defects linked to HS and HE have been elucidated with the help of the existing knowledge of protein 4.1a/4.1b ratio. In literature, both proteins 4.1a and 4.1b are deficient in HE patients (either heterozygous or homozygous). The heterozygous state was characterized by a mild hemolytic state with mild spherocytic elliptocytosis [31]. Patients with mild HE, tend to have a deficiency of protein 4.1. In HS patients, there is a defect in spectrin binding to protein 4.1 [38]. The deficiency could be because of glycophorin C, as it plays a crucial role in the anchoring of protein 4.1 to the membrane skeleton.

Chapter 1.2. Animal Erythrocytes

There exists a huge variation within the cells of erythroid line within the animal kingdom. The differences are in terms of number of cells, size, shape, lifespan and metabolism. The cells also response to injury or anemia differently. In order to study animal erythrocytes in detail, it is essential to get some familiarity with how erythrocytes of different animals look like. There are several differences mentioned in past research for instance, canine erythrocytes seem to have a central pallor which is quite prominent as compared to other animals. This central pallor makes it easier to recognize spherocytic shape changes in canine blood as compared to other species. Below is a table summarizing some basic information of 4 types of animal erythrocytes.

	Canine	**Feline**	**Equine**	**Bovine**
Erythrocyte size	6-8 μm	5-7 μm	5-6 μm	5-6 μm
Erythrocyte life span [39]	100-120 days	70 days	140-150 days	130-160 days
Reticulocytes	1-2 days	Variable	Absent	2-4 days
Blood groups	A dozen but 9 are named after Dog Erythrocyte Antigen (DEA) [40, 41]	AB system [42]	8 major blood types: A, C, D, K, P, Q, U and T	11 major blood group systems in cattle: A, B, C, F, J, L, M, R, S, T and Z.

Table 1. *Comparison of Erythrocytes*

There have been several morphometric studies of different animals reported in the past. The basis of these studies was on linear measurements of erythrocyte size. These studies gave information of the width of erythrocytes of different species and also gave information on unique features observed such as rouleaux formation in equine red blood cells. Dog erythrocytes have been found to be the largest as compared to other species as shown in the table above, with a diameter varying from 6 to 8 μm.

Apart from cell size, comparative animal studies have shown a wide variation of whole blood, plasma viscosity, erythrocyte aggregation and deformability amongst animals such as horse, dog and sheep [43, 44]. Viscosity and aggregation of erythrocytes was studied extensively in horses during submaximal training which was correlated with changes in hemorheological variables. Well trained horses were found to have a more extensive change of fluidity as compared to untrained horses [45].

Another study showed a similarity in K^+-Cl^- transport in equine, bovine and human erythrocytes, volume regulation was investigated. Building on previous knowledge that equine erythrocytes were resistant to hypotonic shock and the cells lost K^+ upon swelling. It was suggested that volume regulatory decrease was achieved by solute efflux via the K^+-Cl^- co-transporter [46].

A study based on the characterization of erythrocytes by comparing aging markers in old and young cells from the same animal has not been conducted in the past. This aspect brings novelty to the current study.

Cell age distribution

The Percoll gradient is a good method to visualize cell density. The density is largely based on the hydration state and the size of the RBCs. The distribution of the RBCs in the gradient is used to calculate the proportions of into low, medium and high-density fractions. Generally speaking, the low-density fraction holds the youngest cells while the high-density fractions contains the old and damaged cells.

Protein 4.1

In studies carried out in the past, band 4.1 from the RBC membranes of cow, sheep, rabbit and guinea pig was split into two sub-bands as observed in human RBCs. In horse, band 4.2 overlapped with band 4.1 [47]. Whereas in horse erythrocytes, band 4.2 protein appeared to be overlapping with band 4.1. It has been reported that cat erythrocytes consist of only 4.1b as the conversion to ‘a; isoform doesn’t take place since Ser is present instead of Asn (site of deamidation in humans as well as other mammals) [48].

Oxidative stress

Growing data suggest that oxidative stress plays a prominent role in the signaling of erythrocyte aging. Oxidative stress results in formation of neo-antigen derived from Band 3, activates pro-apoptotic components and caspase-3, and binds oxidized haemoglobin to high affinity binding sites on Band 3 [49-51]. Haemoglobin and spectrin form a complex that is irreducible and acts as marker of aging as it results in cell damage such as increased rigidity, reduced deformability, erythrophagocytosis as well as echinocytosis [52-54]. Reduced and oxidized glutathione are measured as an indicator for oxidative stress. A study conducted in the past was carried out to assess whether hot seasons affect the oxidative status of transition dairy cows [55]. Studies have not been carried out to profile oxidative stress in normal conditions of bovine or equine erythrocytes.

Adenosine Triphosphate (ATP)

Most of the ATP in the RBCs is used to fuel the Na^+/K^+-pumps and the Ca^{2+}-pumps. As reported in the past, following either exercise or intravenous injection of adrenaline in six thoroughbreds (horses), there was a decrease in ATP concentration [56]. ATP measurements were carried out in relation to infections. No significant correlation between susceptibility to B. argentina and ATP was observed in 25 Droughtmaster and 5 Hereford cattle [57]. Similar to oxidative stress, no studies have been carried out to compare ATP measurements in different fractions of red blood cells.

Phosphatidylserine (PS)

As compared to younger cells, aged erythrocytes tend to have less aminophospholipid translocase activity and higher exposure of PS on cell surface [58]. Vesicles derived from erythrocytes expose PS [59]. Stressful treatments of human erythrocytes *in vitro* have also shown to expose PS [60]. PS exposure in healthy individual erythrocytes are still debated due to the skepticism about the techniques used to isolate older erythrocytes [59, 61].

Band 3

Several cellular changes in older erythrocytes have been identified in the past. Among them, breakdown or clustering of Band 3 has been identified as one of the major pathways leading to a senescent signal [62-64].

Chapter 1.3. Dynamics of Erythrocytes & von Willebrand factor in Sickle Cell Disease

Haemostasis

For human life, constant blood circulation through the blood vessels is vital. Nutrients and oxygen are supplied by blood as carbon dioxide along with waste products are removed through lungs, kidneys and liver. Any obstruction or impairment in circulation may result in hypoxia which results in cell necrosis severely damaging organs. Failing of vital organs results in being fatal. The human body has implemented several safety measures to prevent organs from failing. Blood flows through an enclosed environment with strongly regulated blood pressure. Blood is not exposed to its surrounding as it is surrounded by endothelial cells. Endothelial cells line the inner wall of all blood vessels in the human body. In the event of leakage of blood vessels, the damage is averted by a series of mechanisms such as blood platelets adhesion and blood coagulation. These processes have immense importance and a malfunction can result in severe pathology. Haemostasis is therefore an exceptionally well regulated as it helps in preventing blood leakage into the surrounding tissues.

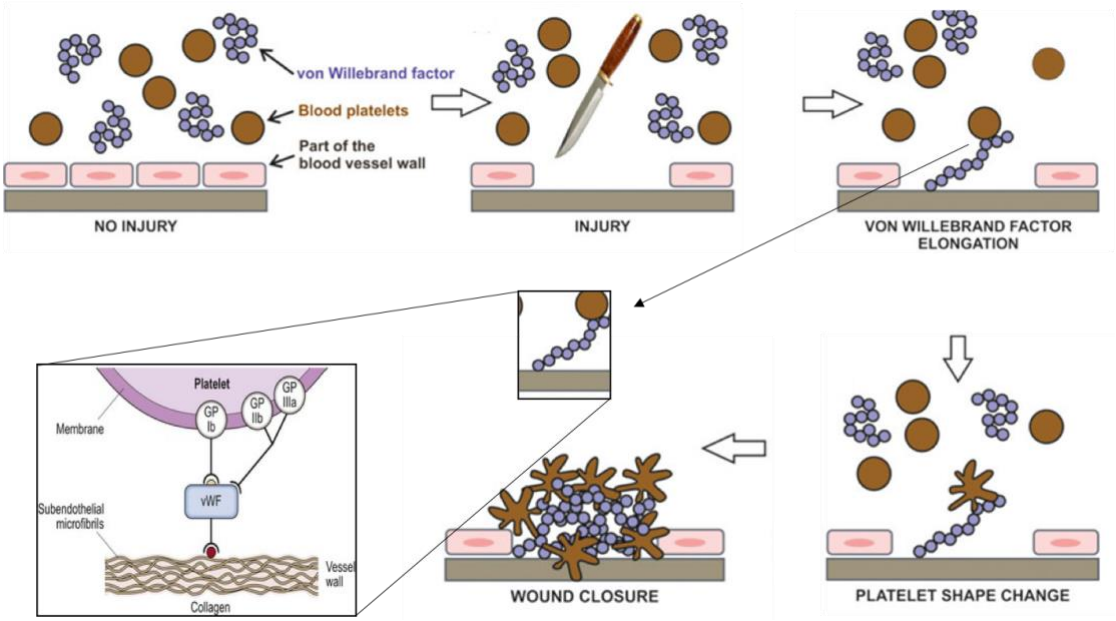

Figure 7. *Platelets and von Willebrand factor acting as blood vessel plumbers at the site of injury [65].*

When endothelium is damaged at the site of injury to a blood vessel, haemostasis is initiated. Platelets are activated by the blood leakage and exposure to the subendothelium (the connective tissue below an endothelial layer). The proteins of the subendothelial matrix adhere to activated platelets forming a plug at the injury site. This is known as ‘primary haemostasis’. This is followed by secondary

haemostasis which is the molecular changes in platelets and tissue factor exposure to plasms Factor VII initiating the activation of 'coagulation system' causing fibrin formation [66, 67]. These two processes guarantee that blood remains within the damaged blood vessels without leakage into tissues.

Primary haemostasis

When the vessel wall is disrupted, platelets bind to extracellular matrix components at the site of damaged endothelium, initiating primary haemostasis. The most essential platelet-supporting proteins are von Willebrand factor (VWF) and collagen [68]. Collagen acts as trigger and has a prominent role in thrombus formation [69]. Collagen type I and III are the major forms present in blood vessels [70]. Platelets bind to collagen via the glycoprotein IV receptor and the integrin α2β1 (GPIa/GPIIa) [71, 72]. Apart from collagen binding, one of the main events taking place in platelet adhesion is the platelet receptor GPIb-V-IX interaction to the A1 domain of VWF is one of the prime events in platelet adhesion [73, 74]

VWF is a large glycoprotein comprising of 2050 amino acids [75]. The basic unit of VWF is a dimer of two 250 kD subunits. These dimers are linked with a disulfide bond to form multimers. The protein is made of several identical subunits. These large multimers of VWF subunits are stored in in the α-granules of platelets and Weibel-Palade bodies of endothelial cells.

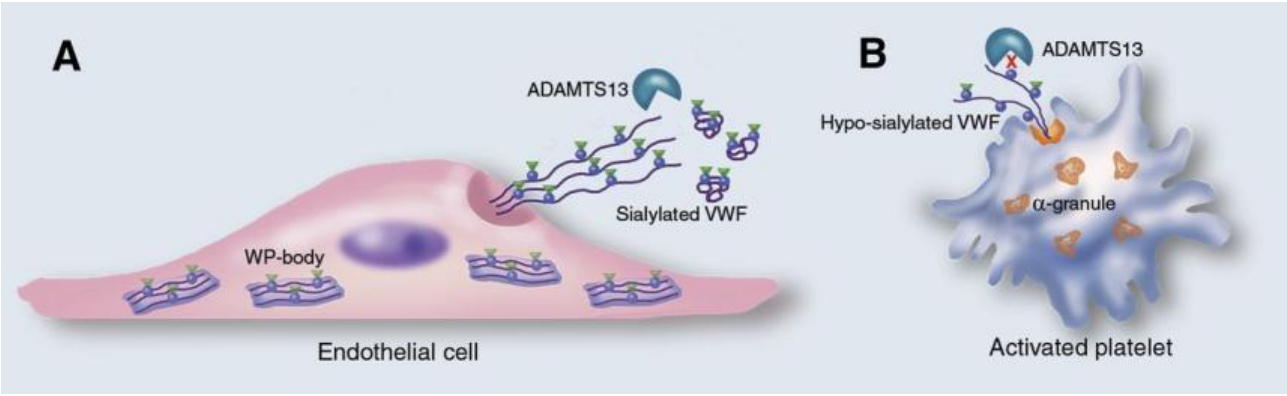

Figure 8. *VWF are stored in endothelial cells as Weibel-Palade bodies (A) and alpha granules of platelets (B) [76].*

VWF are released in the event of platelet or endothelial activation [77]. Upon release by activated endothelial cells, ultra-large VWF strings are formed that bind and capture platelets flowing in the blood stream [78]. Endothelial cells release VWF constantly into the blood stream [79]. When the

blood vessel is damaged, VWF binds to collaged via its A3 domain [80, 81]. Platelet binding to VWF is enhanced by immobilization of VWF on a surface [82]. Exposure of VWF to higher shear stress results in conformational changes within VWF making A1 domain more exposed for platelet binding [83]. The size of VWF multimers is reduced by proteolytic cleavage by ADAMTS13 (a metalloproteinase with a thrombospondin type 1 motif) [84]. Smaller multimers of VWF are not as haemostatically active as large multimers [85]. VWF is eventually cleared from the circulation by liver and spleen macrophages [86, 87].

Platelet activation is mediated by several signals and elevated cytosolic calcium levels is one of the main signals [88]. Upon activation, a multitude of processes take place which enhance primary haemostasis and further contributing to secondary haemostasis. Platelets go through changes upon activation such as releasing α-granule contents, changing shape, increasing adhesiveness and acquiring a pro-hemostatic surface by phosphatidylserine exposure [68]. Increased adhesiveness is achieved by a conformational change and clustering of the integrin αIIbβ3 which mediates stable binding to VWF and fibrinogen [89]. Upon activation, platelets also release ADP, ATP, serotonin, and produce the lipid signalling molecules thromboxane A2 and lysophosphatidic acid which further cause platelet activation [68, 90]. Activated platelets expose phosphatidylserine increasing the formation of tenase (FVIIIa-FIXa) and prothrombinase (FVa-FXa) complexes, resulting in a dramatic growth in thrombin generation [91, 92]. Thrombin produces fibrin clots which captures additional platelets. Thrombin also activates platelets via its G-protein coupled receptors PAR1 (protease-activated receptor 1) and PAR4 [93]. Therefore, phosphatidylserine exposure links primary hemostasis with secondary hemostasis. Activated platelets, eventually contract the clot to form a tight impermeable barrier to halt bleeding [94].

Secondary haemostasis (coagulation)

Blood coagulation can be divided into three separate phases: initiation, amplification, and propagation [95]. Vasculature damage begins the initiation phase exposing subendothelial matrix and cells to the bloodstream. Smooth muscle cells and fibroblasts expose tissue factor (TF), bind coagulation Factor VII (FVII). Following coagulation initiation, phase of amplification takes place. The thrombin produced by the prothrombinase complex activates platelets adhering at sites of injury and amplifies the prothrombinase activity by converting platelet-derived FV into FVa [96-98]. Next, the propagation phase takes place on procoagulant phospholipid surfaces, like activated platelets [99, 100].

Thrombin-activated FXIa converts FIX into FIXa, which associates with thrombin-cleaved FVIIIa [101]. Eventually sufficient amounts of thrombin is produced to from fibrin fibres, which are covalently crosslinked by the thrombin-activated plasma transglutaminase FXIIIa to yield a fibrin clot [102]. The classical intrinsic FXI-FXII pathway (triggered by collagen, polyphosphates, and neutrophil extracellular traps) is activated in parallel with extrinsic TF pathway [103].

There are two major systems to regulate coagulation in order to prevent uncontrolled and widespread clot formation. The two systems are protease inhibitors and the protein C/protein S pathway. Circulating protease inhibitors target the active sites of the coagulation factors and eliminate. The most extensively studied are: tissue factor pathway inhibitor (TFPI) and the serine protease inhibitor (serpin) antithrombin [104-106]. Activated protein C (APC) in complex with protein S supresses tenase and prothrombinase activity by proteolytic inactivation of FVIIIa and FVa [107, 108]. It is well assumed that APC prevents clotting on healthy and uninjured blood vessels instead of downregulating coagulation.

There are two types of bleeding disorders classified into primary and secondary hemostatic defects. Thrombocytopenia, platelet defects and von Willebrand disease come under primary hemostatic disorders [109, 110]. Inherited or acquired deficiencies of coagulation factor come under secondary hemostatic disorders [111]. Amid the primary hemostatic disorders, the most common disorder affection up to 1% if the population is von Willebrand disease (VWD) [111]. VWD is a result of inherited mutation involving the synthesis or function of VWF or acquired by anti-VWF antibodies formation, proteolytic increases and clearance or a reduction in synthesis [112].

Role of von Willebrand factor in Sickle Cell Disease

Sickle cell disease (SCD) is caused by individuals inheriting a mutant β-globin allele (Glu6Val) [113] . This inheritance comes in either two copies or with an allele that specifies defective or deficient β-globin, thus leading to stiff, adhesive and lysis-vulnerable erythrocytes [114, 115]. These characteristics cause the main indicators of SCD, namely haemolytic anaemia and vaso-occlusion, which can impact various different organs. Increased haemolytic rates among patients elevate the potential for pulmonary artery hypertension and leg ulcers [116]. Various adhesive molecules have been associated with sickle vaso-occlusion, such as von Willebrand factor (VWF) [117]. Endothelial cells that have acute activation can discharge large volumes of extremely big and hyper adhesive VWF molecules (ultra-large VWF [ULVWF]), which have the capability to instantaneously bind erythrocytes and platelets, [118, 119] particularly sickle cells [120, 121]. Generally, ULWVF is

cleaved by ADAMTS13 into smaller-sized multimers with less adhesion, thus averting problems such as thrombotic thrombocytopenic purpura [122]. Increased levels of plasma VWF have been discovered in SCD [123, 124], however, a minimal amount of research has focused on the structure and reactivity of this VWF within this condition. In some research, the volume, reactivity and multimer configuration of VWF, as well as the ADAMTS 13 antigen and activity were investigated in SCD individuals, which facilitated the process of establishing a correlation between parameters and haemolysis.

VWF parameters in 13 SCD patients

9:HbSS, 2:Sickle-β^+ thalassemia, 2:Sickle-β^0 thalassemia, 1: HbSC

Parameter	Method	Result
VWF Multimer pattern	1% agarose gel electrophoresis + Western Blotting with polyclonal VWF antibody	Many of the SCD plasmas had **higher VWF levels** and **larger multimers** compared to normal plasma
VWF Antigen concentration	ELISA	**Elevated** in almost all patients from 1.2- to 3.6- fold the concentration in normal plasma
Active VWF	ELISA using llama nanobody AU/VWFa-11 to designate VWF activation factor	**Increased** VWF activation factor in 9 of the 13 patients
Total VWF	By multiplying VWF antigen by VWF activation factor	**Increased** total VWF in 11 out of 13 patients (Total VWF accounts for both VWF quantity and adhesiveness)
ADAMTS13 Antigen	ELISA	**No significant deficiency** in any of the SCD patients
ADAMTS13 activity	Determined by using a peptide substrate using pooled normal plasma as a standard	ADAMTS13-specific activity (Activity/concentration) slightly decreased in 6 patients

Table 2. *Summary of a study that verifies the correlation of vWF and SCD severity.*

Healthy red blood cells do not normally bind to the endothelial cells (EC) lining the vascular wall. Erythrocyte adhesion does occur in several hematologic disorders especially in sickle (SS) cell disease [125-128]. When red cells are bound to the endothelial cells, this causes vaso-occlusive episodes that lead to impaired blood flow, which subsequently generates ischemia and damage to tissues [128]. After it was observed that SS erythrocytes bind to endothelial cells, various different process have been explained that can lead to erythrocyte-EC adhesion [114, 128, 129].

A specific mechanism linked with the binding of SS erythrocytes and ECs that has been expansively researched is through ULVWF multimers [120, 130]. SS erythrocytes binding to ECs can be enhanced immensely by *in vitro* EC-derived ULVWF multimers, however, normal erythrocytes get augmented

only marginally [130]. Research performed on a rat mesocecum model verified that VWF from desmopressin-stimulated ECs enhanced the ability of SS erythrocytes to bind to the venular endothelium [120]. Different researchers established that the seriousness of the sickle-cell condition and the plasma levels of active VWF are correlated [131]. Although it has been widely recognised that SS erythrocytes bind to EC through ULVWF, there has been significantly less focus on the binding of standard erythrocytes. For example, adherence of calcium-loaded erythrocytes to ECs is found to be possible [114]. Based on the findings of these studies, the objective was to determine whether it possible to make enhancements to the ability of erythrocytes to bind to ECs via ULVWF multimers via calcium loading of the erythrocytes. One of the interesting aspects of the study would be to see if this adhesion of calcium-loaded erythrocytes to endothelium-derived VWF is independent of platelet.

Erythrocytes: role in haemostasis

Several mechanisms can explain how hematocrit affects haemostasis. Platelet margination is a process why which erythrocytes influence haemostasis [132]. Erythrocytes tend to move away from the blood vessel when exposed to shear flow owing to their deformability. This movement away of the erythrocytes from the vessel wall results in platelet movement towards the vessel wall by the process of volume exclusion [132]. This process is referred to as platelet margination. The platelet-wall contact then results in adhesion. Apart from this, erythrocytes contribute by releasing compounds that activate platelet and also scavenge inhibitors of platelet activation. ADP is released by erythrocytes which results in activating platelets via purinergic receptors [133, 134]. ADP is released by hemolysis of erythrocytes which causes platelet activation. Moreover, erythrocytes also modulate secondary haemostasis by exposing phosphatidylserine (PS) on their outer leaflet of their membrane [135, 136]. PS exposure provides binding sites for the tenase (FVIIIa-FIXa) and prothrombinase (FVa-FXa) complexes, thereby intensely promoting thrombin formation [92]. PS exposure doesn't take place in erythrocytes under physiological conditions. It is triggered by pathologies like. sickle cell disease or β-thalassemia or during storage in blood banks [137-139]. Erythrocytes can bind to platelets via the erythrocyte membrane protein ICAM-4 and the platelet integrin αIIbβ3 [140, 141]. Adhesion of erythrocyte to endothelial cells is widely studied especially in pathologies like sickle cell disease or β-thalassemia [129, 142].

Chapter 1.4. Glucose-6-phosphate dehydrogenase deficiency

Pentose Phosphate Pathway (PPP)

Along with glycolysis taking place, pentose phosphate pathway is the other major metabolic pathway that occurs in the cell cytosol [143]. PPP gives rise to two essential products: NADPH molecules which help with building other molecules, and ribose-5-phosphate sugar used to make nucleotides (DNA and RNA) [144]. It also generates pentoses (5-carbon sugars) [145].

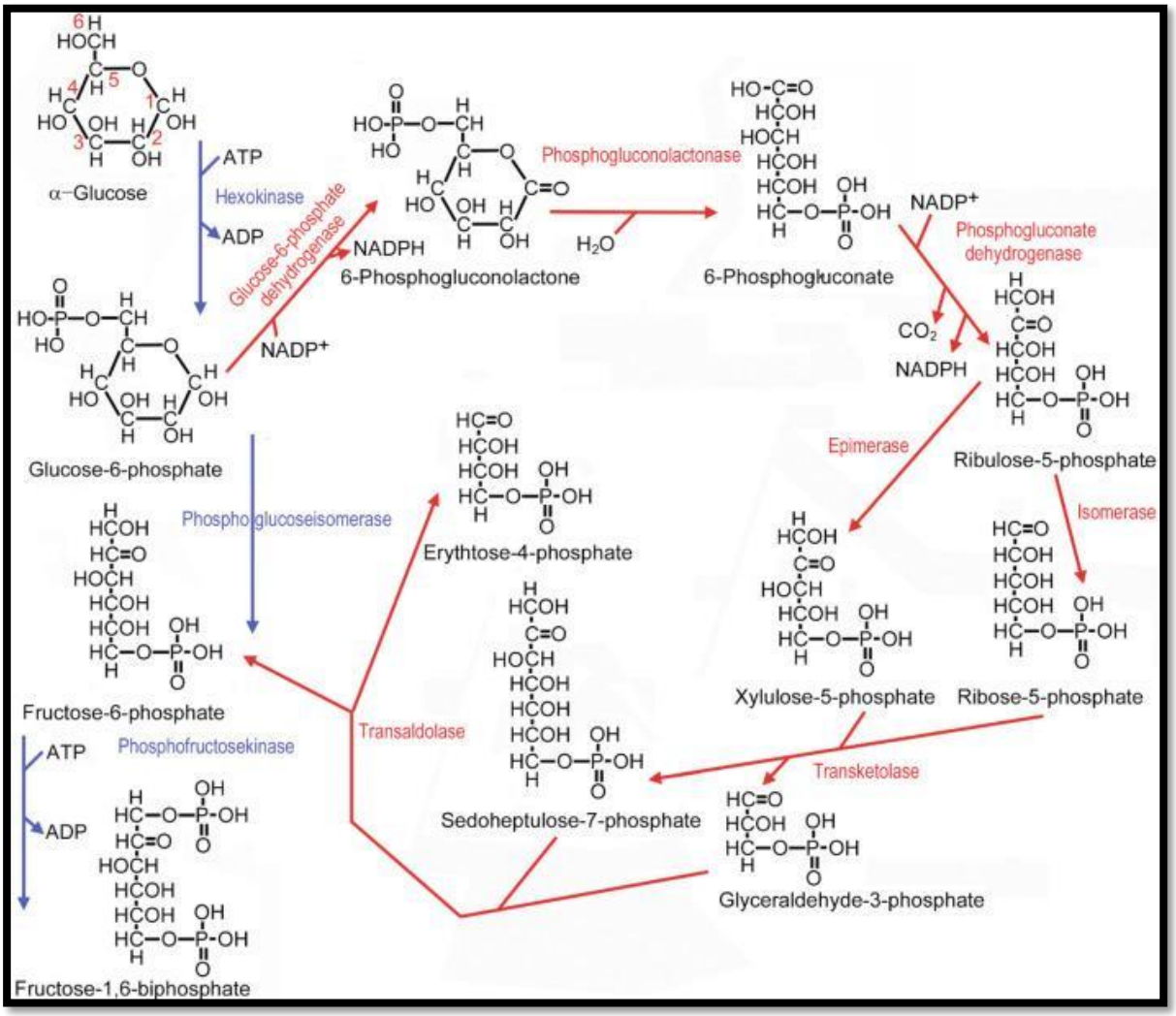

Figure 9. *The pentose phosphate (red lines) alternative to glycolysis (blue lines) [145].*

The pentose phosphate pathway is regulated at the level of its initial enzyme, specifically glucose-6-phosphate dehydrogenase (G6PD), which is managed by the redox condition of the NADP couple, where NADPH has a strong feedback obstruction on this enzyme.

Glucose-6-phosphate dehydrogenase (G6PD)

The pentose phosphate pathway is regulated at the level of its initial enzyme, specifically glucose-6-phosphate dehydrogenase (G6PD), which is managed by the redox condition of the NADP couple, where NADPH has a strong feedback obstruction on this enzyme. The enzyme G6PD is active in each kind of cell that is involved in the standard processing of carbohydrates [146]. It is an important factor within red blood cells. G6PD facilitates the process of protecting red blood cells from being damaged by oxidative agents and untimely destruction [147]. The initial phase in the pentose phosphate pathway is attributable to G6PD, which is a series of chemical reactions that facilitates the conversion of glucose into ribose-5-phosphate. Ribose-5-phosphate is a significant constituent of nucleotides, which are fundamental components of DNA and RNA. This chemical reaction produces NADPH and it is an important factor in the protection of cells from molecules defined as reactive oxygen species, which have the potential to cause harm. G6PD generates NAPDH, which is necessary for red blood cells as they have particularly vulnerability to being damaged by reactive oxygen species because they are deficient in other NADPD-producing enzymes [148].

G6PD deficiency

Glucose-6-phosphate dehydrogenase deficiency is X-chromosome inherited and is the most common red cell enzyme disorder worldwide. Frequent clinical presentations include neonatal jaundice and episodic hemolysis after exposure to oxidative stress [149]. G6PD deficiency is known to affect around 400 million people globally prevalent mostly in Asia, Africa, Middle East as well as the Mediterranean nations [150]. The prevalence of G6PD deficiency is correlated with malaria geographical distribution. It suggests that this deficiency provides slight protection against malaria [151].

Erythrocyte metabolism (detailed)

In regard to humans (as well as all other mammals), there is an absence of mitochondria in red blood cells, which means that it has no operational tricarboxylic acid cycle (TCA) cycle [152]. In this case, glucose is predominantly metabolized through glycolysis, thus producing lactate that is emitted by the cells; this generates 2 ATP for every glucose molecule, which is significantly less than total oxidation (ca 30 ATP), but sufficient to satisfy the energy requirements of the red blood cells. The essential metabolic pathway of glycolysis involves the oxidative breakdown of one glucose into two pyruvates with the capture of some energy as ATP and NADH. Glycolysis is important in the cell because glucose is the main source of fuel for tissues in the body [153].

A certain amount of glucose is oxidized to CO_2 in red blood cells. This largely happens in the PPP or "shunt", in which 1 carbon of glucose is emitted as CO_2, and the extracted energy is utilized in the process of reducing NADP to NADPH, which acts as an antioxidant. The 5-carbon sugars (pentoses) that are produced are subsequently reorganized to a 3-carbon sugar (glyceraldehyde phosphate) that re-enters glycolysis. This explains the utilization of the terminology "shunt", as 5/6 of the glucose carbon that originally enters is returned to glycolysis.

Through variance of the flux via the PPP, it is possible for cells to balance the utilization of ATP (energy) or NADPH (antioxidant). It has been estimated that within the red blood cells of humans, 10-30% of hexokinase flux is redirected via the PPP, and the rest passes through upper glycolysis. This equates to 2-5% of glucose carbon emitted as CO_2, while the rest is metabolized to lactate. This is applicable to the red blood cells of mammals. However, the red blood cells of different vertebrates, such as fish and birds, maintain both their mitochondria and nucleus, and they have a distinctive metabolism [154].

While approximately 90% of proteins within an RBC are comprised of haemoglobin, various different proteins can also be found, such as enzymes within the anaerobic pentose phosphate pathway, which is facilitates the metabolization of around 90% of the glucose that enters the cell (the aerobic pathway handles the remaining 10%). Additionally, certain proteins are responsible for sustaining the oxidation condition of the haemoglobin-bound iron atoms. The iron contained within oxidised haemoglobin, or methaemoglobin, is in the Fe^{3+}(ferric) condition, which does not have the ability to bind oxygen. The iron is converted by the NADH-dependent enzyme methaemoglobin reductase into the Fe^{2+} ferrous condition, which binds O_2 [155]. In fact, NADH represents one of the most important outcomes of the glycolysis in addition to ATP and 2,3–BPG, which facilitate the regulation of O_2 released from haemoglobin. Additionally, NADPH is generated via the anaerobic pathway, and is a co-factor in the process of reducing oxidized glutathione, functioning as a primary reducing agent within the cell to offer protection when faced with oxidative stress. Additional enzymes like superoxide dismutase, glutathione peroxidase, and catalase also assist in the prevention or reversal of oxidation. The movement of oxygen in both directions leads to the creation of reactive oxygen species like superoxide and hydroperoxyl radicals ($\cdot O_2^-$ and $HO_2\cdot$) as well as peroxides such as hydrogen peroxide (H_2O_2), thus making the existence of these defensive proteins essential [156, 157].

Scope of the thesis

This thesis focuses on various aspects of erythrocytes in humans as well as animals. The scope was to identify the role and parameters of erythrocytes that differ with age and in diseases, describing functions of erythrocytes beyond oxygen transport. Work was done in three different laboratories across Europe, resulting in several small projects all connected by the recurring theme of erythrocytes: markers of aging and clinical disorders. Several aspects of erythrocyte biochemistry were studied in the span of this project: morphology, aging, metabolism and insight into pathologies such as sickle cell disease and G6PD deficiency. By means of these new insights, we hope to contribute to future research in the field.

Protein 4.1

Past observations suggest that protein 4.1a ratio to protein 4.1b increases with erythrocyte aging. Since protein 4.1 is bound to other proteins such as spectrin, actin, band 3, glycophorin, calmodulin and myosin, therefore, insight into the role of deamidation of 4.1 can unravel biological significance of how this post translational modification affect its interaction with other proteins. There are high chances that protein 4.1 deamidation modifies other proteins too. Constructed on these evidences, studies were designed to find out more about the conversion of protein 4.1b to 4.1a.

The goals of study at host institute (University of Pavia) and 4.1 study continuation during secondment at Sanquin:

- Protein 4.1 study on a protein and peptide level
- Confirming amino acid difference between the two isoforms
- Conversion of protein 4.1b to 4.1a in human red blood cell under different physiological conditions
- Conversion of protein 4.1b to 4.1a in human red blood cell using different buffers to prepare ghosts
- CD Measurements of peptides
- Conversion of protein 4.1b to 4.1a in healthy and patient human erythrocytes
- Conversion of protein 4.1b to 4.1a in experimentally aged erythrocytes

Study of Animal Erythrocytes

There have been several morphometric studies of different animals reported in the past. The basis of these studies was on linear measurements of erythrocyte size, viscosity and aggregation. A study

based on the characterization of erythrocytes by comparing old and young cells from the same animal has not been conducted in the past. This aspect brings novelty to the current study. The work depicted here was designed to investigate changes observed in animal erythrocytes with age.

The goals of the Secondments at Institute of Veterinary Physiology, University of Zurich

- Defining best conditions for separation of equine and bovine erythrocytes to separate fractions into old and young cells using Percoll gradients
- Measurements of several markers of aging as a comparison between young and old cells: ions (Na^+ & K^+), water, ATP, redox balance (GSH/GSSG), EMA binding, CD71 levels, and intracellular Ca^{2+} levels
- SDS-PAGE of equine and bovine erythrocyte membranes aiming at measuring the ratio between a & b isoforms of protein 4.1 as a cell-age parameter
- Defining best conditions for separation of canine and feline erythrocytes to separate fractions into old and young cells using Percoll gradients
- Acquire images of calcium-loaded feline and canine erythrocytes from different fractions
- Ion measurements of canine erythrocytes
- Designing a FACS protocol for canine erythrocytes

Side Projects: Sickle Cell Disease and G6PD deficiency

There were two ongoing side projects based on red blood cell pathologies. The first study focused on the role of ULVWF and interaction with erythrocytes in SCD. The research question of the second study was if it is possible to correct G6PD deficiency through protein transduction.

The goals of the side projects during Secondments at Blood Cell Research Department, Sanquin, Amsterdam

- Neuraminidase treatment of SCD patient erythrocytes followed by incubation with plasma
- Flow assays to show that activated endothelial cells release ULVWF which mediate adhesion of erythrocytes flowing over the layer of cells
- Confirm ULVWF are present in SCD causing adherence and clotting
- Test efficiency of the Cytofluorometric assay for G6PD deficiency
- Transformation of TAT G6PD
- G6PD activity and protein concentration
- Transduction of eluted protein into red blood cell

Chapter 2. Methods

Chapter 2.1 Lab #1 Department of Biology and Biotechnology, University of Pavia

Blood processing

Blood was attained from healthy donors after informed consent. Blood was mixed with 3.8% (w/v) tri-sodium citrate in a 9:1 ratio. The blood was then filtered through cellulose in order remove leukocytes as well as platelets. Equal parts of α-cellulose and microcrystalline cellulose were present in the cellulose equilibrated in PBS. This filtration step was done to purify erythrocytes from platelets and leukocytes [158].

Erythrocyte membranes (ghosts) preparation

Purified (white) erythrocyte membranes (referred to as 'ghosts' in this thesis) were prepared by a methods described elsewhere [159]. Erythrocytes were incubated for 10 minutes with a serine protease inhibitor: 5mM diisopropyl fluorophosphate (DFP), followed by washing in PBS three times. Packed erythrocytes were then lysed by hypotonic hemolysis with 9 volumes of hypotonic buffer (5mM sodium phosphate 0.5mM EDTA, pH 8.0), at 4°C. After 30 minutes of incubation, the samples were then centrifuged at 26000g repeatedly until white ghost membranes were obtained. The final packed ghosts were diluted to reach the same volume as that of the original packed RBCs from which they were derived, resulting in a protein concentration of approximately 5mg/ml.

Sodium Dodecyl Sulfate Polyacrylamide Gel Electrophoresis (SDS-PAGE)

7% SDS-PAGE gels (Laemmli method [160]) were carried out for analysis of the separation of all proteins in erythrocyte membrane. Ghosts obtained were mixed with 0.5 volumes of 3X sample buffer for SDS-PAGE (50mM Tris/HCL, pH 6.8, 5% SDS (w/v), 0,01% bromophenol blue (w/v), 35% sucrose (w/v), 5mM EDTA, 200mM DTT). Samples loaded on SDS-PAGE gels were carried out for 30 minutes longer for a clear separation of protein 4.1a and 4.1b. 5-15% acrylamide linear gradient gels were also run, method described elsewhere [158]. It was aimed to quantify the two polypeptides of 4.1 after Coomassie blue staining of the gels, digital image acquisition, and densitometric analysis using suitable computer programs (e.g. Scion image/Image J).

Western Blotting and immunodetection

Following SDS-PAGE, the proteins the gel were electro transferred to a polyvinylidene fluoride (PVDF) membrane in a buffer [20mM Tris, 150mM glycine, 20% methanol (v/v) pH 8.3] at a constant current of 200mA for 2 hours. Once the proteins were transferred to the PVDF (activated in methanol prior of use), among the separated proteins, 4.1a and 4.1b bands were detected using primary antibody anti protein 4.1 (EPB41 polyclonal A01, Abnova, Taipei, Taiwan). Antibodies were diluted in the washing buffer [50mM Tris/HCl, pH 7.5, 0.2M NaCl, 1g/l polyethene glycol (PEG) 20000, 0.5ml/I Tween-20, 1g/l BSA]. NaN_3 was added to the solution as a preservative for multiple uses. The washing and immunodetection steps were adapted as described elsewhere [161].

Density gradient

RBCs of different cell age were obtained after separation of the total population of RBCs at 15% haematocrit in a self-forming Percoll gradient, by centrifugation at 33000 x g, 20 °C for 20 min. After centrifugation, the cell suspension was divided into three distinct subsets: bands of low, middle, and high density. Percoll working solution was prepared as described elsewhere [21].

Haematocrit and haemoglobin (Hb) measurements

Haematocrit was measured in micro capillary tubes. The tubes were filled with whole blood or suspensions of RBCs of various dilutions, closed, and centrifuged. Next, the part with packed RBCs was measured with a ruler and divided by the total length, including the liquid part of the total volume. Hb was assayed by adding 25 µl of blood to 2575 µl Drabkin's reagent. The absorbance of the samples at 540 nm was read with a spectrophotometer and multiplied for the factor 0.1594 to give the final value of Hb concentration in the unknown sample in g/ml.

Statistical Analysis

Data was analyzed using GraphPad Prism 8 for MAC (GraphPad Software, La Jolla, CA, USA). Two-way ANOVA was used to analyze results.

Chapter 2.2 Lab #2 Institute of Veterinary Physiology University of Zurich

Blood samples

Blood samples were obtained from the Veterinary Institute in heparinized tubes. All samples were taken in the morning. Samples taken one day earlier were stored in a refrigerator overnight.

Separation of erythrocytes into fractions using Percoll

Erythrocytes were separated into fractions of young, old and mature cells on Percoll density gradient using a technique modified from the initial method described earlier [21]. 13 ml of 85% to 95% isotonic solution was pipetted into centrifugation tubes. The solution contained the following (in mM): 140 NaCl, 4 KCl, 0.75 $MgSO_4$, 10 glucose, 2 $CaCl_2$, 0.015 $ZnCl_2$, 0.2 Gly, 0.2 Glu, 0.2 Ala, 0.1 Arg, 0.6 Gln, 20 HEPES-Imidazole, pH 7.4 at room temperature.1 ml of blood was then added on top of the Percoll solution. Centrifugation of the samples at 45,000g was carried out for 15 minutes at +30 °C (Sorvall RC 5C plus, rotor SM-24, Waltham, MA USA). Fractions were aspirated separately. All three fractions were then washed 3 times in PBS containing 0.1% BSA as haematocrit. RBC volume of each of the fractions was then measured [162].

GSH/GSSG and ATP measurements

The RBCs were lysed, proteins degraded and the result was centrifuged. The supernatant was kept and the pH was adjusted to 7-8. Spectrophotometry was used with Ellman's reagent to measure reduced glutathione by its thiol group. Oxidized glutathione was reduced with NADPH and glutathione reductase before measurement. The percentage of oxidized glutathione was calculated, as well as the amounts of reduced and oxidized glutathione, standardized to haemoglobin [163]. ATP was measured to estimate the balance between the glucose consumption and pump activity of the RBCs using the same supernatant used as for the glutathione measurements. Bioluminescence was used to measure the concentration. The light is a result of a reaction between the ATP and luciferin.

Intracellular K^+ and Na^+ measurements

Flame photometry was used for detection of intraerythrocytic K^+. Briefly, pre-dried pre-weighed 1.5 ml Eppendorf tubes were filled with 1 ml of ice-cold Na^+/K^+-free washing solution containing 100 mM Mg $(NO_3)_2$ and 10 mM imidazole-HNO_3 buffer (pH 7.4 at 4◦C). Aliquots (0.2 ml) of whole blood were injected into 1 ml of washing solution, and RBCs were then sedimented by centrifugation (3000xg, 5 min Eppendorf centrifuge cooled to 4◦C). The washing procedure was repeated three times

and the washing solution removed. Tubes with wet RBC pellets were weighed and dried for 3 days at +80◦C. After weighing, the dry pellet was dissolved in concentrated HNO_3 free from traces of metal ions. K^+ content of RBCs was then detected using Sherwood flame photometer (Sherwood Scientific Ltd., Cambridge, UK) and normalized per dry weight.

Intracellular Ca^{2+} imaging

Ca^{2+} imaging experiments were carried out with RBCs from animal blood samples. Intracellular Ca^{2+} was measured from single cells as Fluo-4 (Thermo Fisher Scientific, Waltham, MA, USA) based fluorescence intensity as described before. Intracellular calcium levels in RBCs was measured using fluorescence live imaging at one thousand times magnification.

Flow Cytometry: Canine Erythrocytes

Gallios Flow Cytometer (Coulter Beckmann Life Sciences, Indianapolis, Indiana, USA) was used to measure forward scatter as an indicator for size and shape. Following Percoll separation, 2 µl of each fraction (light, medium and heavy) of canine erythrocytes was mixed with 1 ml of incubation medium containing Fluophores (Fluo-4, mBBr, EMA). The cells were incubated with the dyes for 1 h at room temperature covered in a dark box. BD Retic-Count solution was used for reticulocyte count. The incubation solution contained: *(mM) 145 NaCl, 4 KCl, 0.15 $MgCl_2$, 1.8 $CaCl_2$, 0.3 alanine, 0.3 glutamate-Na, 0.3 glycine, 10 glucose, 10 HEPES-imidazole, pH 7.40 at room temperature, 0.1% bovine serum albumin (BSA)*. Fluorescence intensity of 100,000 cells was then measured using flow cytometry. During the analysis the following parameters were recorded: forward scatter ±SD, fluorescence intensity (FI) in the whole cell population and in the fraction of RBCs with high Ca^{2+}, EMA binding, mBBE and reticulocytes.

Ghost preparation: Animal Erythrocytes

Heparinized packed erythrocytes were obtained by the Veterinary Institute at University of Zurich. Purified ghost membranes (before or after Percoll separation) were prepared by hypotonic hemolysis of erythrocytes with 9 volumes of hypotonic buffer at 4°C followed by centrifugation at 26000g repeatedly until membranes were obtained. The final packed ghosts are diluted to reach the same volume as that of the original packed RBCs from which they were derived. Dithiothreitol (DTT) was not added to the sample buffer.

SDS-PAGE

Laemmli 7% SDS-PAGE gels were carried out for analysis of the separation of all proteins in erythrocyte membrane. Ghosts obtained were mixed with 0.5 volumes of 3X sample buffer for SDS-PAGE (50mM Tris/HCL, pH 6.8, 5% SDS (w/v), 0,01% bromophenol blue (w/v), 35% sucrose (w/v), 5mM EDTA, 200mM DTT). Samples loaded on SDS-PAGE gels were carried out for 30 minutes longer for a clear separation of protein 4.1a and 4.1b. 5-15% acrylamide linear gradient gels were also run, method described elsewhere [158]. The aim was to be able to quantify the two polypeptides of 4.1 after Coomassie blue staining of the gels, digital image acquisition, and densitometric analysis using suitable computer programs (e.g. Scion image/Image J).

Statistical Analysis

Data was analyzed using GraphPad Prism 8 for MAC (GraphPad Software, La Jolla, CA, USA). Two-way ANOVA was used to analyze results.

Chapter 2.3 Lab #3 Sanquin, Blood Cell Research, Amsterdam

Blood samples

Upon approval of Sanquin's ethics committee, heparinized blood was collected from healthy donors as well as patients, after informed consent in accordance with The Code of Ethics of the World Medical Association (Declaration of Helsinki).

Complete blood count (CBC)

Automatic cell analyzers, ADVIA 2120 (Hematology System, Siemens Healthcare Diagnostics, Forchheim, Germany) and Cell-Dyn Sapphire (Abbott Diagnostics Division, Santa Clara, CA, USA) were used to measure hematological parameters: red blood cell count (RBC), haemoglobin concentration (Hb), and RBC volume percentage (HCT) in all samples.

Experimental aging of erythrocytes

Erythrocytes were isolated from whole blood and centrifuged. The cells were then resuspended in PBS [0.2mM $CuSO_4$ and 5mM ascorbic acid] to get a final concentration of $0.4X10_8$ cells/ml. The cells were then incubated in shaking heating block for 60 minutes at 37°C. The cells were then washed three times with PBS followed by resuspension in HEL HEPES+(with $CaCl_2$) as well as HEPES-(Negative control) to a final concentration of $1X10_8$ cells/ml. Conjugated Annexin V was diluted in both HEPES+ and HEPES- (1:200 dilution). 5µl of diluted erythrocytes and 45µl of diluted annexin-V were pipetted in 96-wells plate, left for 30-minute incubation in the dark on ice. 150µl of HEPES+ and HEPES- were added to respective wells and analyzed by FACS.

Flow Cytometry

All flow cytometry experiments were performed with BD FACS Cantoll or BD LSRII + HTS (BD Biosciences, Franklin Lakes, NJ, USA). The data was analyzed with FACSDiva Software (BD Biosciences, Franklin Lakes, NJ, USA) and FlowJo Software (Tree Star Inc., Ashland, OR, USA).

Erythrocyte calcium loading/depletion

10^8 cells/mL erythrocytes were suspended in HEPES (+) (2.5 mmol/L calcium) buffer, HEPES buffer based on the stipulated calcium concentrations, or HEPES (-) buffer containing a supplement of 5 mmol/L EGTA (ethylene glycol tetra acetic acid) were processed with 1 µmol/L ionomycin for a period of one hour. Subsequently, washing of the erythrocytes was performed with HEPES (+) with

an equivalent concentration of calcium, placed in storage under room temperature conditions and then resuspended before the flow assay experiments. The assays were done in 1% BSA/ HEPES (+) or HEPES (-). Each of the buffers was supplemented with 100 μmol/L histamine.

Endothelial cell culture for flow chamber experiments

The process of culturing pooled human umbilical vein ECs (HUVECs) acquired from (Lonza) was conducted in flasks coated with fibronectin (FN) in EBM-2 medium (Lonza) supplemented with EGM-2 SingleQuot Kit Suppl. & Growth Factors (Lonza). Seeding of the ECs (7.5×10^4 cells/mL) was performed in μ-Slide VI 0.4 ibiTreat flow chambers (Ibidi) that were FN-coated manually. The process of culturing the EC lasted for a total of 5 days prior to starting the flow experiments. When specified, stimulation of the ECs was conducted with 10 ng/mL TNF-α (Peprotech) for a period of 24 hours. HUVECs were utilised until passage 5.

Real-time image capture of erythrocyte binding to endothelial cells during flow

Incubation of 10_8 cells/mL erythrocytes was conducted for 60 minutes using 1 μM ionomycin. Both DMSO and H_2O were utilized as controls. 10_8 cells/mL erythrocytes with no platelets were complemented with 100 μmol/L histamine. Each of the perfusions was conducted using a ProSense syringe pump (NE-1010) at a rate of 0.57 mL/min, which is known to produce shear stress of 0.72 dyne/cm2 and a wall shear rate of $100s^{-1}$. These conditions were adapted according to post-capillary veins or venules conditions as stated elsewhere [83, 164]. The real-time imaging of the erythrocytes and endothelial cells was achieved with the use of a Carl Zeiss Microscopy instrument (Axiovert 200M microscope). The microscope comprised of an Orca-R_2 camera (Hamamatsu) utilizing a 10x air objective.

Western Blotting (VWF)

Western Blots were carried out with the use of the polyclonal primary antibody anti-Human vWF (Dako, A0082, 1:1000 dilution in TBST buffer) as well as an appropriate secondary antibody (Li-Cor, IRDye 800CW, 1:2000 dilution in TBST buffer) provided with Odyssey conjugates. Following the blotting, images were acquired by using Odyssey scanning.

Protein expression using BL21

Expression plasmid TAT-G6PD (Fig 10) was transformed into BL21 via heat shock method [165] and plated on antibiotic selection plate and incubated overnight at 37_oC. A single colony was

resuspended in 10 ml liquid culture with antibiotic. Culture was incubated until OD_{600} reached 0.6. Culture was then induced with IPTG for 3 to 5 hours at 37^{o}C. 6XHis-Tagged Protein was eluted and purified using Ni-NTA Column. Expression was checked by Commassie stained gel, Western Blot or activity assay. Expression was checked in both the total cell extract (soluble + insoluble) and the solution fraction only. G6PD activity was measured by the diagnostic laboratory and the concentration of protein was determined using Pierce BCA Protein Assay Kit [166].

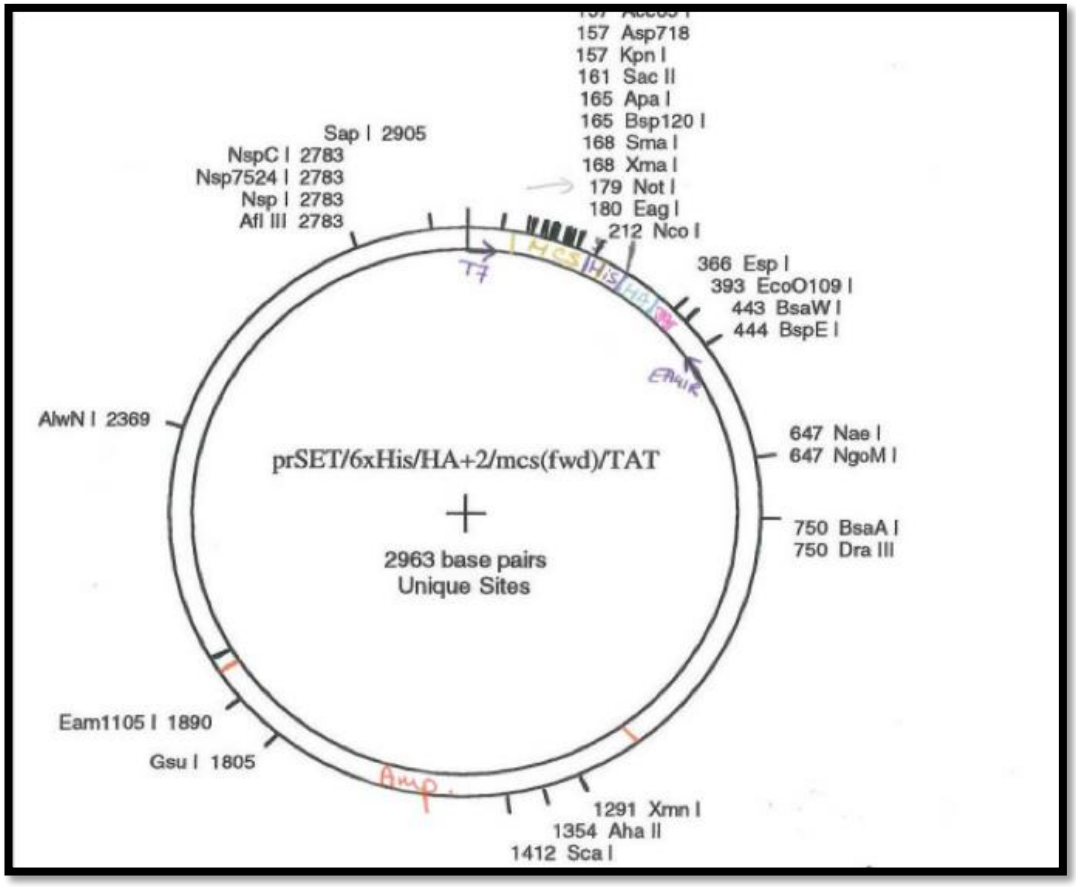

***Figure 10**. Construct of TAT-G6PD.*

Chapter 3. Results

Chapter 3.1: Protein 4.1

The erythrocyte membrane skeleton has been characterized in the past and its general role is to maintain the shape and mechanical properties of RBCs. Protein 4.1 is located in the membrane skeleton and interacts mainly with spectrin, actin, and protein p55 (1). The main function of protein 4.1 is stabilizing cell shape, and providing deformability and mechanical stability to the cell [28]. Protein 4.1 exists as two polypeptides: bands 4.1a and 4.1b are proteins of 80,000 and 78,000 molecular weight respectively. There is a close relation in the primary structure and function of the two polypeptides [29]. In most mammalian RBCs including human, protein 4.1 consists of a doublet of polypeptides, suggesting that post-translational modification of protein 4.1b to 4.1a is a common phenomenon in mammalian RBCs. The post-translation modification has been demonstrated to be a non-enzymatic deamidation process, which takes place at two asparaginyl residues of protein 4.1b. The deamidation at the 502nd asparaginyl residue occurs slowly changing it to aspartate and this is likely the reason for the conversion of 4.1b to 4.1a. It has been observed that protein 4.1a ratio to protein 4.1b increases with RBC ageing. Based on these premises' studies have been carried out to know more about the conversion of protein 4.1b to 4.1a.

Conversion of protein 4.1b to 4.1a in human erythrocytes incubated in vitro

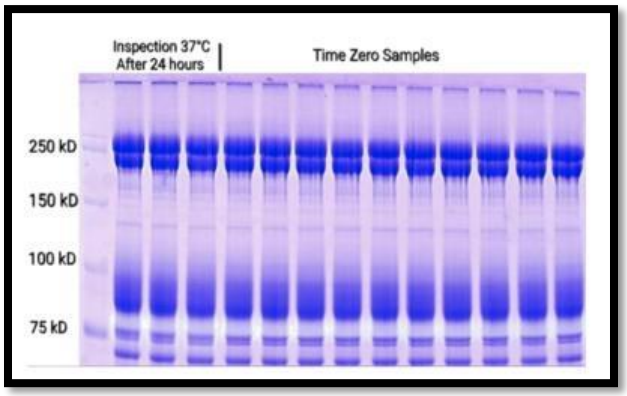

Figure 11. *Time Zero Samples treated and analyzed by SDS-PAGE to quantify protein 4.1a/4.1b ratio.*

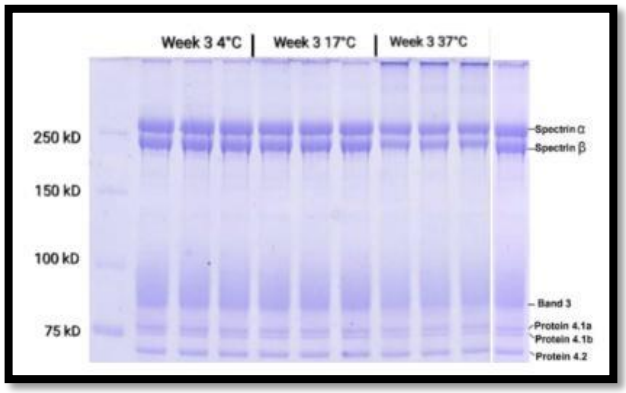

Figure 12. *Week 3 Samples treated and analyzed by SDS-PAGE to quantify protein 4.1a/4.1b ratio.*

Purified RBC membranes (prepared under sterile conditions) were incubated at 4°C, 17°C and 37°C. Samples collected every week, treated and analyzed by SDS-PAGE to quantify protein 4.1a/4.1b ratio. Time zero samples were also analyzed as shown in **Figure 11**. Samples stored at 37 °C showed

a progressive blurring of 4.1 bands and protein aggregates formation from Week 3 onwards as seen in **Figure 12**.

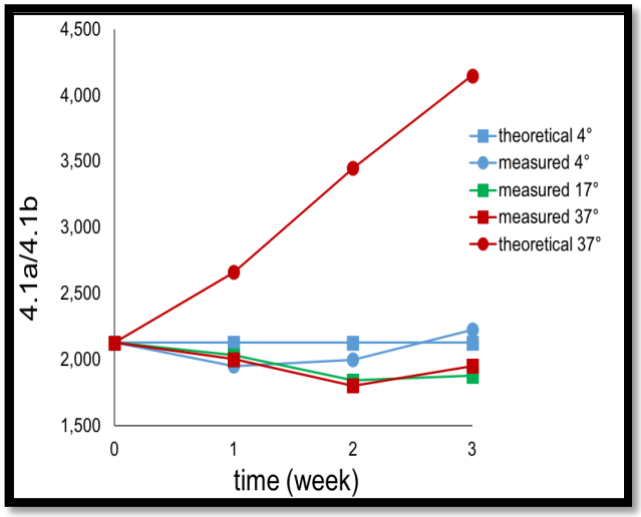

Figure 13. *Theoretical and observed 4.1a 4.1b ratios. The expected 4.1a/4.1b ratio was calculated on the basis of a model that assumes a half-life of 4.1b to 4.1a conversion of 41 days [3]. The 4.1a/4.1b ratio at 4 °C was not expected to change. For ghost incubated at 37 °C, there is a vast difference in the expected and measured ratios. The ratios could have been possibly affected by the aggregation of proteins and potential oxidation in samples stored over the course of the experiment. (**Refer to Figure 12**)*

The expected 4.1a/4.1b ratio shown in **Figure 13** was calculated on the basis of a model that assumes a half-life of 4.1b to 4.1a conversion of 41 days [3]. The 4.1a/4.1b ratio at 4 °C was not expected to change. For ghost incubated at 37 °C, there is a vast difference in the expected and measured ratios.

Confirming amino acid difference between the two isoforms

Studying by M.S. of native protein excised from SDS-PAGE gels

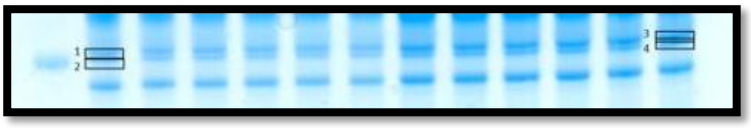

Figure 14. *Gel used for Mass Spectrometry analysis. Band 1= 4.1a, Band 2= 4.1b*

I used MALDI TOF analysis to confirm the sequences of the 2 isoforms of protein 4.1 and to see if it corresponds to previously known information about deamidation of specific amino acid residues.

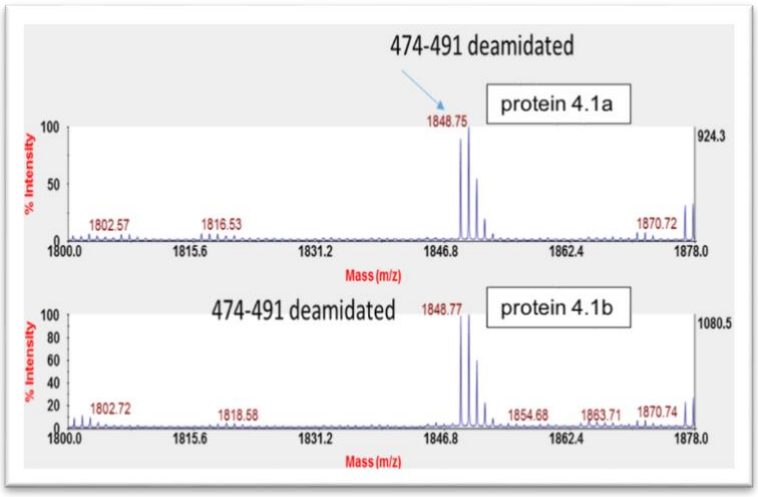

Figure 15. *MALDI TOF spectra of band 1 and 2 reporting peptide ranging from residue 474 to 491 (TLNINGQIPTGEGPPLVK)*

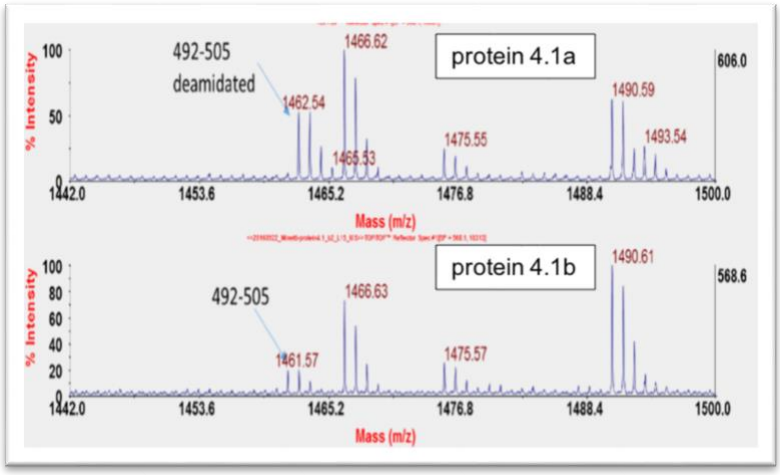

Figure 16*. MALDI TOF spectra of band 1 and 2 reporting peptide ranging from residue 492 to 505 (TQTVTISDNANAVK).*

MALDI TOF spectra of band 1 and 2 as seen in **Figure 15**, reporting peptide ranging from residue 474 to 491 (TLNI**N**GQIPTGEGPPLVK) in which the asparagine **478** is deamidated and this is compatible with the knowledge that both isoforms of 4.1 protein go through deamidation possibly co-translationally at residue 478 which is followed by Glycine, thus generating a sequence particularly suitable to Asn deamidation. MALDI TOF spectra of band 1 and 2 reporting peptide ranging from residue 492 to 505 (TQTVTISD**N**A**N**AVK) are shown in **Figure 16**. Both Asparagine residues are followed by Alanine. In band 1 sample it's evident that at least one of two Asn (500 or 502) is deamidated. Band 2 shows the presence of peptide 492-505 with m/z 1461.5 compatible with the presence the peptide without deamidation. It is known (1) that deamidation of residue 502 is the only

reason for difference in molecular weight of the two isoforms. However, we still need to confirm if deamidation involved Asn 500 or 502.

Studying synthetic peptides *corresponding to the human protein 4.1 sequence centered around Asn 502 (N = 492 to 505 TQTVTISDNA**N**AVK; D = TQTVTISDNA**D**AVK)*

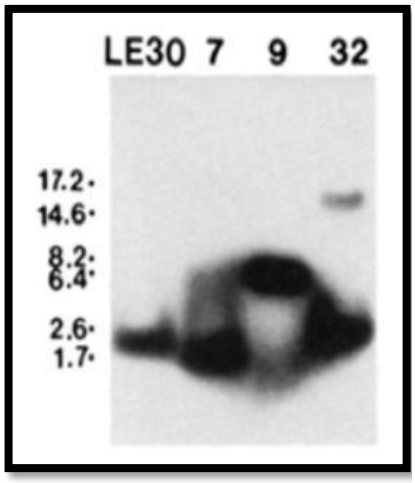

Figure 17. *In the upper part of the figure is the original figure reported in the paper of Inaba et al [2] in which by autoradiography, 502 was found to be responsible for the different mobility in SDS-PAGE of protein 4.1a and 4.1b. Shown here is a 20% acrylamide SDS-PAGE gel where Iodine labeled peptides resulted from proteolytic digestions of carboxyl-terminal fragments of protein 4.1. Similar experiments were repeated where LE7 corresponds to (N) and LE9 corresponds to (D) in* ***Figures 18-21****.*

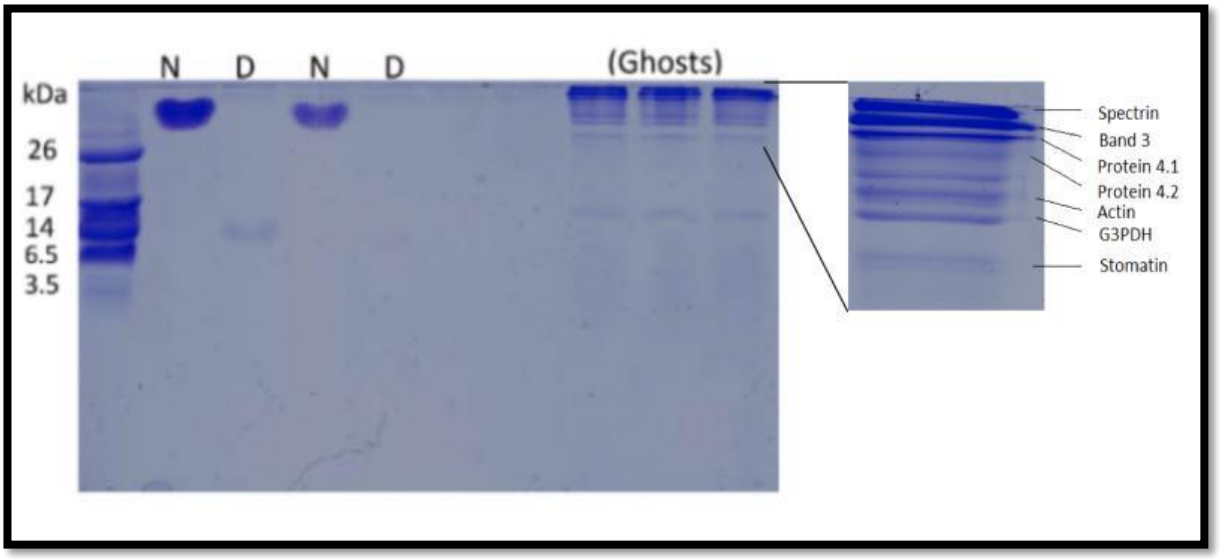

Figure 18*. Varying concentrations of synthetic peptides corresponding to LE7 (N) & LE9 (D) were loaded in a polyacrylamide gel at 20% acrylamide concentration and run with* ***Tris Tricine*** *buffer system. *N = 492 to 505 (TQTVTISDNA**N**AVK) D = TQTVTISDNA**D**AVK*

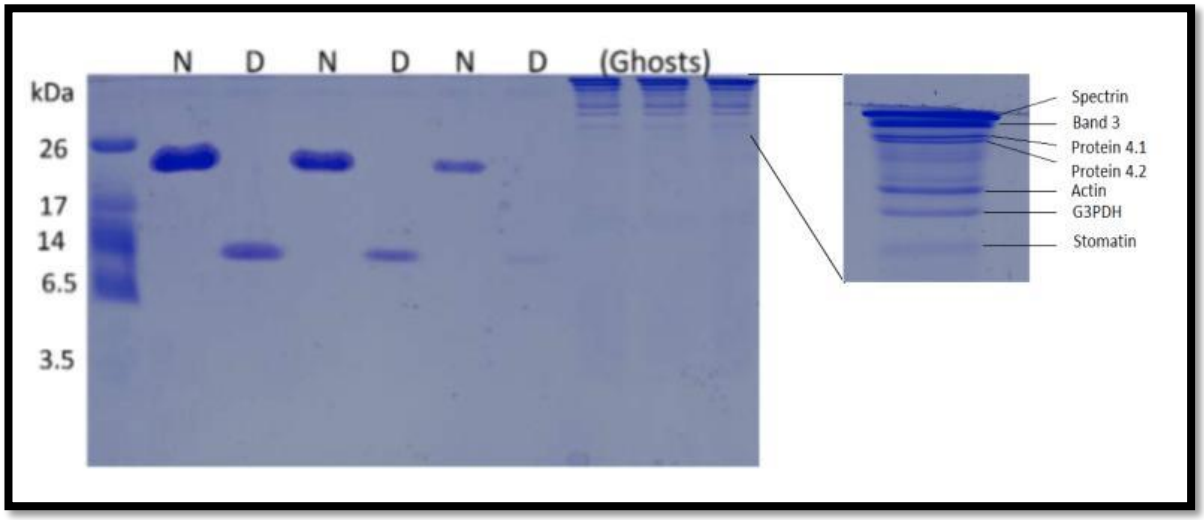

Figure 19*. Varying concentrations of synthetic peptides corresponding to LE7 (N) & LE9 (D) were loaded in a polyacrylamide gel at 20% acrylamide concentration and run with* ***Tris Glycine*** *buffer system. *N = 492 to 505 (TQTVTISDNA**N**AVK) D = TQTVTISDNA**D**AVK*

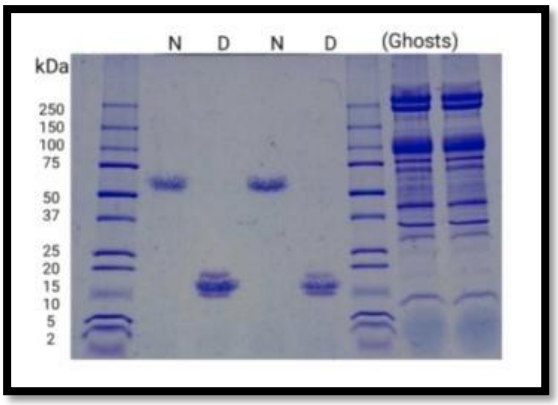

Figure 20*. Varying concentrations of synthetic peptides (2016) corresponding to LE7 (N) & LE9 (D) were loaded in a polyacrylamide gradient gel at 5- 20% acrylamide concentration and run with Tris Glycine buffer system.*

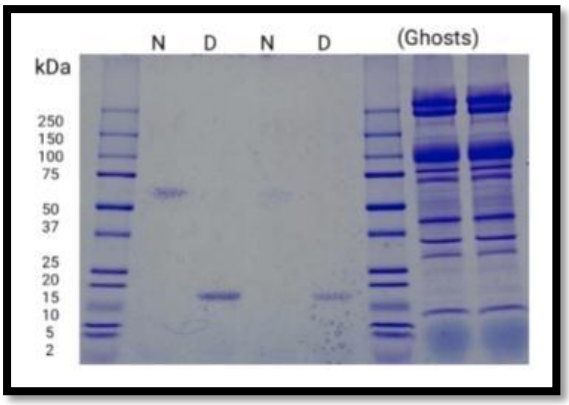

Figure 21. *Varying concentrations of synthetic peptides (2017) corresponding to LE7 (N) & LE9 (D) were loaded in a polyacrylamide gradient gel at 5- 20% acrylamide concentration and run with Tris Glycine buffer system.*

It is shown that even though the two peptides differ only by one amino group still result in a dramatic difference in the molecular mass of 2 kDa similar to native full protein when loaded on SDS-PAGE. Based on these results, two sets of identical synthetic peptides were obtained and run on gels to see the migration pattern. **Figure 17** taken from the original article [2] where 4.1a and 4.1b difference was investigated, LE7 corresponds to the peptide derived from protein 4.1b, and it contains Asn (N)

at position 502, as determined by direct sequencing. LE9 corresponds to the peptide derived from protein 4.1a, and it contains Asp (D) at position 502.Figure 18 and 19 (20% acrylamide concentration) show the migration of peptides in Tris Tricine buffer and **Figure 20 and 21** (5%-20% acrylamide concentration gradient gel) show the migration in Tris Glycine buffer. The peptides do not migrate in the manner expected. Both peptides migrate with an apparent mass larger than expected and peptide D was expected to migrate with an apparent molecular mass higher than N but the results do not conform the expected results. The reason was not clarified however a possible explanation could be that, despite the denaturing conditions, larger aggregates of peptide N are formed in comparison to peptide D, therefore resulting in migration at a higher molecular mass.

CD Measurements of peptides (carried out at University of Parma)

In order to investigate possible effect of deamidation on secondary structure, we carried out the circular dichroism spectra of the two peptides in the far UV range.

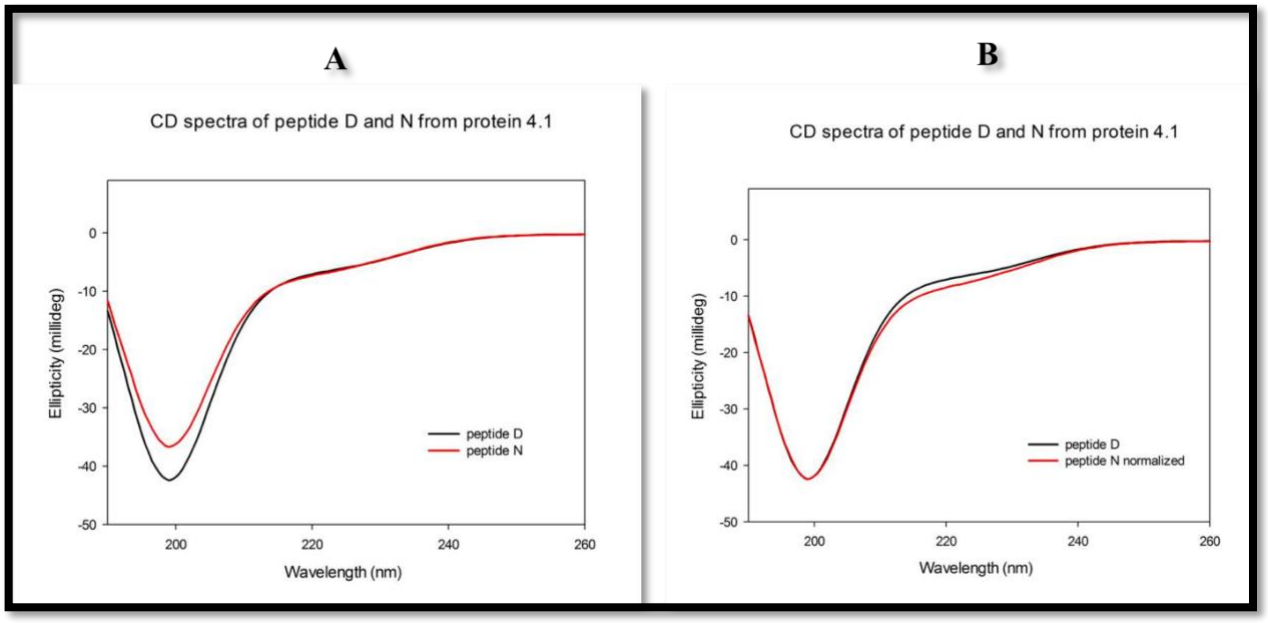

Figure 22. *Analysis of CD spectra of peptide N & D corresponding to the human protein 4.1 sequence centered around Asn 502. Peptide D: TQTVTISDNA**D**AVK, Peptide N: TQTVTISDNA**N**AVK. Spectra on the left **(A)** are the original spectra of peptide D & peptide N. Spectra on the right **(B)** are of peptide D and normalized peptide N.*

Results indicate that the peptides are mainly unstructured and that no striking difference appears between peptide N & D. Since peptide N might be slightly less concentrated than peptide D due to its lower solubility (3-4 little particles of undissolved peptide in a volume of 20 ml were visible), or

order to compare the spectra, a scaling factor was applied so that the two spectra have the same minimum. This allows to compare the two spectra (right panel), which are very similar (same secondary structure of peptide D & N. The analysis of the data was carried on using peptide D, peptide N (left panel) = and normalized peptide N (right panel) data. Results suggest that the peptides are mainly unstructured and peptide N & D show no striking difference.

Neocytolysis study

According to the theory of Neocytolysis [36], erythropoietin (EPO) stimulates the production of RBCs as well as protects young RBCS (neocytes). When there is a decline in plasma EPO, it results in selective clearance of neocytes. It has been suggested that rapid RBC mass reduction occurs in people descending from high altitude where the RBC mass increased as an adaptation to hypoxia. Upon return to sea level, neocytes are cleared selectively [167]. The following results are from experiments set up to detect disappearance of a few percent of younger RBCs from the blood of subjects that were healthy donors. These experiments were set up to mimic what would happen when erythrocytes are exposed to conditions of neocytolysis such as high-altitude hypoxia. Blood was fractionated according to density as shown in **Figure 23**. Purified "ghost" membranes were prepared from each of the three subpopulations of different age as well as reconstituted samples (R3 and R2) R3: The three populations of RBCs were mixed back together but with less young cells than in the original blood (e.g. 8% instead of 12.9%). R2: Only middle-aged and old RBCs were mixed back, no young cells, to mimic a condition of neocytolysis (disappearance of young RBCs). Young erythrocytes are found in the top most layer of Percoll following centrifugation.

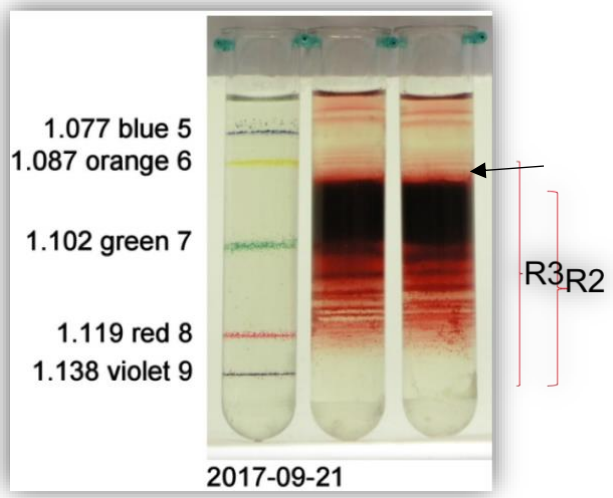

Figure 23. *Erythrocytes from donors were separated according to density in self-forming Percoll gradients. RBCs from normal donors were separated into 3 fractions: light (young), intermediate (middle-aged) and dense (old). Young RBC population is marked by an arrow in the figure.*

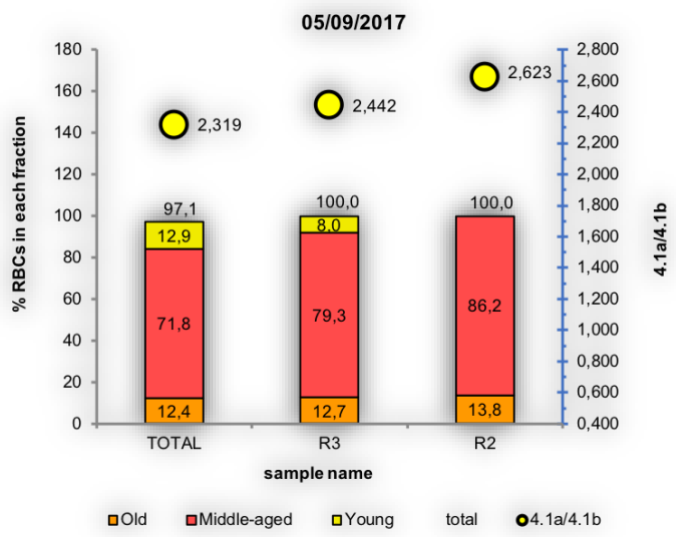

Figure 24. *Representative* ***reconstitution*** *experiment of erythrocyte subpopulations and quantification of the 4.1a/4.1b ratio in the reconstituted samples. The 4.1a/4.1b values are represented by yellow circles above the histogram.*

Figure 24 shows the results obtained from the first experiment. The measured 4.1a/4.1b value of the total population of RBCs was 2.319. Reconstituted (R3) in which young cells were less than in the original blood (8% instead of 12.9%). Similar results were obtained in the subsequent experiments, shown in Figure 25 below.

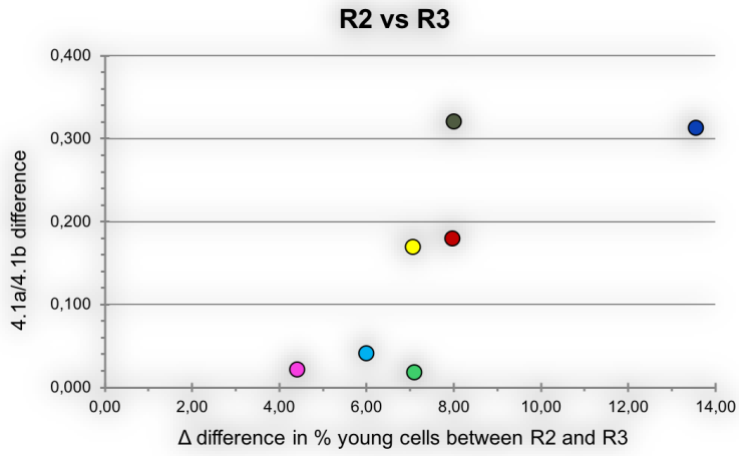

Figure 25*. Difference in the number of young cells between R3 and R2 samples and corresponding difference in the 4.1a/4.1b ratio as measured in 7 independent* ***reconstitution*** *experiment.*

From the results shown in **Figure 23, 24 and 25**, it was concluded that the experimental methodology was suitable for the detection of the disappearance of neocytes from the blood of subjects that are exposed to conditions of enhanced neocytolysis. These preliminary results shed light on the research approach of mimicked neocytolysis and provided a foundation for another project in collaboration with a few partner labs. An independent project named "Neocytolysis: Quantification, characterization, and mechanisms of the destruction of newly formed erythrocytes upon return from high altitude" was then carried out separately.

4.1a/4.1b ratio comparison between ghosts prepared using different buffers

Purified RBC membranes (ghosts) are prepared for protein 4.1a/4.1b quantification by hemolysing the cells by hypotonic buffer followed by centrifugation and running samples on SDS-PAGE gels. Ghosts were prepared in different buffers and it was of interest to check if the two buffers result in variation of 4.1a/4.1b ratio. It is always important to be updated and try different buffers in order to find the best human red blood cell lysis buffer. The two buffers used were adapted from past research and seem to be the most commonly used RBC lysis buffers [168, 169]. **D**: Ghosts prepared in Dodge Buffer *(Hypotonic Phosphate Buffer (25mM Sodium Phosphate Monobasic Monohydrate, pH 7.4 at 4°C)* **T**: Ghosts prepared in Tris Buffer *(Hypotonic Tris buffer (5 mM Tris, 5 mM KCl, pH 7.4 at 4°C)*

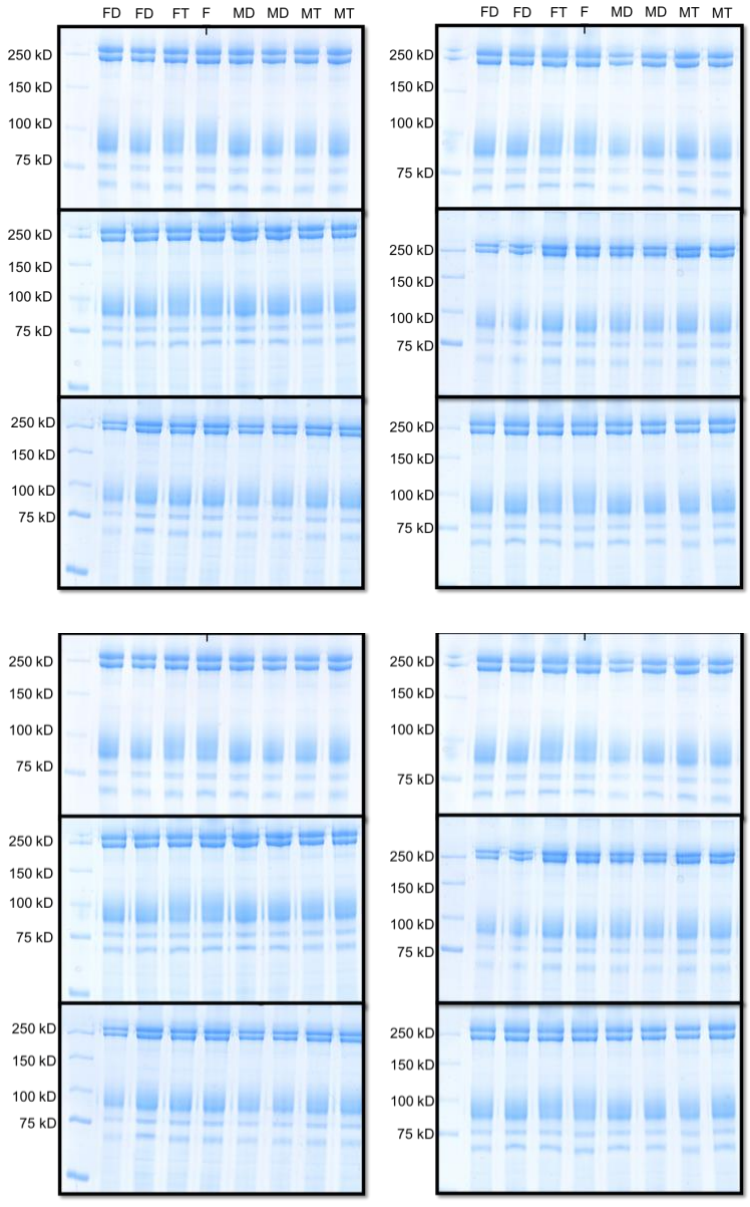

Figure 26. *Ghost samples from the same experiments were loaded on SDS-PAGE gels in duplicates: Female Dodge (FD), Female Tris (FT), Male Dodge (MD), Male Tris (MT).*

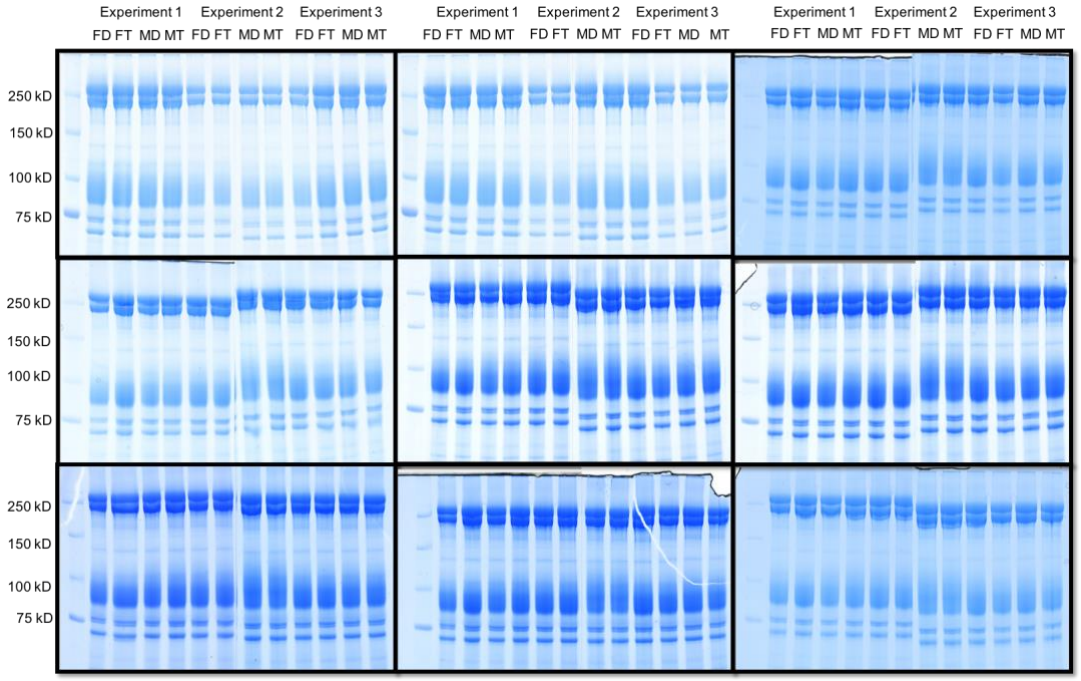

Figure 27. *Ghost samples from three different experiments were loaded on large SDS-Page gels: Female Dodge (FD), Female Tris (FT), Male Dodge (MD), Male Tris (MT).*

The samples were first run on small gels as shown in **Figure 26** and later run on large gels shown in **Figure 27** hoping to get a better separation for 4.1a/4.1b ratio.

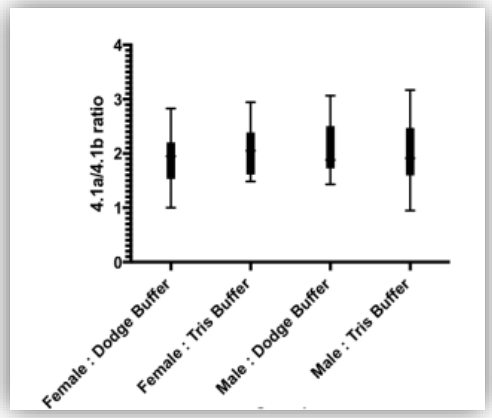

Figure 28. *Protein 4.1a/4.1b ratios from small gels shown in Fig 26.*

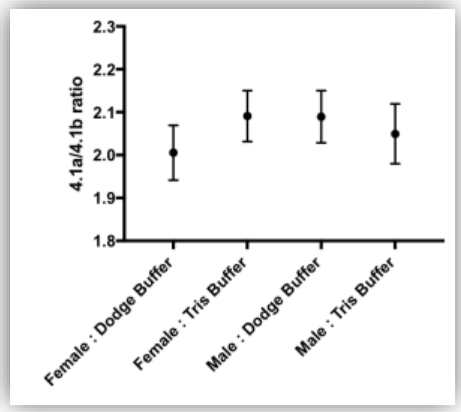

Figure 29. *Protein 4.1a/4.1b ratios from large gels shown in Fig 27.*

No significant difference in the ratio of protein 4.1a/4.1b was observed between the ghosts prepared using different buffers as shown in **Figure 28 and 29**. Two-way ANOVA was used to analyze results. These results suggested the buffer used to prepare ghosts did not introduce any substantial modification in the observed protein ratio between 4.1a and 4.1b.

4.1a/4.1b ratio: Healthy donors and patients

Protein 4.1a/4.1b ratio correlates to the mean erythrocyte life span [48]. The ratio has been reported to differ in membrane skeleton defects in erythrocytes [31]. It was therefore of interest to compare the ratio of ghosts prepared from HS, HE, SCD patients [31, 37] as well as healthy donors. No information on the ongoing treatment of the patients was obtained. Moreover, 4.1a/b measurements were also conducted by Western blotting as shown in **Figure 30**, to increase sensitivity.

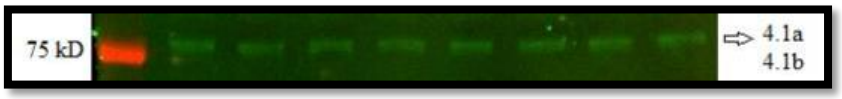

Figure 30. *Western Blot of 4.1 ratio. The gel needed to run for longer time as separation is not clear between the two bands.*

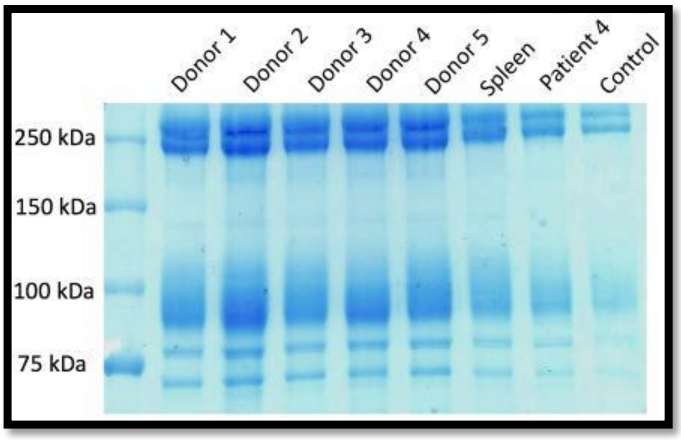

Figure 31. *Ghost samples prepared from healthy donors, spleen of a healthy donor, patient (unknown defect) and control blood samples were loaded on SDS-PAGE gel. Control sample was acquired from year 2016 acquired from the diagnostic group.*

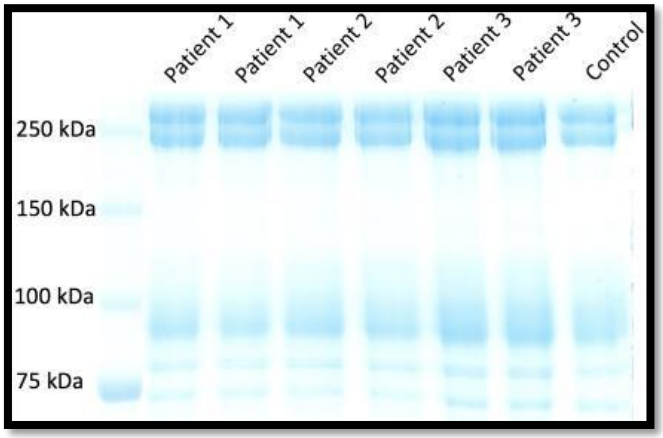

Figure 32. *Ghost samples prepared from patients (patient 1 & 2: HS, patient 3: HE) and control blood samples were loaded on SDS-PAGE gel. Control sample was from year 2016 acquired from the diagnostic group.*

Protein 4.1 study was continued during a secondment at Sanquin to check the difference in the ratio between healthy donors and patients with membrane skeleton defects in erythrocytes.

Flow cytometry results in **Figure 33** confirm experimental aging, however the samples once run on SDS-PAGE gels appeared as smears as visible in **Figure 34** and were not usable for quantification of 4.1a/4.1b ratio.

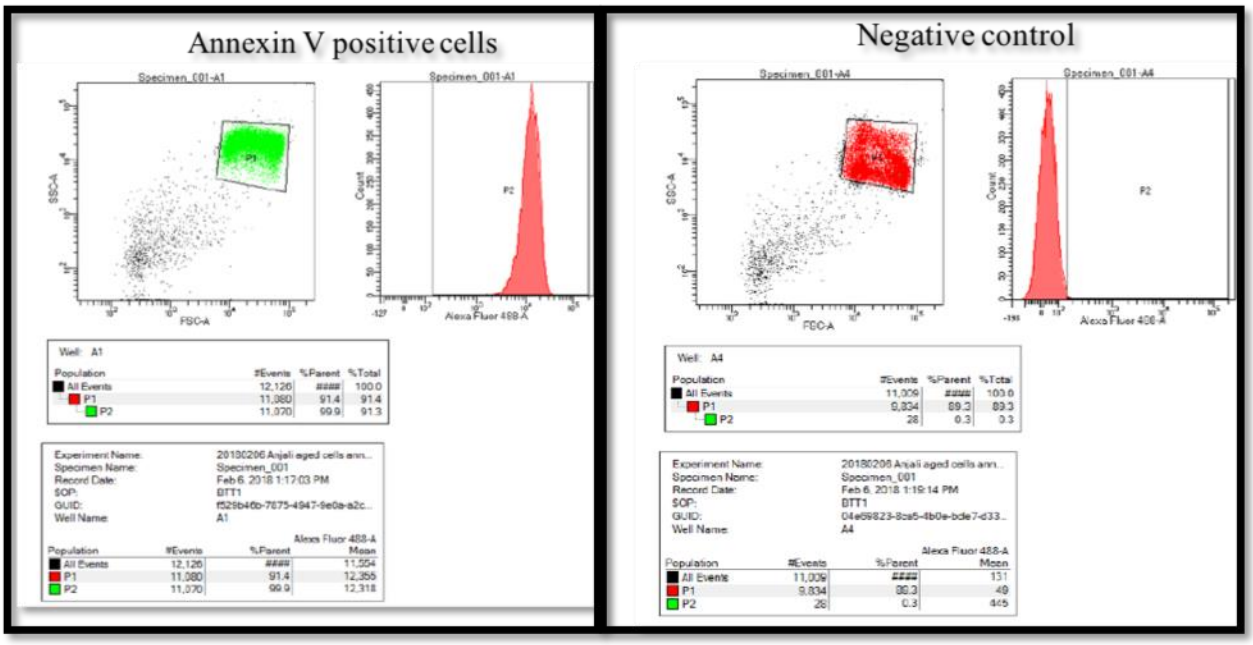

Figure 33. *Flow Cytometry results to confirm experimental aging of erythrocytes. Annexin V was used for copper induced apoptosis detection*

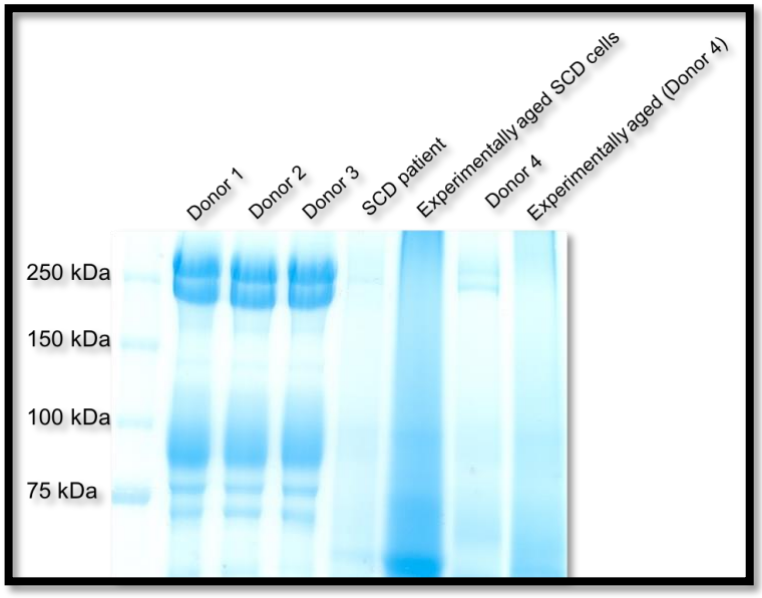

Figure 34. *SDS-PAGE gel of ghosts prepared from donors and experimentally aged red blood cells from sickle cell disease patient and healthy donor. The experimentally aged cells did not however run clearly on the gel; therefore, the ratio was not quantified.*

The gels shown in **Figure 31 and 32** were used to quantify 4.1a/4.1b ratio in healthy donors as well as patient blood samples. The results of protein 4.1a/4.1b ratios are shown in **Figure 35**.

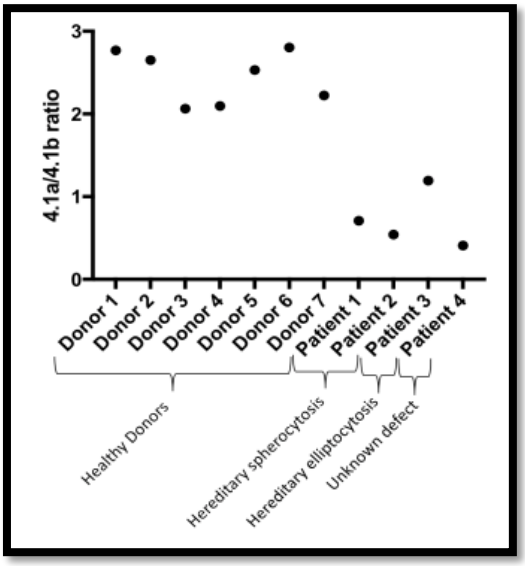

Figure 35. *Observed 4.1a 4.1b ratios from healthy donors as well as patients to see a difference. A clear difference between the ratio is observed.*

Figure 35 show observed protein 4.1a/4.1b ratio to be significantly lower in patients with hereditary elliptocytosis and hereditary spherocytosis. The results were analyzed by two-way ANOVA.

Conclusion on the results obtained from the project "band 4.1 in human erythrocytes"

Deamidation of protein 4.1 of the erythrocyte membrane skeleton was studied on the natural protein as well as on synthetic peptides. In the very early experiment where ghosts were incubated and treated every week, the expected 4.1a/4.1b ratio was calculated on the basis of a model that assumes a half-life of 4.1b to 4.1a conversion of 41 days. The 4.1a/4.1b ratio at 4 °C was not expected to change. For ghost incubated at 37 °C, there is a vast difference in the expected and measured ratios. The ratios could have been possibly affected by the aggregation of proteins and potential oxidation in samples stored over the course of the experiment. The two synthetic peptides N & D adapted from the original study by Inaba et al, when run on gels did not migrate in the manner expected. For further analysis of the peptides, CD measurements were carried out and no striking difference appeared between the two peptides. With further experiments, on the basis of the obtained results of the neocytolysis study, it was concluded that the method was suitable for the detection of the disappearance of a few percent of younger RBCs from the blood of subjects that are exposed to conditions where neocytolysis can

develop. These results were used as a basis for a separate study. The ratios were also checked for ghosts prepared under different conditions such as using different hypotonic buffers. No difference between 4.1a/4.1b ratios of ghosts prepared using the two buffers was observed from the ratios acquired from small gels as well as in large gels. The comparison of ratios observed among the ghosts prepared from male and female blood samples are negligible, with only a slight difference. It can be concluded that the buffer used to prepare ghosts does not affect the ratios. Protein 4.1 study was continued during one of the secondments. During secondment at Sanquin, membranes were prepared from fresh donor blood available locally as well as stored membranes prepared from disease patients. The ratio was observed to be significantly lower in patients with hereditary elliptocytosis and hereditary spherocytosis. As mentioned earlier, both proteins 4.1a and 4.1b are deficient in hereditary elliptocytosis patients (either heterozygous or homozygous). Comparison of the ratios between healthy donors and patients with defective membrane skeleton sheds light on the correlation of protein 4.1 with other proteins of the membrane skeleton. Within the partnership, quantification of 4.1a/4.1b ratio is being used to investigate changes imparted on RBCs by sport and exercise, or of the properties of RBCs from subjects exposed to peculiar environmental conditions such as high-altitude hypoxia. The primary aim of this project was to provide comprehensive knowledge of protein 4.1 which has been classified as the best erythrocyte aging marker. Deamidation is a common reaction that takes place in a time-dependent manner at physiological temperature and pH and there are high chances that it modifies other proteins too. Therefore, further investigation of the role of deamidation of 4.1 in function and catabolism is vital to get a deeper understanding of red blood cell physiology.

Chapter 3.2: Animal Erythrocytes

Erythrocytes differ between different species in terms of the number of cells per ml, shape, lifespan and metabolism. As part of the research project, animal erythrocytes were studied at the Veterinary Institute at the University of Zurich to gain familiarity on characteristics and morphology of erythrocytes from different animals. The work depicted here was designed to investigate aging markers in equine, bovine, feline and canine red blood cells. It was of interest to compare animal and human erythrocytes due to differences in morphology, metabolism and hematopoietic activities. From literature search, it was known that equine blood lacks cells carrying reticulocyte markers such as RNA remnants or CD71 in the circulation [170], and canine erythrocytes lack sodium-potassium pump [171]. With some prior information and curiosity to find more, animal erythrocytes were fractionated into low, medium and heavy density fractions for analysis of markers of aging such as membrane loss, oxidation band 3 abundance and alterations in the intracellular free Ca^{2+}.

Erythrocyte Morphology

Erythrocytes of animals were observed under the microscope at 1000 times magnification to become familiar with the appearances of normal red blood cells reported in Figure 36.

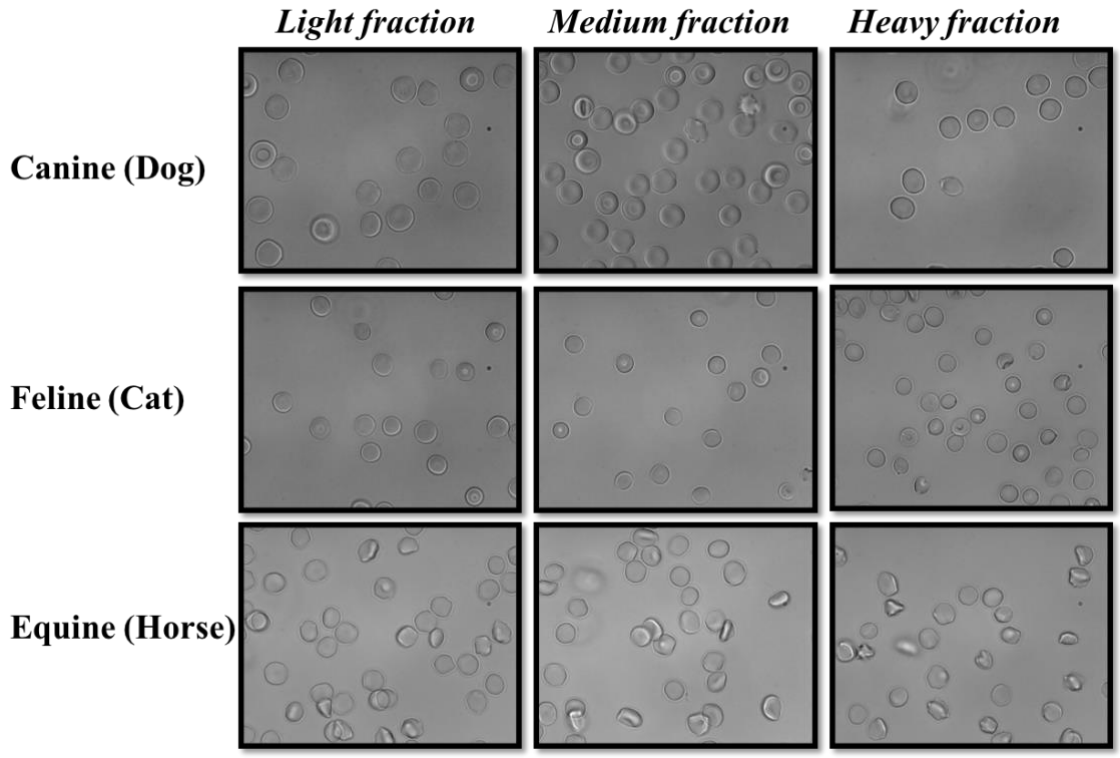

Figure 36. *Erythrocytes from Light, Medium and Heavy fractions of canine, feline and equine blood (1000 X magnification).*

Figure 36 highlight that canine erythrocytes have a prominent central pallor which is visible in the images. Canine erythrocyte appears to be a large, uniform and biconcave disc. Feline erythrocyte seem to be much smaller and more variable in size as compared to canine cells. Equine erythrocytes appear to be of similar size as feline erythrocytes and also lack central pallor.

Camel erythrocytes are reported to be peculiar in shape as compared to other animals. Therefore, the morphology was checked but cells were not studied in detail. Camels have erythrocytes that are small, flat and oval-shaped, as clearly visible in **Figure 37**. As known from literature, the red blood cells of camels protect it from dehydration because the oval-shaped cells can circulate even in thick blood and can significantly expand during rehydration [172].

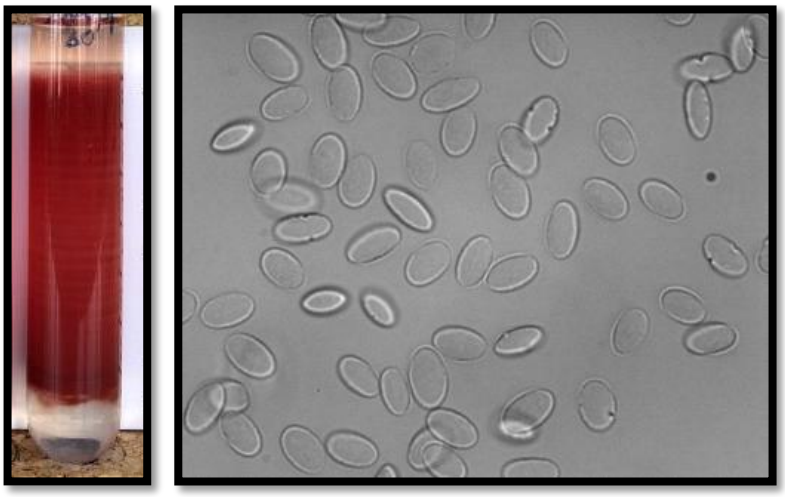

Figure 37. *Gradient Separation of Camelid erythrocytes (90% Percoll, 32-34 °C ,20,000 g, 30 minutes) and an image under the microscope with 1000 times magnification.*
The separation is not ideal as the blood was obtained six days prior to the separation.

During the first secondment at the Veterinary Institute in Zurich, equine and bovine erythrocytes were studied. Canine as well as feline erythrocytes were studied during the second secondment. The animals were selected due to some known peculiarities in the morphology or biochemistry of the erythrocytes. Erythrocytes obtained locally were characterized from the point of view of the cell age distribution by means of gradient separation in subpopulations of different density. Erythrocytes from different density/age were characterized by measurements of ions (Na^+ & K^+), water, ATP, redox balance, EMA binding, CD71 levels, intracellular Ca^{2+} levels, SDS-PAGE of erythrocyte membranes aiming at measuring the ratio between a and b isoform of protein 4.1 as a cell age parameter. Before analyzing markers of aging in different fractions of erythrocytes, Percoll separation was perfected by trying several conditions. **Figure 38** show a few conditions of Percoll separation for both equine and bovine erythrocytes.

Gradient Separation of Equine and Bovine Erythrocytes

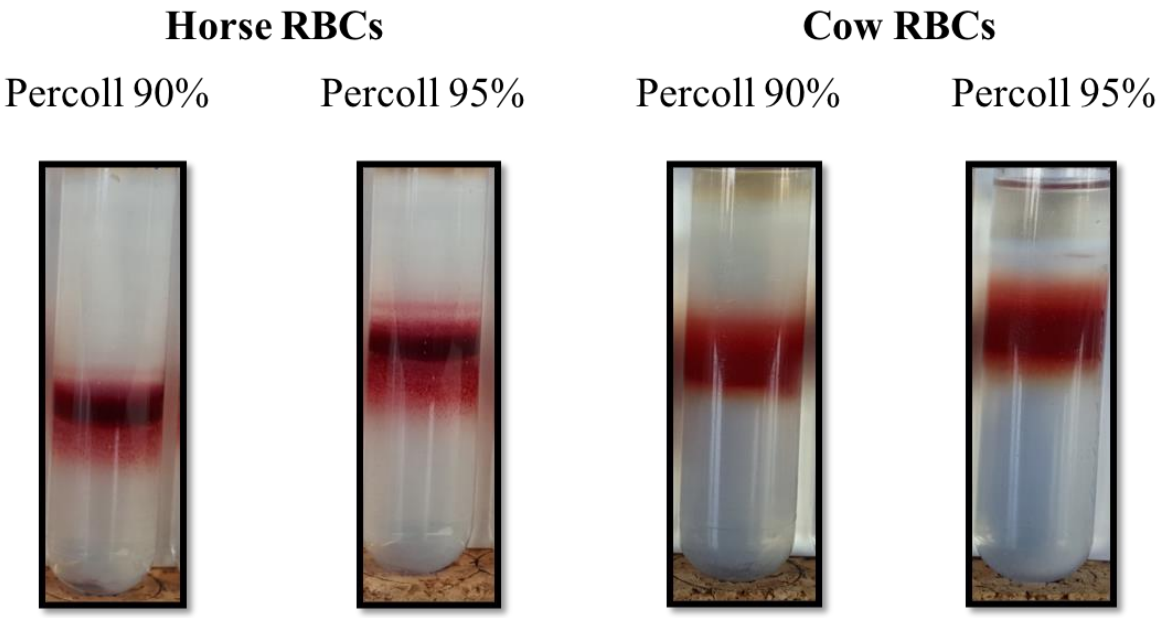

Figure 38. *Gradient Separation of equine and bovine erythrocytes using different Percoll % centrifuged at 32-34 °C , 26,000 g, for 20 minutes.*

The distribution of the RBCs of equine and bovine erythrocytes in the Percoll gradient as seen in Figure 38 is used to calculate the proportions of the low-density fraction (youngest cells) and the high-density fractions (old and damaged cells). Various different conditions were tried and tested to get the best separation for animal erythrocytes. The best conditions were chosen for further experiments. Generally speaking, the low-density fraction holds the youngest cells while the high-density fractions contains the old and damaged cells. Different Percoll %, temperature and centrifugation speed were tried to get the optimal separation. The aim was to prepare 'ghosts' from different fractions of erythrocytes and run on SDS-PAGE gels in order to get 4.1a/4.1b ratio and compare it to human results obtained at the University of Pavia.

The gels shown in **Figure 39 and 40** were run in Zurich with the ghost samples prepared from Bovine and Equine erythrocytes respectively. The samples prepared during the secondment did not include dithiothreitol (DTT), hence making these native gels.

SDS-Page Gels

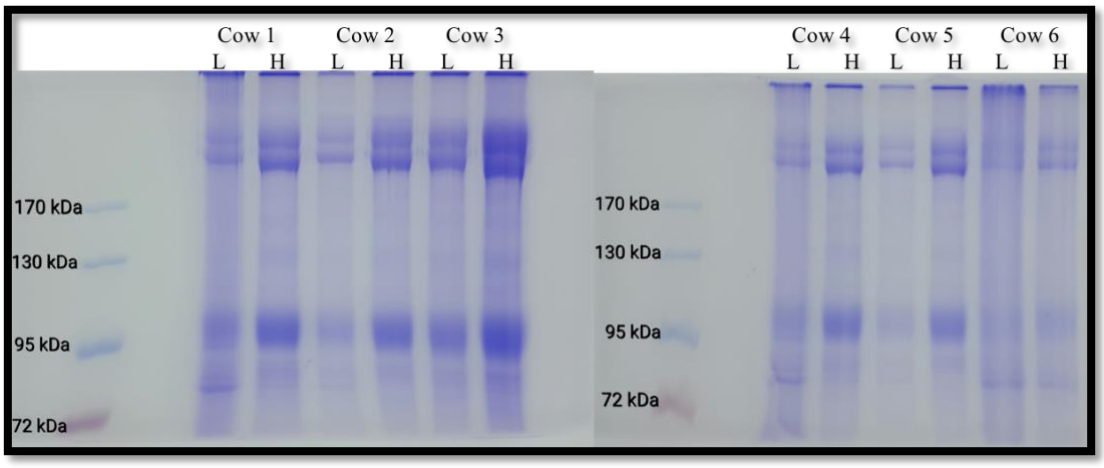

Figure 39. *SDS-Page Gels of erythrocyte membranes prepared from 'Light' & 'Heavy' fractions of bovine erythrocytes.*

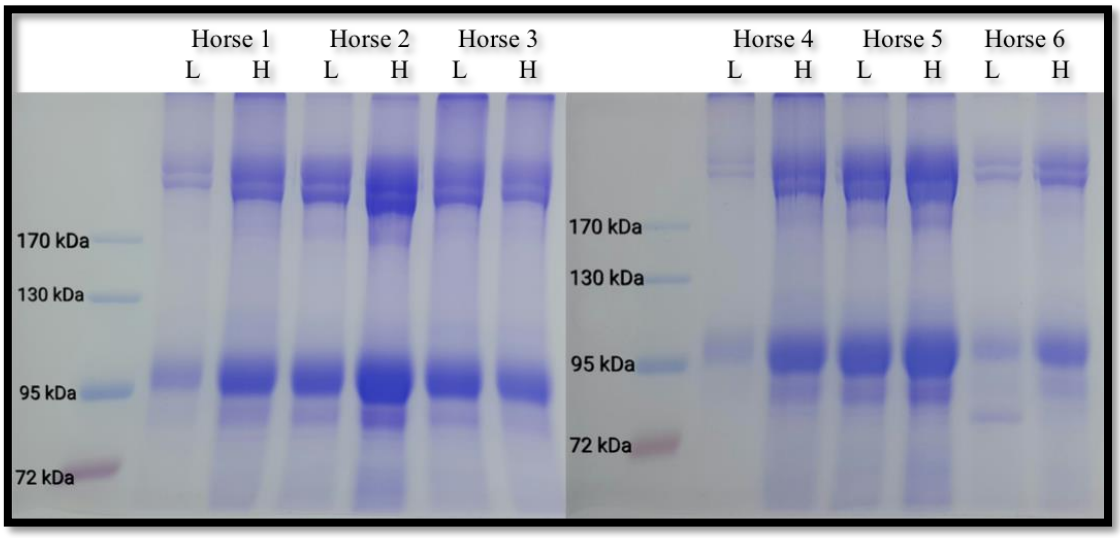

Figure 40. *SDS-Page Gels of erythrocyte membranes prepared from 'Light' & 'Heavy' fractions of equine erythrocytes.*

The gels run in Zurich did not show separate protein 4.1a and 4.b bands, therefore, DTT was used for removing the last traces of tertiary or quaternary structure. Gels were repeated after this treatment at the University of Pavia. However, separation was still not possible as seen in **Figure 41**.

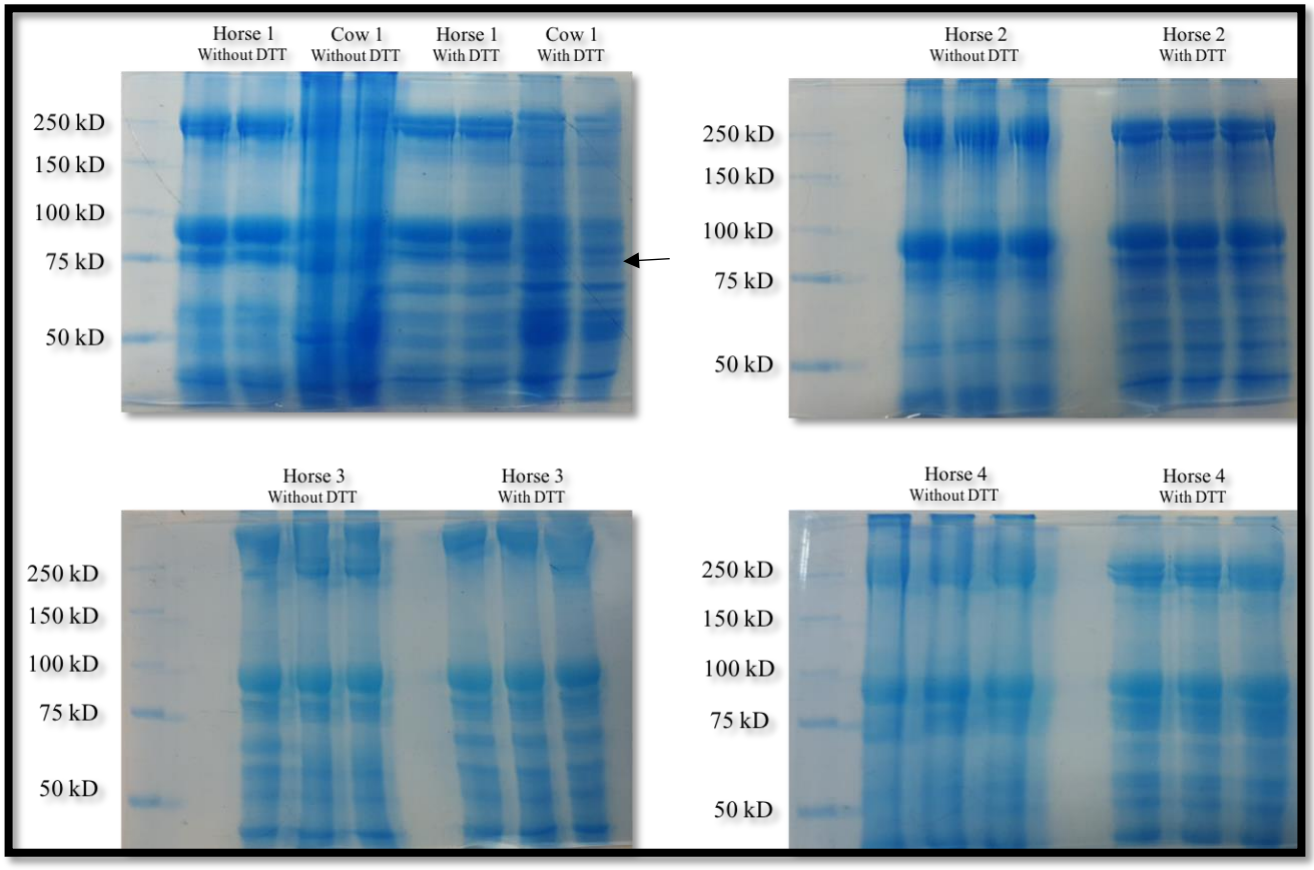

Figure 41. *SDS-Page Gels of equine and bovine erythrocyte membranes prepared from 'Heavy' fractions run without DTT and with DTT (added immediately before loading), samples heated for 15 minutes at 60°C. DTT: 0.156g + 1ml dH_2O (1M)*

The gels in **Figure 41** therefore, show a general profile of the different proteins present in the skeletal membranes of bovine and equine erythrocytes. Protein 4.1a and 4.1b separation was not at all clear and could not be quantified however in the separation of bovine erythrocytes show presence of two extra bands compared to equine erythrocytes (see arrow in Figure 41). This could be due to phosphorylation of the protein in bovine erythrocytes as reported by Riechers et al [173].

Parameters of aging in animal RBCs

Erythrocytes from different animals were isolated and separated into light, medium and high-density fractions on Percoll gradients to study several parameters and red cell aging. Not many studies are available on animal erythrocytes aging. Therefore, most of the knowledge gained from these experiments was novel and not much was available in literature apart from the facts that horses do not have circulating reticulocytes and that dog cells lack a sodium-potassium pump therefore the cells are sodium loaded.

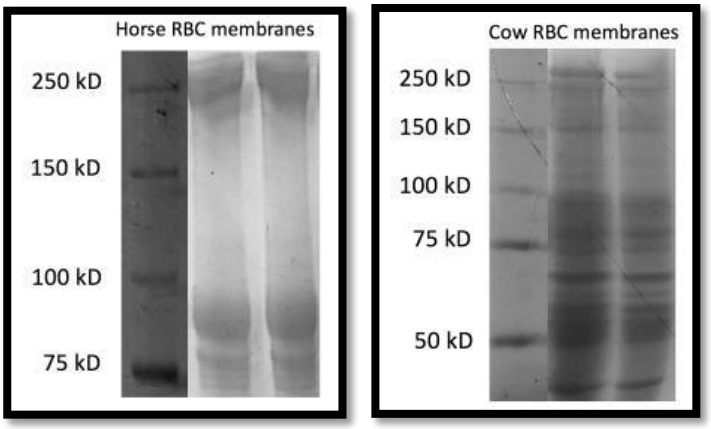

Figure 42. *SDS-Page Gels of equine and bovine erythrocyte membranes prepared from 'Heavy' fractions with DTT. Protein 4.1 ratios still not quantifiable.*

As a known accurate marker of ageing, protein 4.1a/4.1b ratio was tried to be quantified but was not attained. **Figure 42** is adapted from the gels shown in **Figure 41** where gels were run after sample treatment with DTT.

I have then measured the potassium and sodium concentration in separated equine and bovine erythrocytes because they are identified markers of ageing [174]. Results are reported in **Figure 43**.

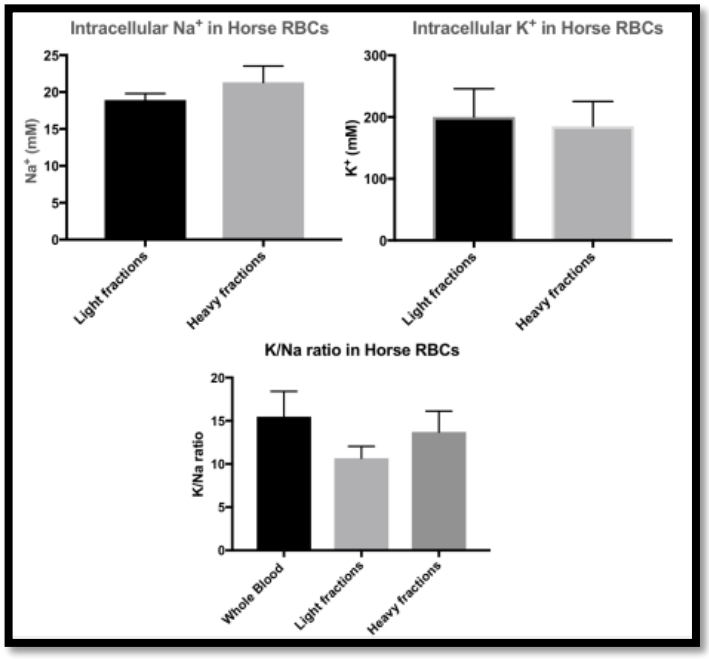

Figure 43. *Measurements of Potassium and Sodium ions in light and heavy fractions of equine and bovine erythrocytes.*

Sodium and potassium levels fluctuate between young and old cells as seen in **Figure 43**. Low sodium and high potassium concentrations were present in young RBCs while compared to old RBC in horse and cow erythrocytes. This complies with the expected results as ageing decreases the activity of Na-K-ATPase, thus the sodium-potassium pump weakens with age resulting in reduction of ion transport across the membrane.

Several other known markers of ageing were studied including ATP, Band 3, Transferrin receptor and PS [17].

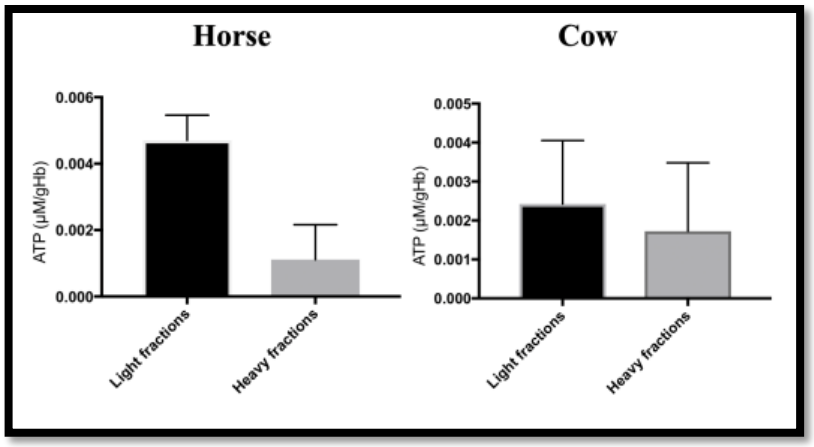

Figure 44. *ATP measurements in light & heavy fractions of equine and bovine erythrocytes.*

With time and age, the cellular processes weaken and the ATP levels reduce which is observed in the measurements where reduction of ATP can be clearly observed in older cells in both equine and bovine erythrocytes shown in **Figure 44**.

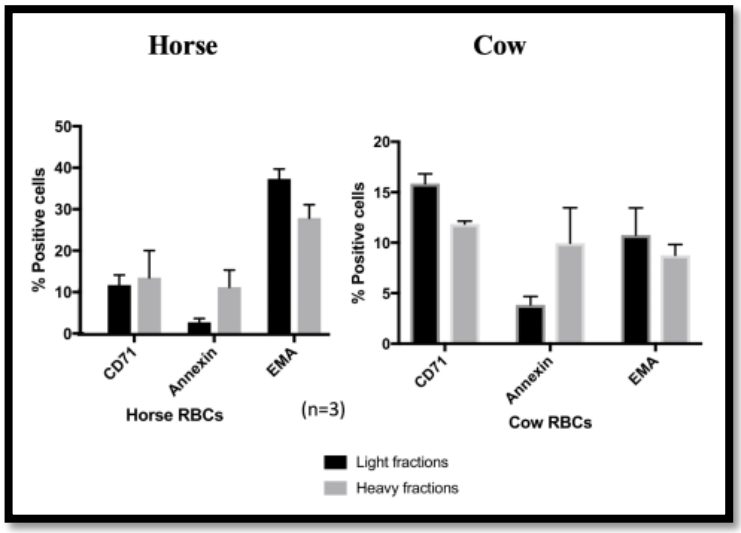

Figure 45. *Band 3, Transferrin receptor, PS measurements in light and heavy fractions of equine and bovine erythrocytes.*

The vesicles shed by the aged red blood cells result in higher PS exposure were quantified by Annexin V staining for both equine and bovine erythrocytes. Band-3 clustering/breakdown occurs in aged cells which follows the results observed. CD71 is slightly elevated in older equine erythrocytes and reduced in older bovine erythrocytes. The results represented in **Figure 45**, therefore follow the trend of these markers of ageing.

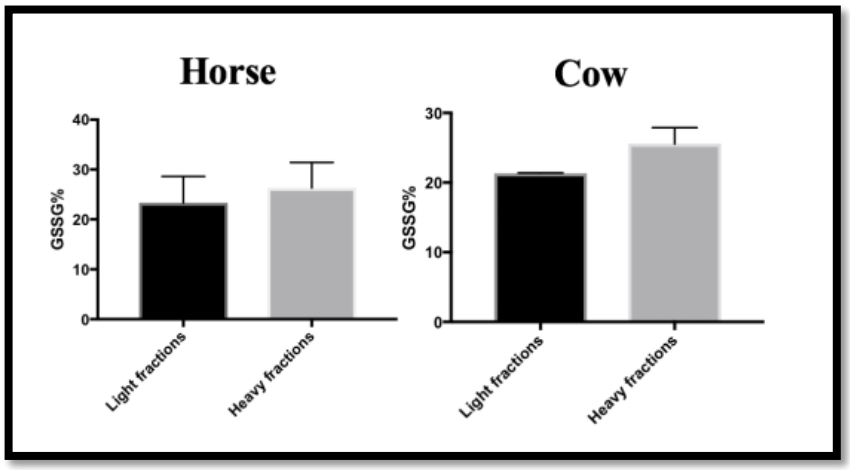

Figure 46. *Oxidative stress measurements in light & heavy fractions of equine and bovine erythrocytes.*

Figure 46 shows an Increase in oxidative stress is observed in both equine and bovine older erythrocytes.

During the secondment scheduled in 2018 at the Veterinary Institute of University of Zurich, canine and feline erythrocytes were available on a daily basis. Therefore, experiments were designed to study erythrocytes of these two species in detail.

Gradient Separation of Feline Erythrocytes

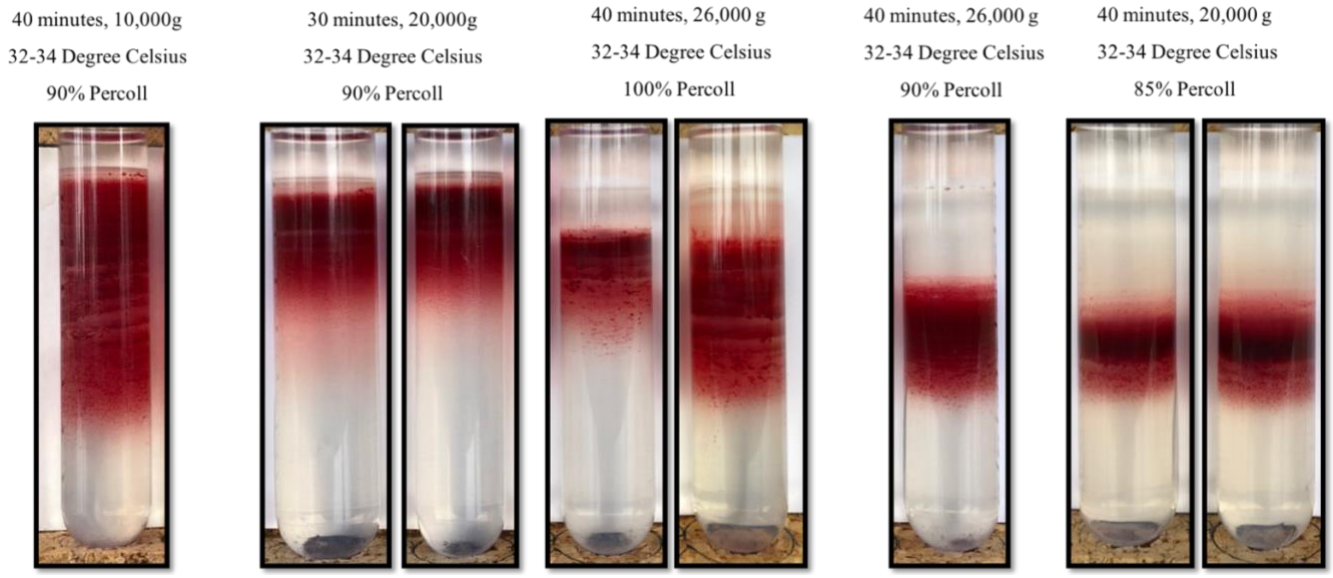

Figure 47. *Density separation of Feline erythrocytes trying different Percoll concentration as well as different centrifugation conditions.*

Various different conditions were tried and tested as shown in **Figure 47** to get the best separation for **feline erythrocytes**. The best conditions were chosen for further experiments shown later. Both feline and canine erythrocytes were to be studied during the second secondment therefore characterization of both were carried out simultaneously.

Gradient Separation of Canine Erythrocytes

Several conditions were tried for separation of **canine erythrocytes** for further experiments. Canine and feline erythrocytes were of great interest as at the institute several pets are checked on a regular basis and therefore people are more willing to get treatments as well as follow up check-ups. Medical records of these animals were not obtained as this was meant to be a blind study. However, records of patient reference number were kept for correlating in future. The biochemistry of canine erythrocytes was therefore of great interest. The main problem to overcome was hemolysis. Due to the recurring hemolysis, most of the time was spent on canine erythrocytes. A few steps were incorporated in the protocol to avoid hemolysis such as adding Bumetanide and Amiloride. **Figure 48** show different conditions of Percoll separation in the presence and absence of Bumetanide and Amiloride. **Figure 49** below show the separation with and without Amiloride, however a new buffer designed specifically for canine erythrocytes was used for these separations. Literature search was conducted to find out the plasma composition of canine and a new buffer was prepared for the sodium loaded canine erythrocytes. The lack a Na-K pump, and the cytoplasmic Na^+ concentration is about equal to that of plasma. It was then decided that the buffer for dog erythrocytes will be prepared in such a way to avoid protons from going inside the blood cells. Therefore, the buffer was prepared with no phosphates. The incorporation of the new buffer showed better results as visible by comparing Figure **48 and 49**.

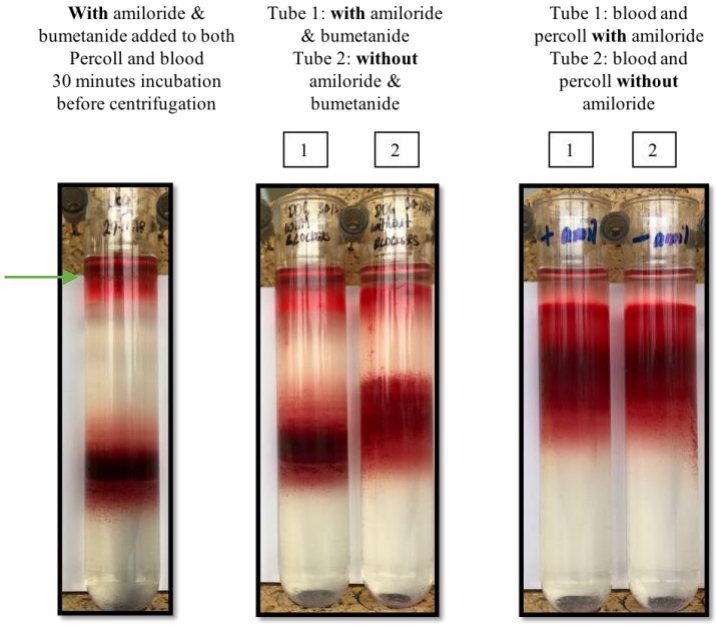

Figure 48. *Density separation of Canine erythrocytes using PBS+0.1% BSA, 40 minutes, 20,000 g, 85% Percoll, 32-34* ℃*. Various different conditions were tried and tested to get the best separation for animal erythrocytes. Hemolysis marked with an arrow.*

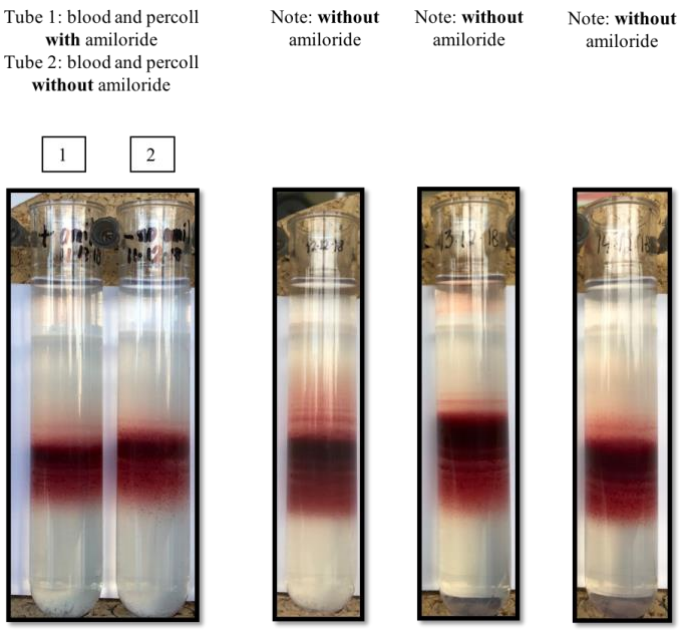

Figure 49. *Density separation of Canine erythrocytes using DOGO BUFFER Hepes-Tris +0.1%BSA+2mM Calcium. 40 minutes, 20,000 g, 85% Percoll, 32-34 ℃. Amiloride was added just to tubes 1 and 2 (on the left)*

Calcium uptake in Feline & Canine Erythrocytes

Calcium uptake by erythrocytes was then compared between the two species. Calcium is the most abundant and one of the most important minerals in the body. It is essential for cell signaling and the proper functioning of muscles, nerves, and the heart. The different fractions of erythrocytes prominently differed from each other in intracellular free Ca^{2+} levels and its distribution within the cells. Figure 50 shows that the heavy fractions of feline erythrocytes tend to accumulate more calcium (marked by arrows) than canine erythrocyte heavy fractions shown in **Figure 51**. Intracellular Ca^{2+} was measured from single cells as Fluo-4 based fluorescence intensity.

Calcium uptake in Feline Erythrocytes

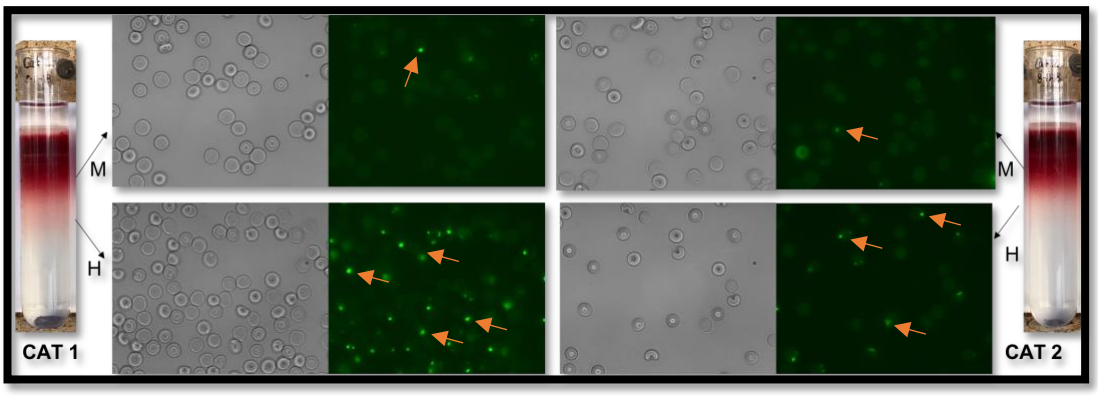

Figure 50. *Images of Calcium-loaded Feline erythrocytes. Separation of fractions M & H, 30 minutes, 32-34 °C , 20,000 g, 90% Percoll. Calcium loaded erythrocytes marked by arrows.*

Calcium uptake in Canine Erythrocytes

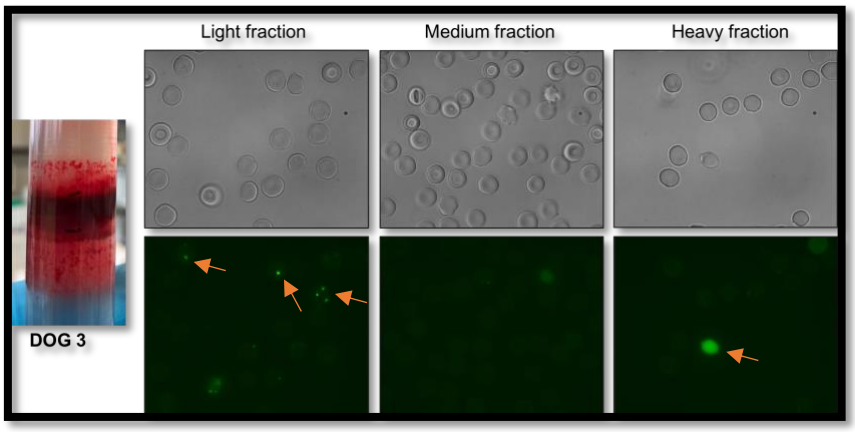

Figure 51. *Images of Calcium-loaded Canine erythrocytes. Separation of fractions L, M & H, 40 minutes, 32-34 °C ,20,000 g, 90% Percoll. Calcium loaded erythrocytes marked by arrows.*

With repetition, the results (not shown) persisted and there seems to be a huge difference in calcium uptake in the canine and feline erythrocyte fractions. Electrolyte's composition differs in the two species affecting electrical impulses which is a plausible explanation for this contrast.

Intracellular Potassium & Sodium ions: Canine Erythrocytes

It is well known that dog red blood cells lack a sodium pump, and yet they are capable of volume regulation in vivo [175]. The lack of sodium pump makes canine erythrocytes particularly rich in intracellular. Sodium and potassium ions were measured in parallel to confirm the data previously reported. **Figure 52** therefore confirmed the known fact that canine erythrocytes are sodium loaded.

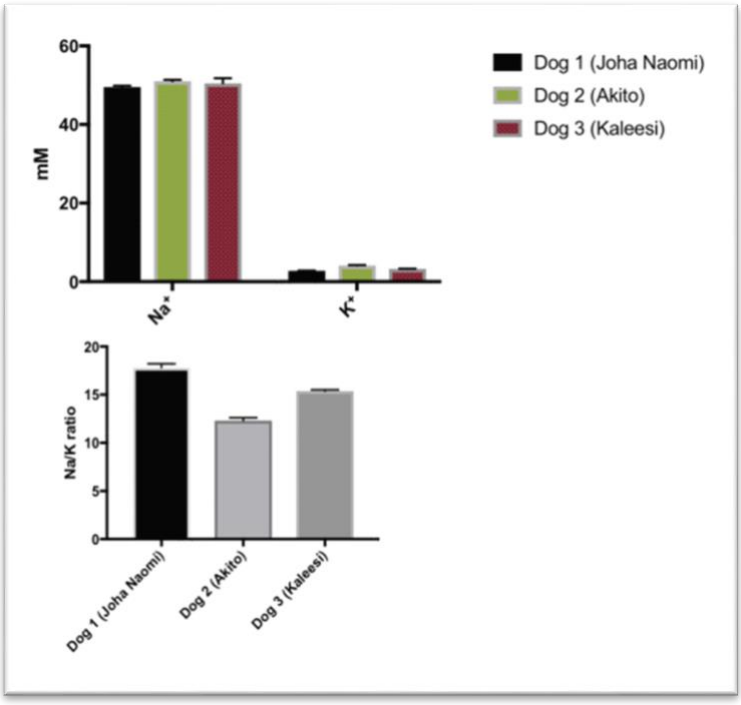

Figure 52. *Intracellular Potassium & Sodium ions of canine erythrocytes (n=3).*

Flow Cytometry: Canine Erythrocytes

Flow cytometry technique was used to analyze the characteristic of erythrocytes. When the cells pass through the laser beam they scatter the light, which is detected as forward scatter (correlating to cell size) and side scatter (correlating to granularity). Light scatter can be used to separate cells into different populations [176]. Besides being useful for assessing specific protein expression, cell viability, apoptosis and death, cellular interactions and cell enrichment, flow cytometry is a sough-after tool for screening, diagnostic and prognostic assays [177]. Here, flow cytometry was used to characterize markers of aging in different population of canine erythrocytes. **Figure 53** shows fluorescence activity observed in light, medium and heavy fractions of canine erythrocytes.

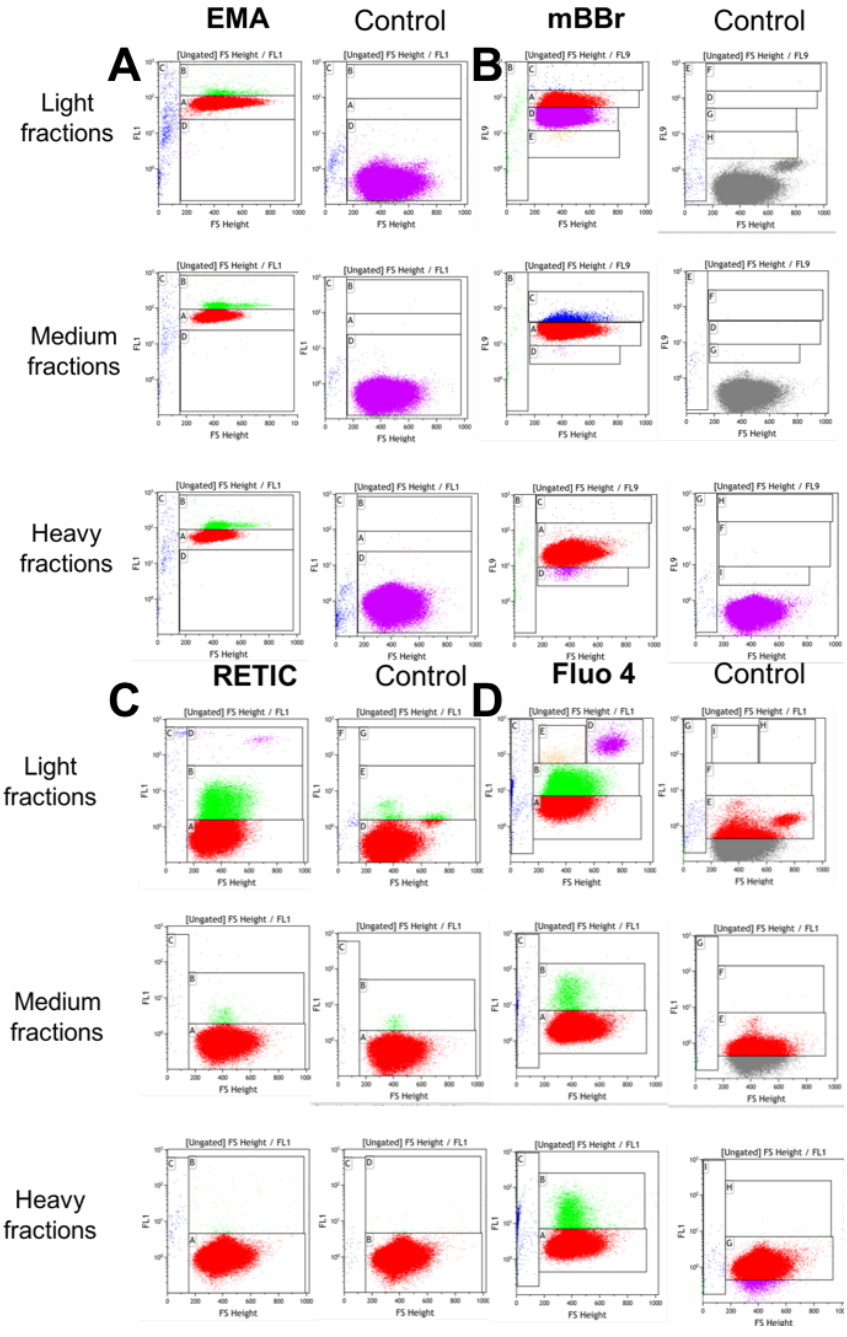

Figure 53. *Fluorescence activity in different fractions of canine erythrocytes for* ***A****: eosin-5-maleimide binding test for band 3 abundance,* ***B****: mBBR for thiols,* ***C****: reticulocyte count,* ***D****: Fluo-4 to visualize cells with free cytosolic calcium.*

The results shown in **Figure 53** are as expected and follow the trend from young to old erythrocytes. The eosin-5′-maleimide (EMA) flow cytometry binding test was used to see the difference in band 3 protein on the surface of canine erythrocytes of different age groups. As clusters increase with aging cells, the pattern is observed as the pollution in Gate B for EMA binding gets dense in aging cells (**Figure 53-A**). Monobromobimane (mBBr) is the fluorescent labeling agent that was used for labeling disulfides and thiols by flow cytometry. The population of cells gated positive for mBBr is much larger in heavy fractions (old cells) as compared to light fractions (young cells) as seen in **Figure 53-B**. BD Retic-Count was used for labeling reticulocyte and as expected the largest population of reticulocytes were observed in the light fractions with barely any cells present in the gating shown for heavy fractions in **Figure 53-C**. Thermo Fluo-4 AM dye was used to visualize populations of cells with free cytosolic calcium. Calcium fluorescence activity in erythrocyte population gradually decreases as the age of the cells increase (from light to heavy fractions) as observed in **Figure 53-D**

CONCLUSION

This study based on the characterization of erythrocytes by comparing old and young cells from the same animal has not been conducted in the past, bringing novelty to the study. The work depicted here was designed to investigate changes observed in animal erythrocytes with age. Measurements of several markers of aging were carried out as a comparison between young and old cells: ions (Na^+ & K^+), water, ATP, redox balance (GSH/GSSG), EMA binding, CD71 levels, and intracellular Ca^{2+} levels. One of the hindrances faced during animal study was difficulty with canine blood as hemolysis was an ongoing problem faced. A significant amount of time was spent trying to overcome this problem resulting in the preparation of a buffer specifically made for sodium loaded canine erythrocytes to reduce hemolysis while handling. The flow cytometry experiments done for bovine, equine and canine erythrocytes gave meaningful data in terms of markers of again in young and old erythrocytes. A perfect separation of cells according to density was obtained by several trials of varying concentration of Percoll as well as centrifugation conditions. The results from animal blood experiments provided in this thesis provide a basis for the possibility of further experiments in profiling animal erythrocytes. The results also add to the existing knowledge about markers of aging and major differences amongst erythrocytes of different species.

Chapter 3.3: Dynamics of Erythrocytes & von Willebrand factor in Sickle Cell Disease

Several mechanisms can explain how hematocrit affects haemostasis: erythrocytes contribute by releasing compounds that activate platelet and also scavenge inhibitors of platelet activation, erythrocytes can bind to platelets via the erythrocyte membrane protein ICAM-4 and the platelet integrin αIIbβ3. Increased levels of plasma von Willebrand factor have been discovered in sickle cell disease [123, 124] and this is plausible due to the thrombophilia of the sickle cell disease condition [178], however, very few studies are reported on the structure and reactivity of this VWF within this condition . Adhesion of erythrocyte to endothelial cells is widely studied especially in pathologies like sickle cell disease or β-thalassemia. This study focused on the role of ULVWF (ultra-large von Willebrand factor [179]) and interaction with erythrocytes in sickle cell disease. Experiments done previously suggested that erythrocytes that were subjected to neuraminidase treatment (that removes sialic acid from erythrocyte membrane), tend to coagulate. Erythrocytes were therefore treated with neuraminidase to make them agglutinable.

Neuraminidase treatment

Erythrocytes were treated with neuraminidase to make them agglutinable and this is clearly visible in the treated cells in **Figure 54**.

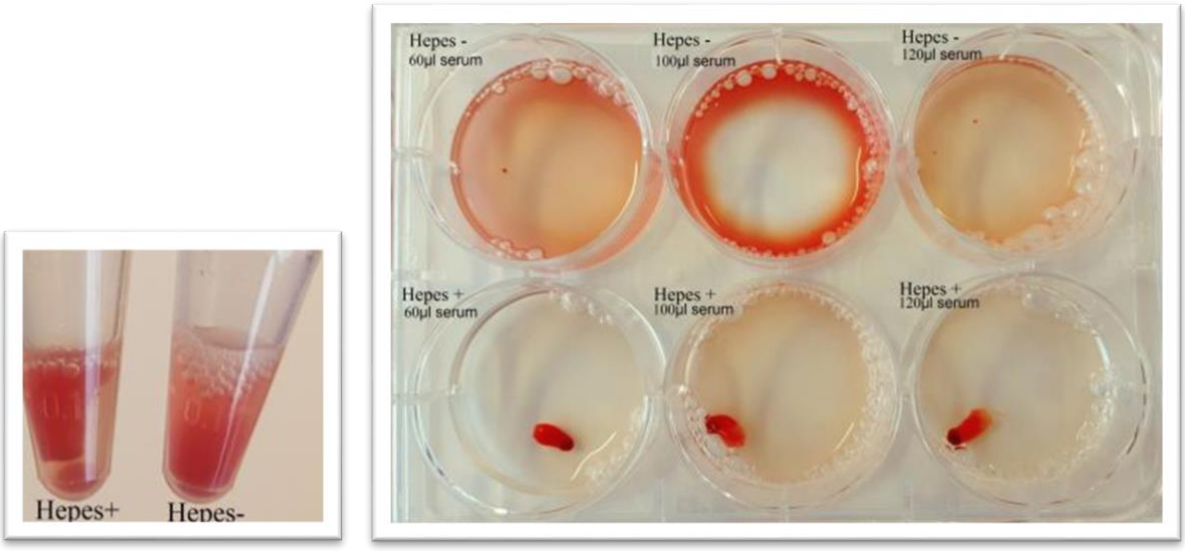

Figure 54. *Neuraminidase treatment (0.1U/mL) at 37°C for 30 minutes followed by Incubation at 37°C for 90 minutes of erythrocytes from healthy donor incubated with different serum concentrations, in the absence and presence of calcium.*

Following neuraminidase treatment, clotting is observed in healthy donor blood in the presence of calcium as shown in **Figure 54.**

The experiments shown in **Figure 55, 56 and 57** were conducted to study the involvement of von Willebrand factor in the severity of Sickle Cell Disease. It had been shown that healthy erythrocytes do not normally bind to the endothelial cells lining the vascular wall [123, 131]. Erythrocyte adhesion does occur in several hematologic disorders especially in sickle (SS) cell disease, due to von Willebrand factor multimers. When patient erythrocytes treated with neuraminidase were incubated with serum from SCD patient, clots were observed as visible in **Figure 55**. When healthy donor erythrocytes were similarly treated, the clots were not formed and this is evident in **Figure 56**. SCD patient erythrocytes incubated with both donor and patient plasma as shown in **Figure 57**. Several combinations were tested to confirm that cells subjected to neuraminidase treatment are more adherent.

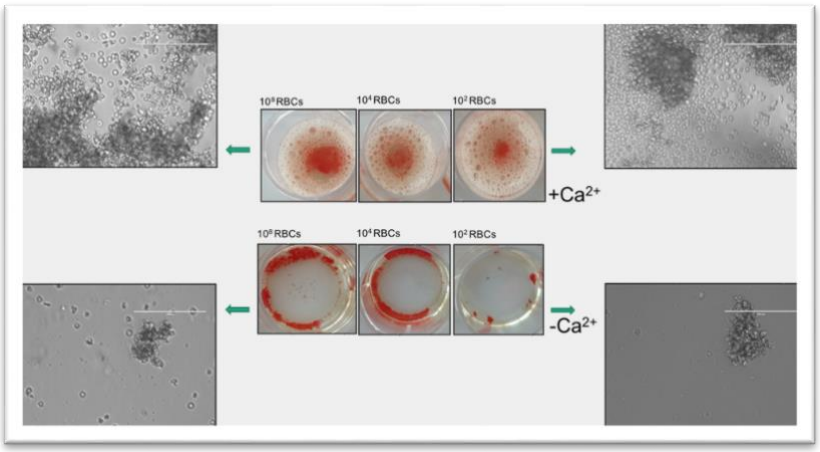

Figure 55. *SCD patient erythrocytes were incubated in 150µl HEPES (pH 7.5) + 80µl plasma at 37°C for 90 minutes after Neuraminidase treatment (0.12mIU/million RBCs, 37°C, 30 minutes).*

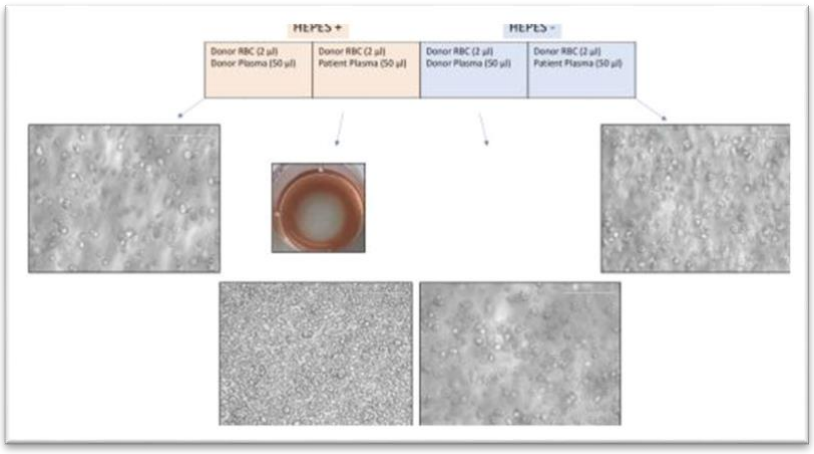

Figure 56. *Neuraminidase treatment (0.1U/mL) at 37°C for 30 minutes followed by Incubation at 37°C for 90 minutes.*

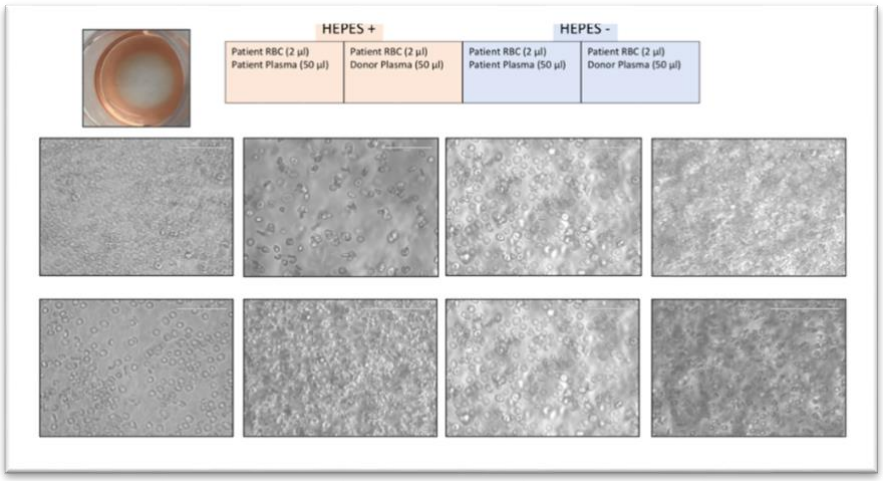

Figure 57. *Neuraminidase treatment (0.1U/mL) at 37°C for 30 minutes followed by Incubation at 37°C for 90 minutes.*

Patient and donor plasma samples were then compared. The patient samples in **Figure 58** have extra bands visible above the 250kDa band. This conforms with the previously known fact about von Willebrand factor existing in the form of ultra large von Willebrand factor in sickle cell disease patient plasma [124].

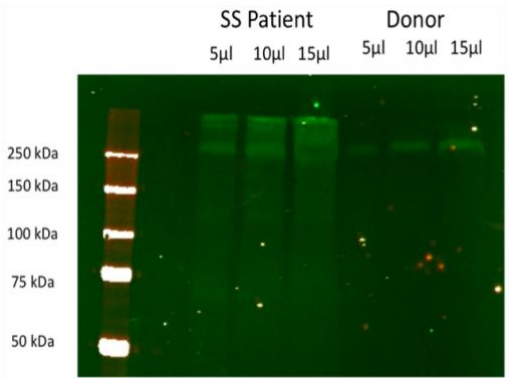

Figure 58. *Comparison of plasma of patient and donor: Sample preparation: Equal volumes of plasma and reducing Sample Buffer, heated for 15 minutes at 60° C. Basic unit of von Willebrand factor is a dimer of two 250kDa subunits.*

Human Erythrocyte Flow Chamber Adhesion Assay

Since there was limited sickle cell disease patient blood, other methods were incorporated to study the role of ULVWF in sickle cell disease. Flow assays were carried out to check adhesion of healthy erythrocytes activated by a calcium influx to histamine-stimulated endothelial cells. In sickle cell disease, erythrocytes have been proven to adhere to endothelial cells enhanced by ULVWF. It was expected to see that calcium loaded erythrocytess strongly adhere to histamine-stimulated primary endothelial cells. Major goal was to confirm that adhesion is mediated by ULVWF by measuring firm adhesion of erythrocytes using a flow chamber assay in the presence of shear stress.

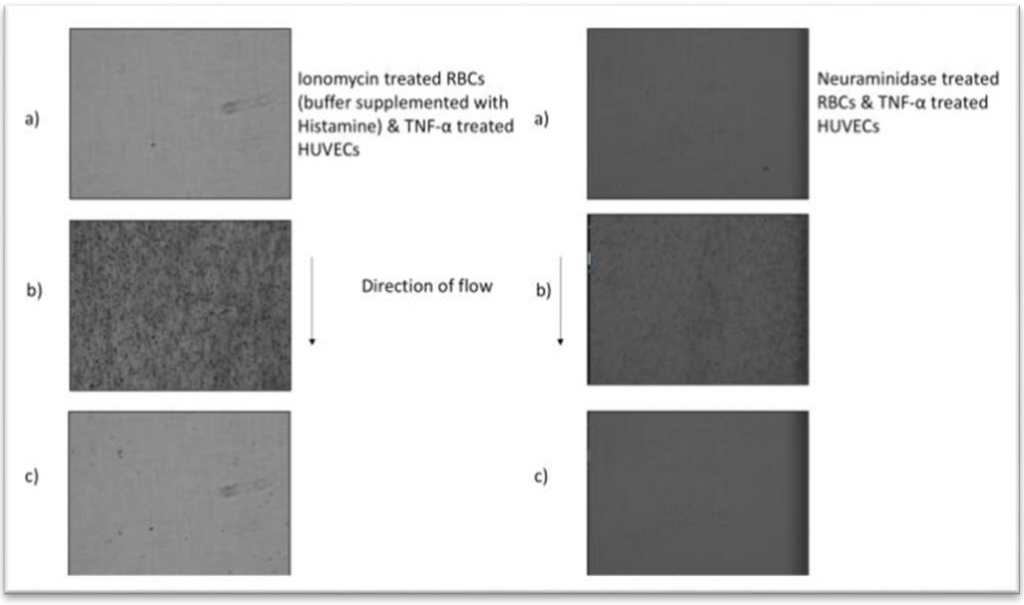

Figure 59. *Calcium loaded erythrocytes over HUVECs. Adhesion was recorded for 10 minutes Images are stills from video: (a) before injecting erythrocytes, (b) during flow of erythrocytes over HUVECs and (c) after the flow of erythrocytes.*

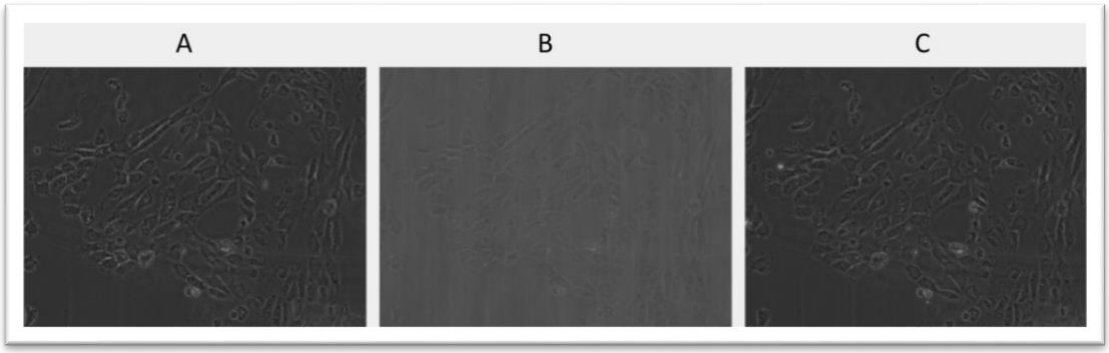

Figure 60. *Adhesion was recorded for 10 minutes Images are stills from video: (a) before injecting erythrocytes, (b) during flow of erythrocytes over HUVECs and (c) after the flow of erythrocytes.*

Ionomycin treated erythrocytes seem to adhere to the HUVECs layer as shown in **Figure 59 and 60**. However, this experiment could not be quantified as the HUVECs monolayer was not confluent enough. Several experiments were conducted for more than a month to optimize the flow assay. HUVECs reached a good confluency and the assay work. Adhesion was not observed in these experiments. The absence of adherence could be caused by the fact that patients were under hydroxyurea treatment. This information was not provided at the time of the experiments but is something that's needs to be looked into. Hydroxyurea is a drug that has been proven to benefit in sickle cell disease. And in the past, it has been proven to decrease erythrocyte adhesion to laminin [180]. Flow assay techniques takes a long period to set up and get quantifiable results, and a good set-up was achieved by the end, however more time is required to get significant results, and a follow-up study is in process.

Chapter 3.4: G6PD deficiency correction

G6PD catalyzes the synthesis of NAPDH, which is necessary for red blood cells as they have particularly vulnerability to being damaged by reactive oxygen species because they are deficient in other NADPD-producing enzymes. The research question of this study was if it is possible to correct G6PD deficiency through protein transduction, which is the internalization of the enzyme into the cells [181]. Protein transduction is an emerging technology being used an alternative to genetic intervention. G6PD deficiency is X-chromosomal inherited and clinical symptoms of the disease are confined to hemizygous men; however, female carriers of the aberrant gene may also suffer. Because of lyonisation (The inactivation of an X chromosome) carriers have a population G6PD deficient and G6PD positive RBC. This makes the diagnosis tricky. The first step to get accurate diagnosis is developing an enzymatic assay that determines enzyme's production of NADPH.

Cytofluorometric assay

Flow cytometry test was developed to determine the fraction of G6PD positive and G6PD deficient RBC in female carriers. Cytofluorometric assay was based on a methaemoglobine reduction method (see methods section on Page 41). The results of the flowcytometry test shown in **Figure 61** were consistent with the G6PD activity determined by the diagnostic lab, making it a reliable assay to diagnose carriers of G6PD deficiency. The reasons for developing the cytofluoremetric enzymatic assay were to determine enzyme's production of NADPH and also because of the difficulty associated to interpret for the mosaic female heterozygotes

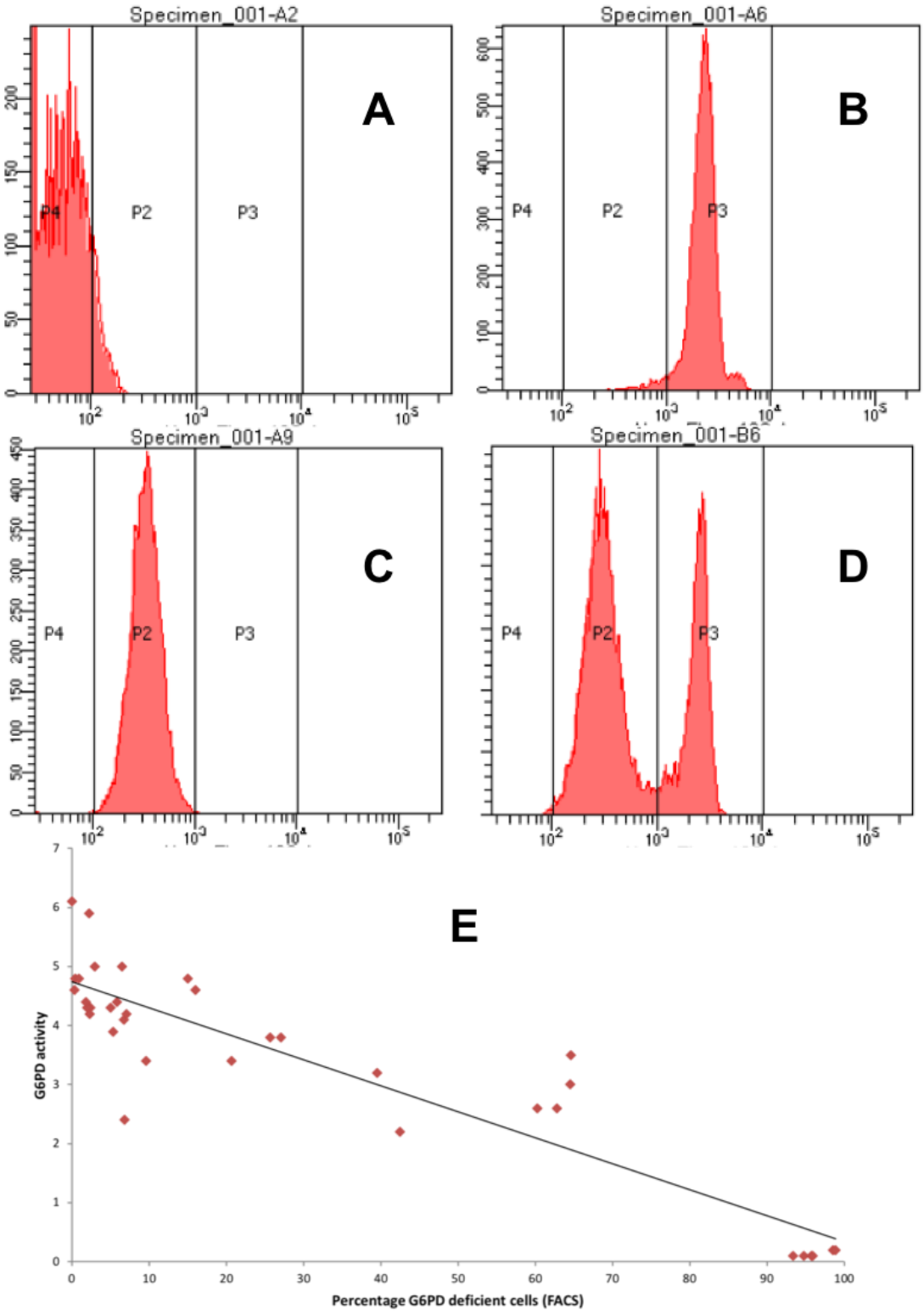

Figure 61. *Results of cytofluorometric assay.* ***A*** *Untreated RBC,* ***B*** *G6PD positive control,* ***C*** *patient G6PD deficiency,* ***D*** *Carrier G6PD deficiency,* ***E*** *Link between the percentage G6PD deficient cells (FACS) and G6PD activity*

The results of the FACS-assay are consistent with the G6PD activity determined by the diagnostic lab. Accuracy of the assay was defined by the consitency of percentage G6PD deficient cells with the results of the chromate inhibition test [182]. Chromate inhibits the activity of glutathione reductase in normal RBC but not in G6PD deficient RBC. Therefore, it was established that the cytofluorometric assay can be a reliable assay to diagnose carriers of G6PD deficiency, making the research question: Is it possible to correct G6PD deficiency through protein transduction?

Recombinant G6PD was prepared as described in method's section (Page 42) and the results of the expression and purification are reported in Figure 62,63, and 64. The expression of G6PD was checked by Commassie stained gel (**Figure 62**), Western blots (**Figure 63**) as well as activity assay (**Figure 64**). G6PD was clearly seen in the eluted protein marked by an arrow at molecular weight 60kDa in **Figure 63**.

Transformation of BL21 cells that took up TAT-G6PD plasmid and produced G6PD protein.

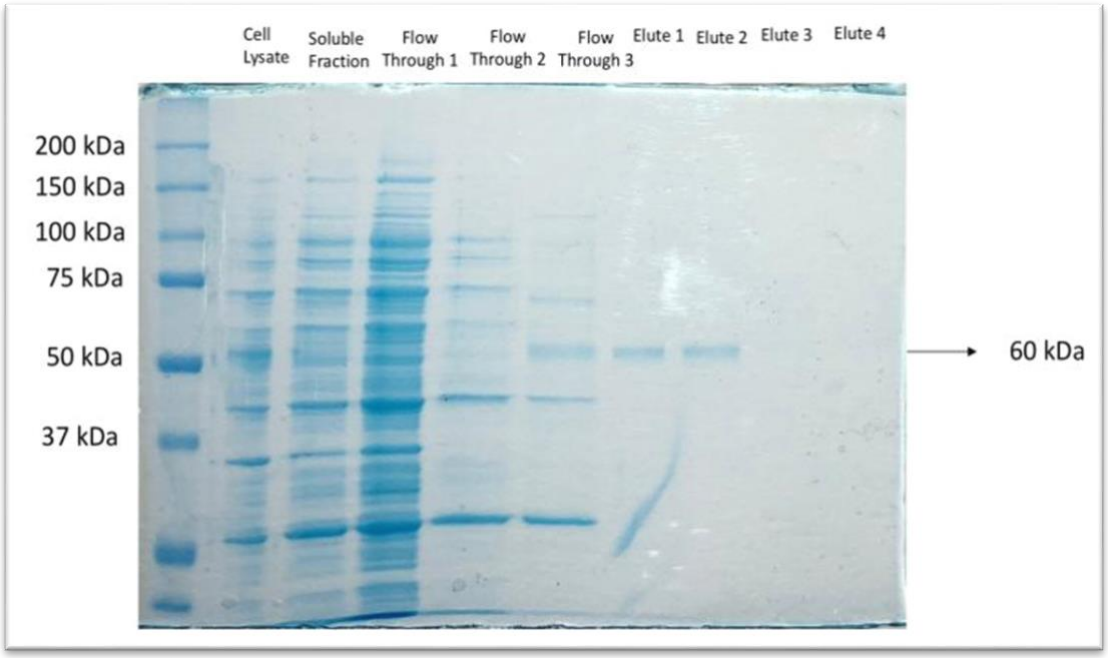

Figure 62. *2018 SDS-PAGE results for G6PD expressed as His-tagged protein in E.coli BL21. Equal portions of cell lysate, soluble fraction, flow through and eluted protein were loaded. The final eluted protein solutions show the specific band of the expressed protein at 60kDa marked with an arrow.*

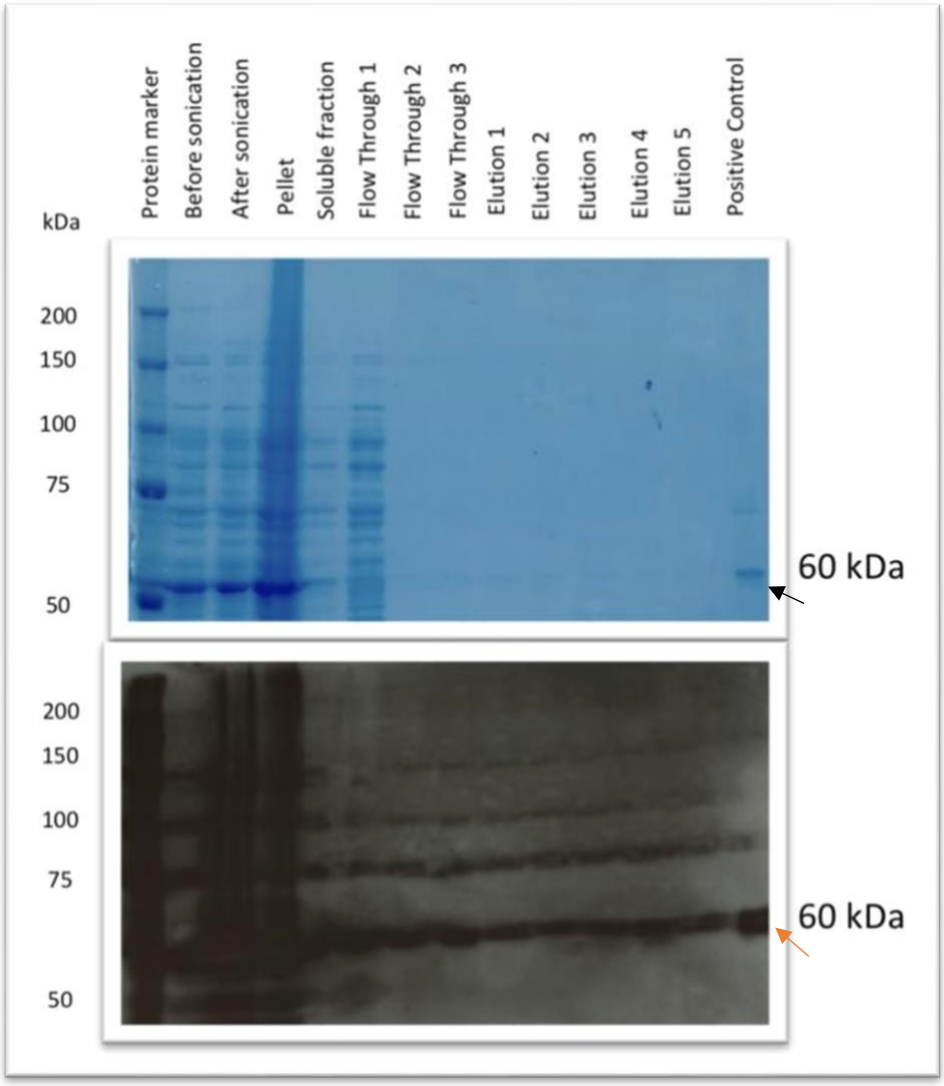

Figure 63. *2010 SDS-PAGE results for G6PD expressed as His-tagged protein in E.coli BL21. Equal portions of cell lysate, soluble fraction, flow through and eluted protein were loaded. The final eluted protein solutions show the specific band of the expressed protein at 60kDa marked with an arrow.*

G6PD eluted from 2018 batch is clearly visible (at 60 kDa) in the SDS-PAGE-gels shown in **Figure 62** but very faint in 2019 batch in **Figure 63** as compared to the control. Most of the protein is found in the pellet which could be due to formation of inclusion bodies.

G6PD activity and protein concentration

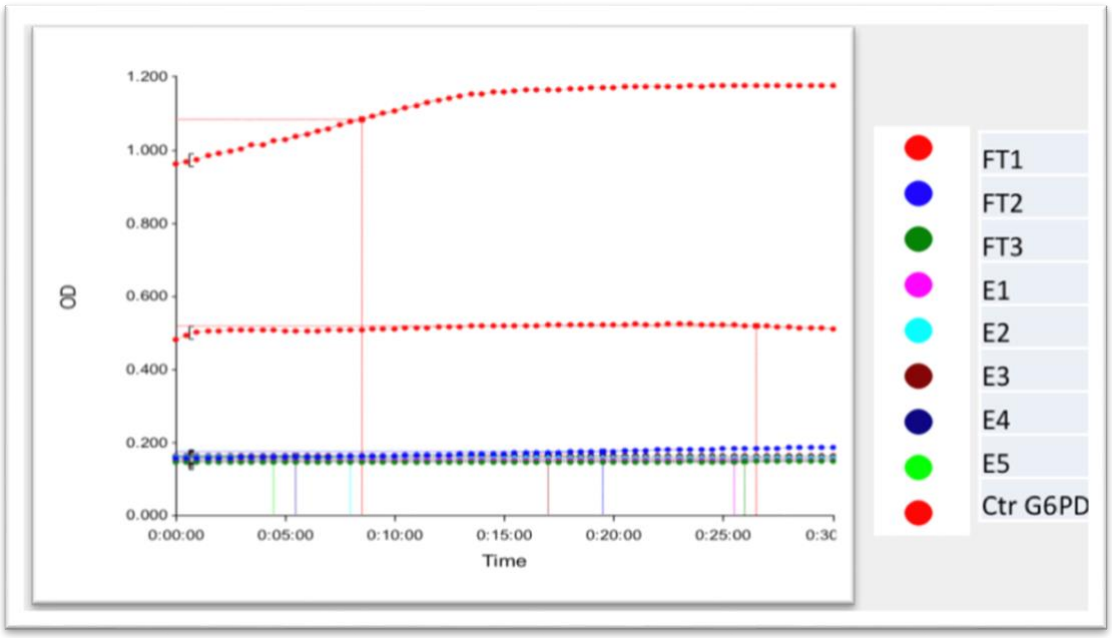

Figure 64. *G6PD activity measured in eluted samples (E1, E2, E3, E4 & E5) and flow throughs (FT1, FT2, FT3). Control G6PD sample provided by the diagnostic lab.*

G6PD activity shown in **Figure 64** is too low in the eluted sample. Most active G6PD is in Flow Through 1.

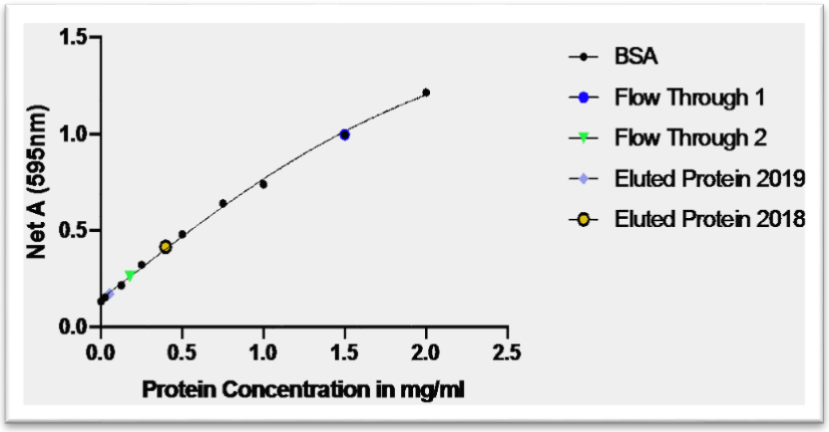

Figure 65. *Biorad Calibration Curve. Protein concentration from 2 batches of produced G6PD (2018 and 2019). Protein purification of the His-tagged protein G6PD was carried out using Ni-NTA matrix. The protein was first bound to the matrix and Flow Through 1 and 2 were collected after washing with increasing concentration of imidazole. The final eluted protein was collected after washing with highest concentration of imidazole. The Flow Through solutions contain a mixture of other proteins and the Eluted Protein contains expressed His-tagged protein G6PD.*

Low quantity of protein is found in eluted samples. Most protein is in Flow Through 1 as shown in Figure 65.

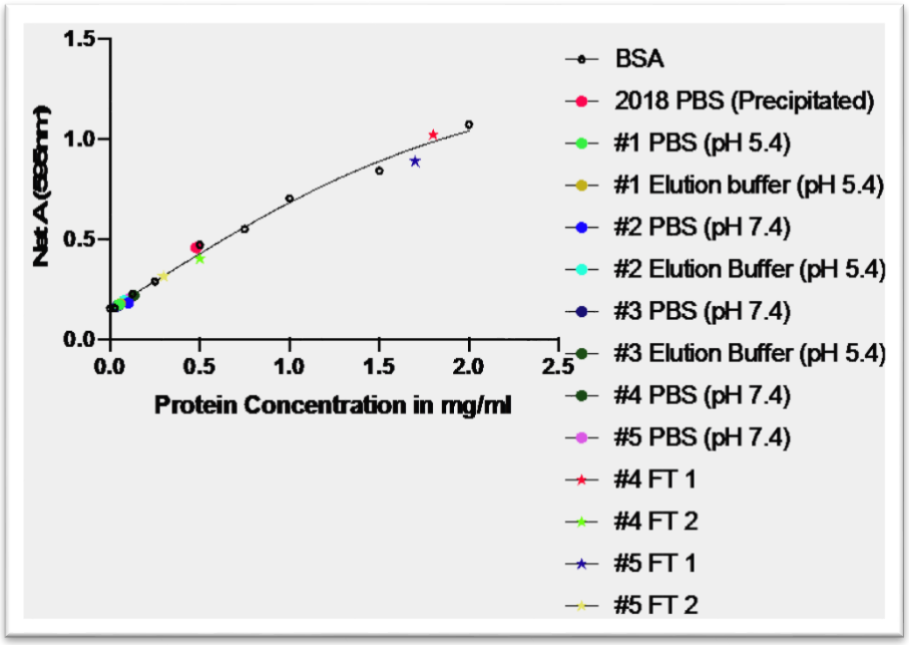

Figure 66. *Biorad Calibration Curve. Protein Concentration of all batches of protein eluted after changing pH of the buffers used in the Ni-NTA columns. The samples were measured in both elution buffer as well as in PBS.*

Most protein (mixture of other proteins along with G6PD) is still present in Flow Through 1 shown in **Figure 66**. The quantity of eluted protein is still low but better than previous results shown in **Figure 65**. Protein eluted after several batches of production was pooled and concentrated to be used for transduction experiments.

Result of Transduction

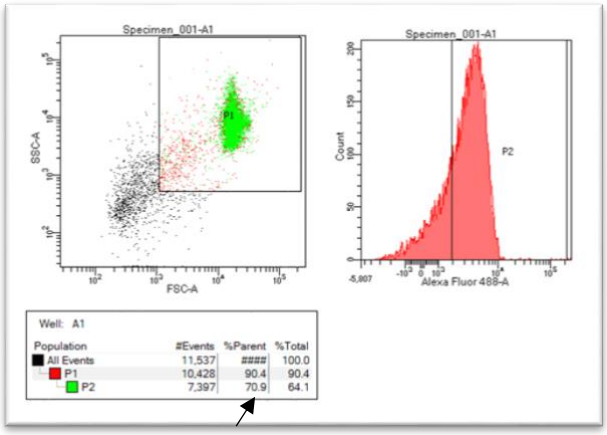

Figure 67. *Fluorescence activity monitored using flow cytometry for RBCs + TAT-G6PD (transduced RBCs) marked by an arrow in the figure.*

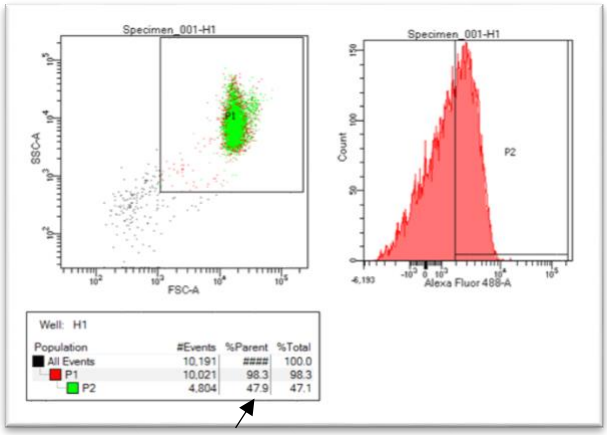

Figure 68. *Fluorescence activity monitored using flow cytometry for RBCs without G6PD marked by an arrow in the figure.*

The research question of this study was if it is possible to correct G6PD deficiency through protein transduction. Therefore, a preliminary study was conducted. Transduced RBCs can be seen in **Figure 67.** The control sample with no G6PD is still very positive as seen in **Figure 68.** The blood was not taken from a patient with G6PD deficiency, but a healthy donor. So, the background is almost high as the G6PD sample because there is already G6PD present. So far very minimal increase in G6PD is observed after protein transduction. An increase of 23% can be seen by comparing P2 % Parent values. The P2 % Parent value in transduced RBCs is 70.9% in Figure 67 and value without transduction is 47.9% in Figure 68. The results are preliminary and the assay needs to be optimized.

CONCLUSION

Several batches of G6PD were produced by expression in BL21 bacteria and the activity as well as concentration of the proteins were measured. The concentration and the activity of the TAT-G6PD is very low as shown in **Figure 64, 65 and 66**. The bacterial culture needs to be upscaled. The majority of the protein remains in the pellet instead of the supernatant. This is because of the formation of inclusion bodies. A preliminary experiment for transduction was conducted after production of G6PD in small amounts several times and pooled together. There is a 23% increase in G6PD positive cells in the transduced population (erythrocytes with added G6PD) as seen in **Figure 68** (marked with an arrow). The major aim of the pilot study was accomplished as TAT-G6PD was successfully transduced in to a small percentage of the erythrocytes. However, the concentration of the protein was very low which can possibly be improved by optimizing the conditions of the protein induction. There were some limitations but overall these experiments provided a base for a further study being carried out by another student at red cell group at Sanquin. With further optimization of the transduction methods, a cytofluoromtric assay, that has already been set up as shown in Figure 61, will then be performed on the transduced G6PD deficient RBC.

Chapter 4. Discussion

Chapter 4.1: Protein 4.1

Characterization of the rate of conversion of protein 4.1b to 4.1a

Purified RBC membranes ("ghosts") were re-suspended in hypotonic phosphate pH 7.4. The suspension was distributed into aliquots and incubated at 4 °C, 17 °C or 37 °C. After every week samples were collected, treated and analyzed by SDS-PAGE to quantify protein 4.1a/4.1b ratio. The ratios altered slightly with time at the lower temperatures. There was progressive blurring of the 4.1a and 4.1b bands which translated into an increasingly difficult quantification of the ratio. This phenomenon, as it turned out, was dependent on damage, possibly oxidative in nature, suffered especially by protein 4.1 when incubated at higher temperatures. From week 3 onwards (Fig 12), gels showed the presence of high-molecular weight protein aggregates, non-reducible by thiols. After this initial unsuccessful approach, it was concluded that experiments need to be designed by preparing ghosts with oxygen-free buffers, resealing them against a buffer with high potassium and 2mM glutathione, and incubating them in sealed vials under nitrogen. In Fig 13, the expected 4.1a/4.1b ratio was calculated on the basis of a model that assumes a half-life of 4.1b to 4.1a conversion of 41 days. The 4.1a/4.1b ratio at 4 °C was not expected to change. For ghost incubated at 37 °C, there is a vast difference in the expected and measured ratios. The ratios could have been possibly affected by the aggregation of proteins and potential oxidation in samples stored over the course of the experiment.

Confirming amino acid difference between the two isoforms

Protein 4.1 study was continued with confirming the one amino acid difference between the two isoforms [2], by studying synthetic peptides corresponding to the human protein 4.1 sequence centred around Asn 502, and by purification of the natural protein verified by mass spectrometry. The aim of MALDI TOF analysis was to confirm the sequences of the 2 isoforms of protein 4.1 and see if it corresponds to previously known information about deamidation of specific amino acid residues. The bands were excised from the gel shown in Fig 14. Fig 15 shows the MALDI TOF spectra of protein 4.1a and protein 4.1b reporting peptide ranging from residue 474 to 491 (TLNINGQIPTGEGPPLVK) in which the Asn 478 is deamidated and this is compatible with the knowledge that both isoforms of 4.1 protein go through deamidation possibly co-translationally at residue 478 which is followed by Gly. Fig 16 shows the MALDI TOF spectra of protein 4.1a and protein 4.1b reporting peptide ranging

from residue 492 to 505 (TQTVTISDNANAVK). Both Asn residues are followed by Ala. In protein 4.1a sample it's evident that at least one of two Asn (500 or 502) is deamidated. Protein 4.1b shows the presence of peptide 492-505 with m/z 1461.6 compatible with the presence the peptide without deamidation. It is known that deamidation of residue 502 is the sole reason for difference in molecular weight of the two isoforms. However, it still needs to be confirmed if it was N at 500 or 502 which was deamidated.

In the original article where the difference between protein 4.1a and 4.1b was investigated, an experiment was performed in which some peptides derived from the C-terminal end of protein 4.1 by CNBr-cleavage were further proteolyzed with lysylendopeptidase, labelled with ^{125}-I, run in a 20% polyacrylamide gel and then autoradiographed. The result is shown in Fig. 17. LE7 corresponds to the peptide derived from protein 4.1b, and it contains Asn (N) at position 502, as determined by direct sequencing. LE9 corresponds to the peptide derived from protein 4.1a, and it contains Asp (D) at position 502. It is shown that even though the two peptides differ only by one amino group still result in a dramatic difference in the molecular mass of 2 kDa similar to native full protein when loaded on SDS-PAGE. Varying concentrations of synthetic peptides corresponding to LE7 (N) and LE9 (D) were analysed by SDS-PAGE as in the original article (Fig. 18 and 19). The same peptides from 2 separate batches (Fig 20 2016 batch, Fig 21 2017 batch) were loaded in a polyacrylamide gradient gel at 5-20% acrylamide concentration and run with Tris Glycine buffer system. The two synthetic peptides N & D, when run on gels (Fig 18-21), do not migrate in the manner expected. Both peptides migrate with an apparent mass larger than expected and peptide D was expected to migrate with an apparent molecular mass higher than N but the results do not comply. The reason was not identified however a possible explanation could be larger aggregates form by peptide N polymers as compared to peptide D, therefore resulting in migration at a higher molecular mass, contrary to expectation.

CD Measurements of peptides (University of Parma)

Peptides were dissolved in soluble in NaP buffer 20 mM pH 7.5. Spectra on the left are the original spectra. Since peptide N might be slightly less concentrated than peptide D due to its lower solubility (we could see 3-4 little particles of undissolved peptide in a volume of 20 ml), in order to compare the spectra, we applied a scaling factor so that the two spectra have the same minimum. This allows to compare the two spectra (right panel), which are very similar (same secondary structure of peptide D & N. The analysis of the data was carried on using peptide D, peptide N (A) and normalized peptide N (B) data. Results indicate that the peptides are mainly unstructured and that no striking difference

appears between peptide N & D. Therefore, the peptide forms of the two isomers do not explain or provide insight into the biochemistry of the full protein form of both protein 4.1a and 4.1b.

Neocytolysis study

Experiments were conducted to study neocytolysis where blood was fractionated according to density (Fig 23) and the youngest population is either removed or added in small percentage to see the impact on 4.1a/4.1b ratio. The data obtained in the first preliminary experiment are shown in the graph of Figure 24. It can be observed that in the total population of RBCs the measured 4.1a/4.1b value was 2.319. After separation of cells into young, middle-aged and old subpopulations, according to the percentages shown inside the respective areas of the histogram bar, a new total population of RBCs was reconstituted (R3) in which young cells were less than in the original blood (8% instead of 12.9%). This can be seen by the 4.1a/4.1b ratio being higher than the original blood (2.442 vs 2.319). An even higher 4.1a/4.1b value was measured in a reconstituted population of RBCs (R2) to which the previously isolated young RBCs were not added back (2.623 vs 2.442). Similar results were obtained in the subsequent experiments, shown in Figure 25. The inconsistency observed here is the different 4.1a/4.1b value in R3 compared to total population of cells (which should be similar as these two populations have similar composition). The difference in the 4.1a/4.1b values between the R3 and R2 populations goes in the expected direction, with a higher 4.1a/4.1b value in the R2 population, which contains fewer young cells, than in the R3 population.

On the basis of the obtained results, it was concluded that the method was suitable for the detection of the disappearance of a few percent of younger RBCs from the blood of subjects that are exposed to conditions where neocytolysis can develop. These preliminary results shed light on the research approach of mimicked neocytolysis and provided a foundation for another project (NEOCYTOLYSIS) in collaboration with a few labs around Europe.

4.1a/4.1b ratio comparison between ghosts prepared using different buffers

Ghosts were prepared from female and male donors using two different buffers: Dodge (D) & Tris (T). **D**: Ghosts prepared in Dodge Buffer *(Hypotonic Phosphate Buffer (25mM Sodium Phosphate Monobasic Monohydrate, pH 7.4 at 4°C).* **T**: Ghosts prepared in Tris Buffer *(Hypotonic Tris buffer (5 mM Tris, 5 mM KCl, pH 7.4 at 4°C)*

As shown in Fig 28, no difference between the two buffers was observed from the ratios acquired from small gels in Figure 26. However male and female blood samples vary just little. Samples from three independent experiments were then run on large gels (Fig 27) to get a better separation. The observed 4.1a/4.1b ratio did not vary much (Fig 29) and it confirmed that the buffer used to prepare ghosts does not affect the ratios, however as expected, ratios differed slightly amongst male and female samples.

4.1a/4.1b ratio: by experimental aging of erythrocytes

At the beginning of apoptosis, PS is relocated to the external membrane serving as a recognition signal for phagocytes. In the presence of calcium, Annexin V is used to detect apoptosis due to strong and specific interaction with exposed phosphatidylserine. In this experiment, Annexin V was used for copper induced apoptosis detection. Flow cytometry results in Fig 33 confirm experimental aging, however the samples once run on SDS-PAGE gels appeared as smears and were not usable for quantification of 4.1a/4.1b ratio.

4.1a/4.1b ratio: Healthy donors and patients

Protein 4.1 study was continued during the secondment at Sanquin where membranes were prepared from fresh donor blood available locally as well as stored membranes prepared from disease patients. The aim was to quantify the two polypeptides of 4.1 after Coomassie blue staining of the gels, digital image acquisition, and densitometric analysis using Image J. Moreover, 4.1a/b measurements were also conducted by Western blotting as shown in Fig 30, to increase sensitivity. By western blotting is it also possible to load in SDS-page gel whole erythrocytes instead of ghosts (membranes), thus avoiding the preparation of ghost membranes which requires large blood volumes and likely miniaturizing this assay for situations where sample sizes are critical (sports, children, hypoxia conditions and other pathologies). Due to limited availability of patient samples, a few samples were processed as shown in Fig 35. The ratio was observed to be significantly lower in patients with

hereditary elliptocytosis and hereditary spherocytosis. As mentioned earlier, both proteins 4.1a and 4.1b are deficient In HE patients (either heterozygous or homozygous). The heterozygous state was characterized by a mild hemolytic state with mild spherocytic elliptocytosis [31].

A deficiency of protein 4.1 has also been described in a patient with mild HE. In HS patients, there is a defect in spectrin binding to protein 4.1 [38]. Since glycophorin C may play a role in the anchoring of protein 4.1 to the plasma membrane, it is possible that the primary deficiency maybe be due to glycophorin C.

Chapter 4.2: Animal Erythrocytes

Erythrocyte Morphology

Erythrocytes of animals were observed under the microscope (Fig 36) to become familiar with the appearances of normal red blood cells. As mentioned earlier, canine erythrocytes have a prominent central pallor. As known through literature, camels have erythrocytes that are small, flat and oval-shaped as seen in Fig 37. Camelid Erythrocytes were not studied, but the morphology was observed for their unique shape. As seen in Fig 36, the canine erythrocyte appears to be a large, uniform and biconcave disc. Feline erythrocyte seem to be much smaller and more variable in size as compared to canine cells. Feline erythrocytes do not seem to have a central pallor. It is known that haemoglobin present in feline erythrocytes is more prone to oxidant injury as compared to other species. This is because feline haemoglobin contains eight oxidizable sulfhydryl groups. Therefore, low numbers (<10%) single, small Heinz bodies can be seen on feline erythrocytes even in healthy cats [183]. Equine erythrocytes appear to be of similar size as feline erythrocytes and also lack central pallor.

Gradient Separation of Equine and Bovine Erythrocytes

As mentioned earlier, the Percoll gradient is a good method to visualize cell density. The density is largely based on the hydration state and the size of the RBCs. The distribution of the RBCs in the gradient is used to calculate the proportions of into low, medium and high-density fractions. Generally speaking, the low-density fraction holds the youngest cells while the high-density fractions contains the old and damaged cells. Various different conditions were tried and tested to get the best separation for animal erythrocytes. As shown in Fig 38, 90% and 95% of Percoll concentration were chosen after trying several different Percoll percentages and centrifugation conditions. Eventually the protocol was adapted for centrifugation 32-34 ℃ , 26,000 g, for 20 minutes.

SDS-Page Gels Equine and Bovine Erythrocyte Ghosts

The ghost samples prepared from the light and heavy fractions of both horse and cow erythrocytes were not usable for quantification. This was because the protocol at the lab in Zurich did not include addition of dithiothreitol. Dithiothreitol (DTT) reduces disulfide bonds (sulfur-sulfur linkages between two cysteine residues), removing the last traces of tertiary or quaternary structure. Hence,

the gels run in Zurich (a few shown in Fig 39 & 40), were native gels and 4.1a and 4.1b separation was not possible.

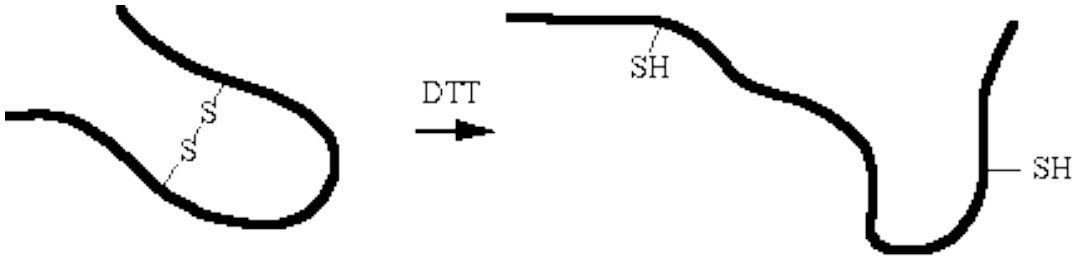

Figure 69. *DTT function [184]*

The left-over samples were transported to Pavia and native samples were run along with after adding DTT. The gels from Fig 41 were however still not usable for quantification as seen in Fig 42. However, 2 sub bands at the location of protein 4.1 were observed which complies with literature.

Measurements of different parameters in young and old erythrocytes

During the two secondments, erythrocytes from different animals were isolated and separated into light, medium and high-density fractions on Percoll gradients to study several parameters and red cell aging. The parameters planned to study during the secondment in Zurich have be studied in specific conditions or animals after a fitness regime (horses that are runners) or cows that's are lactating. There haven't been many studies where young and old erythrocytes of the same animal were studied and cellular parameters compared. Therefore, most of the knowledge gained from these experiments was novel and not much was available in literature apart from the facts that horses do not have reticulocytes in circulation [185] and that dog cells lack a sodium-potassium pump [186].

The major task was characterization of the red blood cells of different density/age by measurements of ions (Na^+ & K^+), water, ATP, redox balance (GSH/GSSG), EMA binding, CD71 levels, and intracellular Ca^{2+} levels. The results obtained by studying the markers of aging in animal blood were in line with human RBCs, which has been studied extensively.

For instance, two markers of red cell aging are sodium and potassium and the levels fluctuate between young and old cells. Low sodium and high potassium concentrations were present in young RBCs while compared to old RBC in horse and cow erythrocytes. Analysis had differences among Light (young) and Heavy (old) cells. Sodium levels were slightly lower in younger cells as compared to

older cells, and Potassium levels higher in younger cells as compared to older cells as shown in Figure 43.

There are easily recognizable changes in erythrocytes that occur with age. Since erythrocytes do not contain a mitochondrion, they do not use any of the oxygen they transport. As known, red blood cells produce the energy carrier adenosine triphosphate (ATP) by glycolysis of glucose and lactic acid fermentation on the resulting pyruvate. With time and age, the cellular processes weaken and the ATP levels reduce which is observed in the measurements where reduction of ATP can be clearly observed in older cells in (Fig 44). Erythrocytes as they age have more oxidative stress which impairs oxygen delivery. Erythrocytes need to deform and squeeze through capillaries that are narrower than themselves, and this gets difficult as oxidative stress damages the membrane skeleton of the cells. Oxidative stress therefore plays role in the elimination of aged and damaged erythrocytes [187, 188]. Increase in oxidative stress is observed in both equine and bovine older erythrocytes as seen in Fig 46.

Flow Cytometry: Bovine and Equine Erythrocytes

An antibody for CD71 was used as a marker for reticulocytes, eosin-5-maleimide which binds to band 3 protein and is a marker for membrane abundance, and annexin-V which binds to external phosphatidylserine and is a marker for clearance by macrophages. Fluorescent indicator Fluo-4 penetrates the cell membrane and is activated when it binds to internal Ca^{2+}. These receptors were measured by flow cytometry for light and heavy fractions of horse and cow erythrocytes as shown in Fig 45. The vesicles shed by the aged red blood cells result in higher PS exposure quantified by Annexin V staining as shown in Fig 45 for both equine and bovine erythrocytes. As mentioned earlier, Band-3 clustering/breakdown occurs in aged cells which follows the results observed. It has been shown in the past that dysregulation of iron metabolism contributes to age-related pathologies. During aging, there is accumulation of iron taking place at several sites in the body: hepatocytes and Kupffer cells of the liver, kidney brain and skeletal muscle. The mechanisms of iron retention associated with aging are unclear but could be due to either enhanced iron uptake or reduced iron export in tissues, resulting from dysregulation of iron transport proteins. CD71 (transferrin receptor) is responsible for importing iron into the cell and it is regulated in response to the iron concentration inside the cell. As observed in the results, CD71 is slightly elevated in older equine erythrocytes and reduced in older bovine erythrocytes.

Gradient Separation of Feline and Canine Erythrocytes

Percoll Separation for Dog erythrocytes were still not ideal after trying several conditions (Fig 48). However, the main problem to overcome was Hemolysis in dog erythrocytes. A few steps were incorporated in the protocol to avoid hemolysis such as adding Bumetanide and Amiloride (30 minutes incubation) to both Percoll solution as well as erythrocytes [189, 190]. Next step was to find out osmolarity of dog erythrocytes though literature search and prepare a new buffer. It was known that sodium is the major cation inside dog erythrocytes. Dog erythrocytes contain 10 times more Na^+ than K^+. The lack a Na-K pump, and the cytoplasmic Na^+ concentration is about equal to that of plasma [191]. It was then decided that the buffer for dog erythrocytes was to avoid protons from going inside the blood cells. There the buffer should be prepared with no phosphates.

CONSTITUENTS OF DOG RED CELLS AND PLASMA

	Na	K	Cl	Water
		meq/kg water		*percent wet wt*
Cells	161.9±2.3	7.8±0.5	80.1±5.2	63.6±0.5
Plasma	165.3±2.1	4.6±0.2	122.7±3.9	91.7±0.2

Concentration ratios

$Na_{plasma}/Na_{cells} = 1.02\pm0.02$

$K_{plasma}/K_{cells} = 0.59\pm0.04$

$Cl_{cells}/Cl_{plasma} = 0.65\pm0.04$

Table 3. *Serum or plasma osmolality of canine erythrocytes [186].*

New buffer for Dog Erythrocytes was prepared:

Hepes buffered saline solution	MW (g/mol)	1X	Conc (mM)	10X	250ml (10X)
NaCl *Sodium chloride*	58.44	9.643g	165	96.43 g	24.11 g
KCl *Potassium chloride*	74.55	342.93 mg	4.6	3.429 g	857.33 mg
HEPES	238.30	4.77	20	47.66 g	11.93 g
Tris 1M Stock to set pH to 7.4	*MW=121.14, 1M, Prepare 100 ml (12.13g)*				
Calcium from 1M stock	1mM or 2mM, add later to 1X buffer before use				
Magnesium Chloride Hexahydrate $MgCl_26H_2O$	203.31	30.49 mg	0.15	304.97 mg	76.24 mg
Glucose	180.156	1.8g	10	18 g	4.5 g

Table 4. *DOGO buffer prepared to use for canine erythrocytes.*

As seen in Figure 49, a better separation of fractions with no hemolysis was observed in density separation of dog erythrocytes as compared to Fig 48. Being sodium loaded cells, dog erythrocytes had a much higher concentration of Sodium compared to Potassium and this was confirmed by intracellular potassium and sodium ions as shown in Fig 55.

Calcium uptake in Feline and Canine Erythrocytes

There is a huge difference in Calcium uptake in the erythrocyte fractions of Cats and Dogs. Cat erythrocyte heavy fractions tend to accumulate more calcium than Dog erythrocyte heavy fractions. Fig 50 & 51 depicts the representative confocal images of fluo-4 fluorescence intensity proportional to the amount of free calcium in feline and canine erythrocytes. Sequestration of calcium in the intracellular vesicles is observed in feline erythrocytes. The difference in calcium uptake is observed between the two species as the electrolyte's composition differ in the two species affecting electrical impulses. In some cells, the intracellular sequestration of calcium can occur as way to maintain low levels of cytoplasmic calcium levels [192]. This might be the case in feline erythrocytes.

Flow Cytometry: Canine Erythrocytes

Figure 53 shows the Fluorescence activity observed in different density fractions of canine erythrocytes separated by Percoll. The eosin-5′-maleimide (EMA) flow cytometry binding test was used to see the difference in band 3 protein on the surface of canine erythrocytes of different age groups. As erythrocytes age, haemoglobin denatures and band 3 clustering takes places. Band 3 clustering occurs due to hemichromes formed from denatured haemoglobin cross-linking the protein. EMA binding targets these clusters [193]. As clusters increase with aging cells, the pattern is observed as the pollution in Gate B for EMA binding gets dense in aging cells. Monobromobimane (mBBr) is the fluorescent labeling agent that was used for labeling disulfides and thiols by flow cytometry. It has been suggested in the past that with cell aging, plasma glutathione decreases and oxidized forms of thiols increase. Total cysteine has also been reported to increase with age which results in more disulfide bridges [194]. This knowledge correlates to the observations as the population of cells gated positive for mBBr is much larger in heavy fractions (old cells) as compared to light fractions (young cells). BD Retic-Count was used for labeling reticulocyte and as expected [195] the largest population of reticulocytes were observed in the light fractions with barely any cells present in the gating shown for heavy fractions. Thermo Fluo-4 AM dye was used to visualize populations of cells with free

cytosolic calcium. Calcium pump present in the plasma membrane of cells is driven by ATP and decreases in activity with age [196]. This can be observed in the results where the calcium fluorescence activity in erythrocyte population gradually decreases as the age of the cells increase (from light to heavy fractions).

Chapter 4.3: Dynamics of Erythrocytes & von Willebrand factor in Sickle Cell Disease

Preliminary experiments proposed that cells that were subjected to neuraminidase treatment (that removes sialic acid from erythrocyte membrane), tend to coagulate. Cells were treated with neuraminidase to make them agglutinable. Several combinations (Fig 55-57) were tried where it was noticed that cells subjected to neuraminidase treatment are more adherent. Clotting is observed in healthy donor blood in the presence of calcium as shown in Fig 54. Aggregation and clotting are observed in sickle erythrocytes when incubated with sickle patient plasma. When healthy donor erythrocytes are incubated with patient plasma, similar results are observed. Therefore, there is something present in the patient plasma (possible ULVWF) that causes clotting/aggregation. The treatment was done to speed up coagulation process and compare treated/untreated cells incubated with serum of SCD patients or healthy donors.

Fig 58 shows a comparison of plasma of patient and donor where samples were prepared with equal volumes of plasma and reducing sample buffer, heated for 15 minutes at 60° C. Basic unit of vWF is a dimer of two 250kDa subunits. Single subunits of 250kDa are visible in patient as well as donor samples. In patient samples, extra bands visible above the 250kDa band. This complies with the what is known previously about vWF existing in the form of ULWVF in sickle cell disease patient plasma.

Due to limited supply of SCD patient blood, other methods were incorporated to study the role of ULVWF in SCD. It has been shown in the past that activated endothelial cells (EC) release ULVWF which mediate adhesion of erythrocytes flowing over the layer of cells. So as a follow up step, adhesion of healthy erythrocytes activated by a calcium influx to endothelial cells were recorded. Flow assays were carried out to check adhesion of healthy erythrocytes activated by a calcium influx to histamine-stimulated endothelial cells. In SCD, erythrocytes have been proven to adhere to EC enhanced by ULVWF. It was expected to see that calcium loaded RBCs strongly adhere to histamine-stimulated primary ECs. Major goal was to confirm that adhesion is mediated by ULVWF by measuring firm adhesion of erythrocytes using a flow chamber assay in the presence of shear stress.

Ionomycin treated erythrocytes seem to adhere to the HUVECs layer (Fig 59 & 60). However, this experiment could not be quantified as the HUVECs monolayer was not confluent enough and this experiment needs to be repeated. Several experiments were conducted for more than a month to optimize the flow assay. HUVECs reached a good confluency and the assay work. However, adhesion

was not observed. The absence of adherence could be because of patient treatment with hydroxyurea. This information was not provided at the time of the experiments but is something that's needs to be looked into. Hydroxyurea is a drug that has been proven to benefit in sickle cell disease. And in the past, it has been proven to decrease erythrocyte adhesion to laminin [180].

The aim was to confirm that ULVWF is what causes adherence of calcium-loaded erythrocytes to endothelial cells, and also the reason for normal RBCs as well as sickle RBCs to coagulate when incubated with plasma from SCD patient. Something to look into is what is causing these ULVWF from not being cleaved. Aggregation involves platelet activation and clotting further involves deposition and maturation of fibrin. It is however, not known which inhibitors the clots are sensitive towards. In future research being continued at Sanquin, aggregates can be isolated and blotted for vWF, fibrin and other clotting factors. By testing the stability of aggregates and clots to several drugs such as Aggrastat, Pefabloc and Hirudin, a new potential therapy to avoid coagulation and vaso-occlusion in SCD could be introduced. Furthermore, a study can be done to evaluate protein 4.1a/4.1b ratios before and after treatment of sickle cells with the various anti-coagulant drugs. This could provide some information about the changes occurring in the membrane skeleton due to sickle cell disease.

Chapter 4.4: G6PD deficiency

G6PD: transformation, activity and concentration

Research aim was to develop a flowcytometry test that can determine the fraction of G6PD positive and G6PD deficient RBC in female carriers. Cytofluorometric assay was based on a methaemoglobine reduction method, the principle explained elsewhere [197]. The results of the flowcytometry test shown in Fig 61 were consistent with the G6PD activity determined by the diagnostic lab. Therefore, the cytofluorometric assay was found to be a reliable assay to diagnose carriers of G6PD deficiency.

The research question was if it is possible to correct G6PD deficiency through protein transduction. G6PD from different batches can be seen on Coomassie and Western Blot in Fig 62 & 63. G6PD activity shown in Fig 64 is too low in the eluted sample. Most active G6PD is in Flow Through 1. Low quantity of protein in eluted samples. Most protein is in Flow Through 1 as shown in Fig 65.

Problems faced were that the concentration and the activity of the TAT-G6PD was very low and majority of the protein remained in the pellet instead of the supernatant. Protein precipitation occured while changing buffer (pH of elution buffer needed to be corrected according to the isoelectric point of the G6PD) [198]. Isoelectric point is pH at which the amino acids does not migrate in an electric field. It is the pH at which the amino acid is neutral. It was found out that His-tagged proteins bind best to Ni-agarose resin if the pH is slightly basic (7.8-8). If the pH gets more acidic, the Histidine residues get protonated and therefore not bind to Ni^{2+} resin anymore.

The isoelectric point of the enzyme G6PD was found to be 6.3-6.4 from previous studies by the diagnostic group. The buffers used for the elution of protein of interest (G6PD) were then adjusted to pH 5.3-5.4 that was 1 unit less than the isoelectric point. For proteins prepared with the old buffers, the samples were dialyzed overnight in the new buffers.

Upon adjusting the pH of the buffers, a lot of protein was still in flow through 1. Fig 66 shows the protein concentration of all batches of protein eluted after changing isoelectric point of the buffers used in the Ni-NTA columns. Most protein is still in Flow Through 1. But the protein concentration increased compared to earlier batches.

Transduction: FACS results (preliminary data)

Several batches of proteins were then prepared, eluted and dialyzed to PBS pH 7.4. The protein concentration was very low so 10 ml of the solution was concentrated using a centrifugal concentrator falcon tube followed by transduction TAT-G6PD into G6PD deficient RBC. (Transduction method not included here). In the past TAT-G6PD was successfully transduced in to 20,8% of the RBC. A cytofluorometric assay was performed on the transduced RBC.

The control sample with no G6PD is still very positive. The blood was not taken from a patient with G6PD deficiency, but a healthy donor. So, the background is almost high as the G6PD sample because there is already G6PD present. There is a 23% increase in G6PD positive cells in the transduced population (Fig 67 & 68). The results from the FIX & PERM Cell Permeabilization assay (not shown), show high background in the control (with no G6PD) as compared to the G6PD sample. The results are preliminary and the assay needs to be optimized. Further study on this topic is being conducted by a fellow student at Sanquin.

Conclusions and Future Scope

Protein 4.1

The major function of protein 4.1 is stabilizing cell shape and providing deformability and mechanical stability to the cell. Past observations suggest that protein 4.1a ratio to protein 4.1b increases with erythrocyte aging. Constructed on these evidences, studies were designed to find out more about the conversion of protein 4.1b to 4.1a. The two bands of protein 4.1 were studied on a protein level as well as peptide level. MALDI TOF analysis was done to confirm the sequences of the 2 isoforms of protein 4.1 and it corresponded to previously known information about deamidation of specific amino acid residues. Several different experiments were carried out to get more insight into the mechanism of the deamidation, where a few were inconclusive. Since protein 4.1 is bound to other proteins such as spectrin, actin, band 3, glycophorin, calmodulin and myosin, therefore, insight into the role of deamidation of 4.1 can unravel biological significance of how this post translational modification affect its interaction with other proteins. There are high chances that protein 4.1 deamidation modifies other proteins too.

Within the partnership, quantification of 4.1a/4.1b ratio is being used to investigate changes imparted on RBCs by sport and exercise, or of the properties of RBCs from subjects exposed to peculiar environmental conditions such as high-altitude hypoxia. The primary aim of this project was to provide comprehensive knowledge of protein 4.1 which has been classified as the best erythrocyte age marker. Deamidation is a common reaction that takes place in a time-dependent manner at physiological temperature and pH and there are high chances that it modifies other proteins too. Therefore, the role of deamidation of 4.1 is vital to get a deeper understanding of red blood cell physiology. The project also aimed to answer questions as to why specifically neocytes are and how is it related to the decrease in EPO levels. Analysis of the changes in protein 4.1 of RBCs isolated from mountain climbers in a separate study will shed some light on this issue.

It is still needed to confirm that deamidation of residue 502 is the only reason for the difference in molecular weight of the two isoforms. The CD measurements of the peptides showed that the two forms were unstructured and that no striking difference appeared between them. Thus, the role of 4.1 deamidations is vital to get a deeper understanding of red blood cell physiology with a detailed protein and peptide level study. It would be thought-provoking to find out if the ratio gets altered in diseases such as ovalocytosis and spherocytosis resulting in shortened erythrocyte lifespan.

Quantification of 4.1a/4.1b ratio is easily carried out in Coomassie-stained gels or by Western blotting. As the protein ratio 4.1a/4.1b can be used in the approximation of the age of erythrocyte population, it has the potential to substitute for invasive techniques of cell labeling that can generate artefacts. There are possibilities of the ratio to shed light over the aging situation of RBCs at a given time point in healthy donors and also in patients. One of the goals of this project was to study physiological factors that may affect the life span of RBCs. Human RBCs of different age were studied to gain a deeper insight into the biochemical alterations that RBCs undergo as they age in the circulation with a particular focus on the neocytolytic process. The preliminary results shared in this thesis were used as a foundation for another project.

Study of Animal Erythrocytes

There have been several morphometric studies of different animals reported in the past. The basis of these studies was on linear measurements of erythrocyte size, viscosity and aggregation. A study based on the characterization of erythrocytes by comparing old and young cells from the same animal has not been conducted in the past. This aspect brings novelty to the current study. The work depicted here was designed to investigate changes observed in animal erythrocytes with age. The study of erythrocyte morphology in animals was done along with flow cytometry to compare membrane receptors between young and old cell populations. Measurements of several markers of aging were carried out as a comparison between young and old cells: ions (Na^+ & K^+), water, ATP, redox balance (GSH/GSSG), EMA binding, CD71 levels, and intracellular Ca^{2+} levels. One of the major achievements of this study was preparation of a buffer specifically made for sodium loaded canine erythrocytes to reduce hemolysis while handling.

The data from animal blood experiments provided in this thesis provides a basis for the possibility of further experiments in profiling animal erythrocytes, adding on to existing knowledge about their markers of aging and also major differences amongst different species. With more information about the circulation of erythrocytes in animals, storage can be improvised. The flow cytometry experiments done for bovine, equine and canine erythrocytes gave meaningful data in terms of markers of again in young and old erythrocytes. A perfect separation of cells according to density was obtained by several trials of varying concentration of Percoll as well as centrifugation conditions.

Future prospects of continuation of the study could lead to optimization for better erythrocyte storage and transfusion. Protein 4.1a/4.1b is classified a reliable cell age marker, however it was not possible

to measure in the animal samples obtained. Fig 70 shows an interesting distribution of the life span of erythrocytes in different species as well as 4.1a/4.1b ratios observed in whole blood. With an improved protocol to prepared erythrocyte membranes in the future, it will be interesting to check the ratios in cells of different age and also in commonly known pathologies.

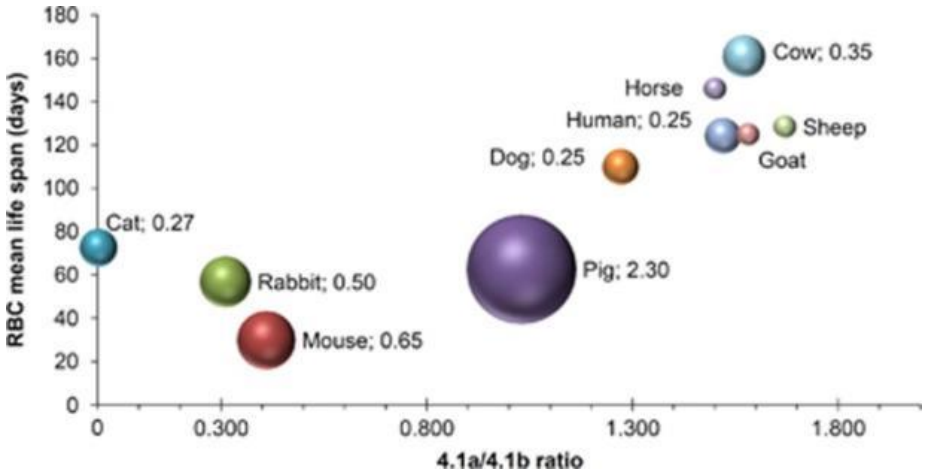

Figure 70. *Summary of protein 4.1a/4.1b ratio in different species of mammals [199].*

Dynamics of Erythrocytes & von Willebrand factor in Sickle Cell Disease

The first side project done at Sanquin discusses the involvement of von Willebrand factor in the severity of Sickle Cell Disease. It had been shown that healthy erythrocytes do not normally bind to the endothelial cells lining the vascular wall. Erythrocyte adhesion does occur in several hematologic disorders especially in sickle (SS) cell disease, due to von Willebrand factor multimers. When neuraminidase treated patient erythrocytes were incubated with serum from SCD patient, clots were observed. When healthy donor erythrocytes are incubated with patient plasma, similar results are observed. However, there was not always enough sickle cell plasma for these experiments and this was one of the main limitations experienced. Other method that was incorporated to study the role of ULVWF in SCD was live time imaging and recording of adhesion of healthy erythrocytes activated by a calcium influx to endothelial cells activated by histamine. These flow assays were conducted several times and needed optimization. With every experiment, the endothelial cells needed five days to grow before addition of cytokine (TNFα). The microscope and flow assay chamber with an inbuilt incubator had to be booked much in advance as it is in the shared facility of the department. Despite thorough literature search and protocol planning, not a lot of data was collected for this side project due to technical issues and time restraint. Since the study will be continued, the results obtained will be providing as a preliminary base for reference.

G6PD deficiency

The second side project was based on the correction of Glucose-6-phosphate dehydrogenase (G6PD) deficiency through protein transduction. Several batches of G6PD were produced by expression in BL21 bacteria and the activity as well as concentration of the proteins were measured. A preliminary experiment for transduction was conducted. There were some limitations to the experiments but overall it provided a base for a further study being carried out by another student at red cell group at Sanquin. By discussing the results and experiment approach with experts in the field, suggestions were given for improvement which creates opportunity for progress in the future. Use of a different bacterial system that has already been successfully used for protein expression will be incorporated into the protocol. The bacterial cell line is available through one of the partner institutes in Bristol, UK. It was not possible to acquire these cells during the planned secondment due to time constraints. Following further experiments, aggregates will be checked with HPLC within Sanquin facility. There are possibilities of better protein extraction methods, however a possibility of using zwitterion was eliminated as it is known to affect protein activity. As inclusions bodies were observed, chaperones could be used in order to elongate the protein in bacterial cells.

References

1. Arivis. *Relevance consortium project in brief*. Available from: http://relevance.arivis.com/.
2. Inaba, M., et al., *Deamidation of human erythrocyte protein 4.1: possible role in aging.* Blood, 1992. **79**(12): p. 3355-61.
3. Minetti, G., et al., *Cell age-related monovalent cations content and density changes in stored human erythrocytes.* Biochim Biophys Acta, 2001. **1527**(3): p. 149-55.
4. Stephen N. Sarikas, W.C.O., *Laboratory Investigations in Anatomy & Physiology*. 2006: Pearson Benjamin Cummings.
5. Kaestner, L. and A. Bogdanova, *Regulation of red cell life-span, erythropoiesis, senescence, and clearance.* Front Physiol, 2014. **5**: p. 269.
6. Beutler, E., *Red cell metabolism: a manual of biochemical methods*. 2 ed. 1975: Grune & Stratton. 160.
7. An, X. and N. Mohandas, *Erythroblastic islands, terminal erythroid differentiation and reticulocyte maturation.* Int J Hematol, 2011. **93**(2): p. 139-143.
8. Tauzin, L., V. Campos, and M. Tichet, *Cellular endogenous NAD(P)H fluorescence as a label-free method for the identification of erythrocytes and reticulocytes.* Cytometry A, 2018. **93**(4): p. 472-479.
9. Fisher, J.W., et al., *Erythropoietin production by interstitial cells of hypoxic monkey kidneys.* Br J Haematol, 1996. **95**(1): p. 27-32.
10. Naets, J.P. and M. Wittek, *Erythropoiesis in anephric man.* Lancet, 1968. **1**(7549): p. 941-3.
11. Ji, P., M. Murata-Hori, and H.F. Lodish, *Formation of mammalian erythrocytes: chromatin condensation and enucleation.* Trends Cell Biol, 2011. **21**(7): p. 409-15.
12. Bessis, M., *[Erythroblastic island, functional unity of bone marrow].* Rev Hematol, 1958. **13**(1): p. 8-11.
13. Bessis, M.C. and J. Breton-Gorius, *Iron metabolism in the bone marrow as seen by electron microscopy: a critical review.* Blood, 1962. **19**: p. 635-63.
14. Lehninger AL, N.D., *Lehninger's Principles of Biochemistry*. 5 ed. 2008: Freeman, New York.
15. Huisjes, R., et al., *Squeezing for Life - Properties of Red Blood Cell Deformability.* Front Physiol, 2018. **9**: p. 656.
16. Nelson, R.A., Jr., *The immune-adherence phenomenon; an immunologically specific reaction between microorganisms and erythrocytes leading to enhanced phagocytosis.* Science, 1953. **118**(3077): p. 733-7.

17. Aminoff, D., A. Rolfes-Curl, and E. Supina, *Molecular biomarkers of aging: the red cell as a model.* Arch Gerontol Geriatr, 1992. **15 Suppl 1**: p. 7-15.
18. Willekens, F.L., et al., *Hemoglobin loss from erythrocytes in vivo results from spleen-facilitated vesiculation.* Blood, 2003. **101**(2): p. 747-51.
19. Piomelli, S. and C. Seaman, *Mechanism of red blood cell aging: relationship of cell density and cell age.* Am J Hematol, 1993. **42**(1): p. 46-52.
20. Bosch, F.H., et al., *Characteristics of red blood cell populations fractionated with a combination of counterflow centrifugation and Percoll separation.* Blood, 1992. **79**(1): p. 254-60.
21. Lutz, H.U., et al., *Density separation of human red blood cells on self forming Percoll gradients: correlation with cell age.* Biochim Biophys Acta, 1992. **1116**(1): p. 1-10.
22. Mueller, T.J., et al., *Membrane skeletal alterations during in vivo mouse red cell aging. Increase in the band 4.1a:4.1b ratio.* J Clin Invest, 1987. **79**(2): p. 492-9.
23. Mebius, R.E. and G. Kraal, *Structure and function of the spleen.* Nat Rev Immunol, 2005. **5**(8): p. 606-16.
24. Arias, C.F. and C.F. Arias, *How do red blood cells know when to die?* R Soc Open Sci, 2017. **4**(4): p. 160850.
25. Han, B.G., et al., *Protein 4.1R core domain structure and insights into regulation of cytoskeletal organization.* Nat Struct Biol, 2000. **7**(10): p. 871-5.
26. BERKELEY, U.O.C.-. *The amazing flexibility of red blood cells*. Super-resolution microscopy reveals fine detail of cellular mesh underlying cell membrane, 2018.
27. Lux, S.E.t., *Anatomy of the red cell membrane skeleton: unanswered questions.* Blood, 2016. **127**(2): p. 187-99.
28. Diakowski, W., M. Grzybek, and A.F. Sikorski, *Protein 4.1, a component of the erythrocyte membrane skeleton and its related homologue proteins forming the protein 4.1/FERM superfamily.* Folia Histochem Cytobiol, 2006. **44**(4): p. 231-48.
29. Leto, T.L. and V.T. Marchesi, *A structural model of human erythrocyte protein 4.1.* J Biol Chem, 1984. **259**(7): p. 4603-8.
30. Goodman, S.R., et al., *Erythrocyte membrane skeletal protein bands 4.1 a and b are sequence-related phosphoproteins.* J Biol Chem, 1982. **257**(8): p. 4564-9.
31. Tchernia, G., N. Mohandas, and S.B. Shohet, *Deficiency of skeletal membrane protein band 4.1 in homozygous hereditary elliptocytosis. Implications for erythrocyte membrane stability.* J Clin Invest, 1981. **68**(2): p. 454-60.

32. Takakuwa, Y., et al., *Restoration of normal membrane stability to unstable protein 4.1-deficient erythrocyte membranes by incorporation of purified protein 4.1.* J Clin Invest, 1986. **78**(1): p. 80-5.
33. Noah E. Robinson, A.B.R., *Molecular Clocks: Deamidation of Asparaginyl and Glutaminyl Residues in Peptides and Proteins*. 2004: Althouse Press. 419.
34. Baines, A.J., H.C. Lu, and P.M. Bennett, *The Protein 4.1 family: hub proteins in animals for organizing membrane proteins.* Biochim Biophys Acta, 2014. **1838**(2): p. 605-19.
35. Scott, C., G.W. Phillips, and A.J. Baines, *Properties of the C-terminal domain of 4.1 proteins.* Eur J Biochem, 2001. **268**(13): p. 3709-17.
36. Risso, A., et al., *Neocytolysis: none, one or many? A reappraisal and future perspectives.* Front Physiol, 2014. **5**: p. 54.
37. Palek, J., *Hereditary elliptocytosis, spherocytosis and related disorders: consequences of a deficiency or a mutation of membrane skeletal proteins.* Blood Rev, 1987. **1**(3): p. 147-68.
38. Goodman, S.R., et al., *Identification of the molecular defect in the erythrocyte membrane skeleton of some kindreds with hereditary spherocytosis.* Blood, 1982. **60**(3): p. 772-84.
39. Adili, N., M. Melizi, and H. Belabbas, *Species determination using the red blood cells morphometry in domestic animals.* Vet World, 2016. **9**(9): p. 960-963.
40. Symons, M. and K. Bell, *Expansion of the canine A blood group system.* Anim Genet, 1991. **22**(3): p. 227-35.
41. Symons, M. and K. Bell, *Canine blood groups: description of 20 specificities.* Anim Genet, 1992. **23**(6): p. 509-15.
42. Knottenbelt, C.M., et al., *Determination of the prevalence of feline blood types in the UK.* J Small Anim Pract, 1999. **40**(3): p. 115-8.
43. Bodey, A.R. and M.W. Rampling, *A comparative study of the haemorheology of various breeds of dog.* Clin Hemorheol Microcirc, 1998. **18**(4): p. 291-8.
44. Windberger, U., et al., *Whole blood viscosity, plasma viscosity and erythrocyte aggregation in nine mammalian species: reference values and comparison of data.* Exp Physiol, 2003. **88**(3): p. 431-40.
45. Stoiber, B., et al., *Whole blood, plasma viscosity, and erythrocyte aggregation as a determining factor of competitiveness in standard bred trotters.* Clin Hemorheol Microcirc, 2005. **32**(1): p. 31-41.
46. Gibson, J.S., et al., *Volume-sensitive KCl co-transport and taurine fluxes in horse red blood cells.* Exp Physiol, 1993. **78**(5): p. 685-95.

47. Matei, H., L. Frentescu, and G. Benga, *Comparative studies of the protein composition of red blood cell membranes from eight mammalian species.* J Cell Mol Med, 2000. **4**(4): p. 270-276.
48. Inaba, M. and Y. Maede, *Correlation between protein 4.1a/4.1b ratio and erythrocyte life span.* Biochim Biophys Acta, 1988. **944**(2): p. 256-64.
49. Rettig, M.P., et al., *Evaluation of biochemical changes during in vivo erythrocyte senescence in the dog.* Blood, 1999. **93**(1): p. 376-84.
50. Kiefer, C.R. and L.M. Snyder, *Oxidation and erythrocyte senescence.* Curr Opin Hematol, 2000. **7**(2): p. 113-6.
51. Tellone, E., et al., *Oxidative effects of gemfibrozil on anion influx and metabolism in normal and Beta-thalassemic erythrocytes: physiological implications.* J Membr Biol, 2008. **224**(1-3): p. 1-8.
52. Snyder, L.M., et al., *Demonstration of haemoglobin associated with isolated, purified spectrin from senescent human red cells.* Br J Haematol, 1985. **61**(3): p. 415-9.
53. Snyder, L.M., et al., *Irreversible spectrin-haemoglobin crosslinking in vivo: a marker for red cell senescence.* Br J Haematol, 1983. **53**(3): p. 379-84.
54. Fortier, N., et al., *The relationship between in vivo generated hemoglobin skeletal protein complex and increased red cell membrane rigidity.* Blood, 1988. **71**(5): p. 1427-31.
55. Bernabucci, U., et al., *Markers of oxidative status in plasma and erythrocytes of transition dairy cows during hot season.* J Dairy Sci, 2002. **85**(9): p. 2173-9.
56. Snow, D.H. and V. Martin, *Effects of exercise and adrenaline on equine erythrocyte ATP content.* Res Vet Sci, 1990. **49**(1): p. 77-81.
57. Bachmann, A.W., et al., *Erythrocyte adenosine triphosphate levels in cattle infected with Babesia argentina.* Tropenmed Parasitol, 1976. **27**(3): p. 372-6.
58. Mandal, D., et al., *Fas-, caspase 8-, and caspase 3-dependent signaling regulates the activity of the aminophospholipid translocase and phosphatidylserine externalization in human erythrocytes.* J Biol Chem, 2005. **280**(47): p. 39460-7.
59. Willekens, F.L., et al., *Erythrocyte vesiculation: a self-protective mechanism?* Br J Haematol, 2008. **141**(4): p. 549-56.
60. Lang, F., et al., *Mechanisms and significance of eryptosis.* Antioxid Redox Signal, 2006. **8**(7-8): p. 1183-92.
61. Connor, J., C.C. Pak, and A.J. Schroit, *Exposure of phosphatidylserine in the outer leaflet of human red blood cells. Relationship to cell density, cell age, and clearance by mononuclear cells.* J Biol Chem, 1994. **269**(4): p. 2399-404.

62. Pantaleo, A., et al., *Naturally occurring anti-band 3 antibodies and red blood cell removal under physiological and pathological conditions.* Autoimmun Rev, 2008. **7**(6): p. 457-62.
63. Kay, M., *Immunoregulation of cellular life span.* Ann N Y Acad Sci, 2005. **1057**: p. 85-111.
64. Kay, M.M., et al., *Band-3 polymers and aggregates, and hemoglobin precipitates in red cell aging.* Blood Cells, 1988. **14**(1): p. 275-95.
65. Aponte-Santamaria, C., et al., *Force-sensitive autoinhibition of the von Willebrand factor is mediated by interdomain interactions.* Biophys J, 2015. **108**(9): p. 2312-21.
66. Davie, E.W. and O.D. Ratnoff, *Waterfall Sequence for Intrinsic Blood Clotting.* Science, 1964. **145**(3638): p. 1310-2.
67. Macfarlane, R.G., *An Enzyme Cascade in the Blood Clotting Mechanism, and Its Function as a Biochemical Amplifier.* Nature, 1964. **202**: p. 498-9.
68. Versteeg, H.H., et al., *New fundamentals in hemostasis.* Physiol Rev, 2013. **93**(1): p. 327-58.
69. Kuijpers, M.J., et al., *Complementary roles of glycoprotein VI and alpha2beta1 integrin in collagen-induced thrombus formation in flowing whole blood ex vivo.* FASEB J, 2003. **17**(6): p. 685-7.
70. Morton, L.F. and M.J. Barnes, *Collagen polymorphism in the normal and diseased blood vessel wall. Investigation of collagens types I, III and V.* Atherosclerosis, 1982. **42**(1): p. 41-51.
71. Santoro, S.A., *Identification of a 160,000 dalton platelet membrane protein that mediates the initial divalent cation-dependent adhesion of platelets to collagen.* Cell, 1986. **46**(6): p. 913-20.
72. Tandon, N.N., U. Kralisz, and G.A. Jamieson, *Identification of glycoprotein IV (CD36) as a primary receptor for platelet-collagen adhesion.* J Biol Chem, 1989. **264**(13): p. 7576-83.
73. Phillips, D.R., *An evaluation of membrane glycoproteins in platelet adhesion and aggregation.* Prog Hemost Thromb, 1980. **5**: p. 81-109.
74. Adachi, T., et al., *Identification of amino acid residues essential for heparin binding by the A1 domain of human von Willebrand factor.* Biochem Biophys Res Commun, 2006. **339**(4): p. 1178-83.
75. Titani, K., et al., *Amino acid sequence of human von Willebrand factor.* Biochemistry, 1986. **25**(11): p. 3171-84.
76. Lenting, P.J. and C.V. Denis, *Platelet von Willebrand factor: sweet resistance.* Blood, 2013. **122**(25): p. 4006-7.

77. Wagner, D.D., *Cell biology of von Willebrand factor.* Annu Rev Cell Biol, 1990. **6**: p. 217-46.
78. De Ceunynck, K., S.F. De Meyer, and K. Vanhoorelbeke, *Unwinding the von Willebrand factor strings puzzle.* Blood, 2013. **121**(2): p. 270-7.
79. Giblin, J.P., L.J. Hewlett, and M.J. Hannah, *Basal secretion of von Willebrand factor from human endothelial cells.* Blood, 2008. **112**(4): p. 957-64.
80. van Genderen, P.J., et al., *Acquired von Willebrand disease caused by an autoantibody selectively inhibiting the binding of von Willebrand factor to collagen.* Blood, 1994. **84**(10): p. 3378-84.
81. Cruz, M.A., et al., *Interaction of the von Willebrand factor (vWF) with collagen. Localization of the primary collagen-binding site by analysis of recombinant vWF a domain polypeptides.* J Biol Chem, 1995. **270**(18): p. 10822-7.
82. Tsuji, S., et al., *Role and initiation mechanism of the interaction of glycoprotein Ib with surface-immobilized von Willebrand factor in a solid-phase platelet cohesion process.* Blood, 1996. **88**(10): p. 3854-61.
83. Kroll, M.H., et al., *Platelets and shear stress.* Blood, 1996. **88**(5): p. 1525-41.
84. Levy, G.G., et al., *Mutations in a member of the ADAMTS gene family cause thrombotic thrombocytopenic purpura.* Nature, 2001. **413**(6855): p. 488-94.
85. Moake, J.L., et al., *Involvement of large plasma von Willebrand factor (vWF) multimers and unusually large vWF forms derived from endothelial cells in shear stress-induced platelet aggregation.* J Clin Invest, 1986. **78**(6): p. 1456-61.
86. Lenting, P.J., et al., *An experimental model to study the in vivo survival of von Willebrand factor. Basic aspects and application to the R1205H mutation.* J Biol Chem, 2004. **279**(13): p. 12102-9.
87. van Schooten, C.J., et al., *Macrophages contribute to the cellular uptake of von Willebrand factor and factor VIII in vivo.* Blood, 2008. **112**(5): p. 1704-12.
88. Varga-Szabo, D., A. Braun, and B. Nieswandt, *Calcium signaling in platelets.* J Thromb Haemost, 2009. **7**(7): p. 1057-66.
89. Ma, Y.Q., J. Qin, and E.F. Plow, *Platelet integrin alpha(IIb)beta(3): activation mechanisms.* J Thromb Haemost, 2007. **5**(7): p. 1345-52.
90. Moolenaar, W.H. and A. Perrakis, *Insights into autotaxin: how to produce and present a lipid mediator.* Nat Rev Mol Cell Biol, 2011. **12**(10): p. 674-9.
91. Bevers, E.M., et al., *Generation of prothrombin-converting activity and the exposure of phosphatidylserine at the outer surface of platelets.* Eur J Biochem, 1982. **122**(2): p. 429-36.

92. Kung, C., E. Hayes, and K.G. Mann, *A membrane-mediated catalytic event in prothrombin activation.* J Biol Chem, 1994. **269**(41): p. 25838-48.
93. Coughlin, S.R., *Thrombin signalling and protease-activated receptors.* Nature, 2000. **407**(6801): p. 258-64.
94. Cines, D.B., et al., *Clot contraction: compression of erythrocytes into tightly packed polyhedra and redistribution of platelets and fibrin.* Blood, 2014. **123**(10): p. 1596-603.
95. Hoffman, M. and D.M. Monroe, 3rd, *A cell-based model of hemostasis.* Thromb Haemost, 2001. **85**(6): p. 958-65.
96. Holmsen, H. and H.J. Day, *Thrombin-induced platelet release reaction and platelet lysosomes.* Nature, 1968. **219**(5155): p. 760-1.
97. Chesney, C.M., D. Pifer, and R.W. Colman, *Subcellular localization and secretion of factor V from human platelets.* Proc Natl Acad Sci U S A, 1981. **78**(8): p. 5180-4.
98. Monkovic, D.D. and P.B. Tracy, *Activation of human factor V by factor Xa and thrombin.* Biochemistry, 1990. **29**(5): p. 1118-28.
99. Monroe, D.M. and M. Hoffman, *What does it take to make the perfect clot?* Arterioscler Thromb Vasc Biol, 2006. **26**(1): p. 41-8.
100. Walsh, P.N., et al., *Functional characterization of platelet-bound factor XIa: retention of factor XIa activity on the platelet surface.* Blood, 1986. **68**(1): p. 225-30.
101. Lollar, P., G.J. Knutson, and D.N. Fass, *Stabilization of thrombin-activated porcine factor VIII:C by factor IXa phospholipid.* Blood, 1984. **63**(6): p. 1303-8.
102. Kattula, S., J.R. Byrnes, and A.S. Wolberg, *Fibrinogen and Fibrin in Hemostasis and Thrombosis.* Arterioscler Thromb Vasc Biol, 2017. **37**(3): p. e13-e21.
103. Verhoef, J.J., et al., *Polyphosphate nanoparticles on the platelet surface trigger contact system activation.* Blood, 2017. **129**(12): p. 1707-1717.
104. Huang, Z.F., T.C. Wun, and G.J. Broze, Jr., *Kinetics of factor Xa inhibition by tissue factor pathway inhibitor.* J Biol Chem, 1993. **268**(36): p. 26950-5.
105. Pedersen, A.H., et al., *Recombinant human extrinsic pathway inhibitor. Production, isolation, and characterization of its inhibitory activity on tissue factor-initiated coagulation reactions.* J Biol Chem, 1990. **265**(28): p. 16786-93.
106. Rao, L.V. and W. Ruf, *Tissue factor residues Lys165 and Lys166 are essential for rapid formation of the quaternary complex of tissue factor.VIIa with Xa.tissue factor pathway inhibitor.* Biochemistry, 1995. **34**(34): p. 10867-71.
107. Suzuki, K., et al., *Inactivation of human coagulation factor V by activated protein C.* J Biol Chem, 1983. **258**(3): p. 1914-20.

108. Marlar, R.A., A.J. Kleiss, and J.H. Griffin, *Mechanism of action of human activated protein C, a thrombin-dependent anticoagulant enzyme.* Blood, 1982. **59**(5): p. 1067-72.
109. Kumar, R. and M. Carcao, *Inherited abnormalities of coagulation: hemophilia, von Willebrand disease, and beyond.* Pediatr Clin North Am, 2013. **60**(6): p. 1419-41.
110. van Ommen, C.H. and M. Peters, *The bleeding child. Part I: primary hemostatic disorders.* Eur J Pediatr, 2012. **171**(1): p. 1-10.
111. Rodeghiero, F., G. Castaman, and E. Dini, *Epidemiological investigation of the prevalence of von Willebrand's disease.* Blood, 1987. **69**(2): p. 454-9.
112. Goodeve, A.C., *The genetic basis of von Willebrand disease.* Blood Rev, 2010. **24**(3): p. 123-34.
113. Ingram, V.M., *Gene mutations in human haemoglobin: the chemical difference between normal and sickle cell haemoglobin.* Nature, 1957. **180**(4581): p. 326-8.
114. Hebbel, R.P., et al., *Abnormal adherence of sickle erythrocytes to cultured vascular endothelium: possible mechanism for microvascular occlusion in sickle cell disease.* J Clin Invest, 1980. **65**(1): p. 154-60.
115. Schwartz, R.S., et al., *Increased adherence of sickled and phosphatidylserine-enriched human erythrocytes to cultured human peripheral blood monocytes.* J Clin Invest, 1985. **75**(6): p. 1965-72.
116. Kato, G.J., et al., *Lactate dehydrogenase as a biomarker of hemolysis-associated nitric oxide resistance, priapism, leg ulceration, pulmonary hypertension, and death in patients with sickle cell disease.* Blood, 2006. **107**(6): p. 2279-85.
117. Chen, J. and J.A. Lopez, *Interactions of platelets with subendothelium and endothelium.* Microcirculation, 2005. **12**(3): p. 235-46.
118. Arya, M., et al., *Ultralarge multimers of von Willebrand factor form spontaneous high-strength bonds with the platelet glycoprotein Ib-IX complex: studies using optical tweezers.* Blood, 2002. **99**(11): p. 3971-7.
119. Dong, J.F., et al., *ADAMTS-13 rapidly cleaves newly secreted ultralarge von Willebrand factor multimers on the endothelial surface under flowing conditions.* Blood, 2002. **100**(12): p. 4033-9.
120. Kaul, D.K., et al., *Sickle erythrocyte-endothelial interactions in microcirculation: the role of von Willebrand factor and implications for vasoocclusion.* Blood, 1993. **81**(9): p. 2429-38.
121. Mohandas, N. and E. Evans, *Sickle erythrocyte adherence to vascular endothelium. Morphologic correlates and the requirement for divalent cations and collagen-binding plasma proteins.* J Clin Invest, 1985. **76**(4): p. 1605-12.

122. Moake, J.L., et al., *Unusually large plasma factor VIII:von Willebrand factor multimers in chronic relapsing thrombotic thrombocytopenic purpura.* N Engl J Med, 1982. **307**(23): p. 1432-5.
123. Krishnan, S., et al., *Increased von Willebrand factor antigen and high molecular weight multimers in sickle cell disease associated with nocturnal hypoxemia.* Thromb Res, 2008. **122**(4): p. 455-8.
124. Schnog, J.J., et al., *ADAMTS13 activity in sickle cell disease.* Am J Hematol, 2006. **81**(7): p. 492-8.
125. Hovav, T., et al., *Enhanced adherence of beta-thalassaemic erythrocytes to endothelial cells.* Br J Haematol, 1999. **106**(1): p. 178-81.
126. Wautier, M.P., et al., *Increased adhesion to endothelial cells of erythrocytes from patients with polycythemia vera is mediated by laminin alpha5 chain and Lu/BCAM.* Blood, 2007. **110**(3): p. 894-901.
127. Smith, B.D. and G.B. Segel, *Abnormal erythrocyte endothelial adherence in hereditary stomatocytosis.* Blood, 1997. **89**(9): p. 3451-6.
128. Stuart, M.J. and R.L. Nagel, *Sickle-cell disease.* Lancet, 2004. **364**(9442): p. 1343-60.
129. Hebbel, R.P., et al., *Erythrocyte adherence to endothelium in sickle-cell anemia. A possible determinant of disease severity.* N Engl J Med, 1980. **302**(18): p. 992-5.
130. Wick, T.M., et al., *Unusually large von Willebrand factor multimers increase adhesion of sickle erythrocytes to human endothelial cells under controlled flow.* J Clin Invest, 1987. **80**(3): p. 905-10.
131. Chen, J., et al., *The rate of hemolysis in sickle cell disease correlates with the quantity of active von Willebrand factor in the plasma.* Blood, 2011. **117**(13): p. 3680-3.
132. Vahidkhah, K., S.L. Diamond, and P. Bagchi, *Platelet dynamics in three-dimensional simulation of whole blood.* Biophys J, 2014. **106**(11): p. 2529-40.
133. Murugappa, S. and S.P. Kunapuli, *The role of ADP receptors in platelet function.* Front Biosci, 2006. **11**: p. 1977-86.
134. Valles, J., et al., *Erythrocytes metabolically enhance collagen-induced platelet responsiveness via increased thromboxane production, adenosine diphosphate release, and recruitment.* Blood, 1991. **78**(1): p. 154-62.
135. Burger, P., et al., *Potassium leakage primes stored erythrocytes for phosphatidylserine exposure and shedding of pro-coagulant vesicles.* Br J Haematol, 2013. **160**(3): p. 377-86.
136. Rubin, O., et al., *Red blood cell-derived microparticles isolated from blood units initiate and propagate thrombin generation.* Transfusion, 2013. **53**(8): p. 1744-54.

137. Ibrahim, H.A., et al., *Erythrocyte phosphatidylserine exposure in beta-thalassemia.* Lab Hematol, 2014. **20**(2): p. 9-14.
138. Wood, B.L., D.F. Gibson, and J.F. Tait, *Increased erythrocyte phosphatidylserine exposure in sickle cell disease: flow-cytometric measurement and clinical associations.* Blood, 1996. **88**(5): p. 1873-80.
139. Dinkla, S., et al., *Phosphatidylserine exposure on stored red blood cells as a parameter for donor-dependent variation in product quality.* Blood Transfus, 2014. **12**(2): p. 204-9.
140. Hermand, P., et al., *Red cell ICAM-4 is a novel ligand for platelet-activated alpha IIbbeta 3 integrin.* J Biol Chem, 2003. **278**(7): p. 4892-8.
141. Du, V.X., et al., *New insights into the role of erythrocytes in thrombus formation.* Semin Thromb Hemost, 2014. **40**(1): p. 72-80.
142. Relevy, H., et al., *Blood banking-induced alteration of red blood cell flow properties.* Transfusion, 2008. **48**(1): p. 136-46.
143. Metere, A., et al., *Carbon monoxide signaling in human red blood cells: evidence for pentose phosphate pathway activation and protein deglutathionylation.* Antioxid Redox Signal, 2014. **20**(3): p. 403-16.
144. Stincone, A., et al., *The return of metabolism: biochemistry and physiology of the pentose phosphate pathway.* Biol Rev Camb Philos Soc, 2015. **90**(3): p. 927-63.
145. Laurence Cole, P.R.K., *Human Physiology, Biochemistry and Basic Medicine*. Sugars, Fatty Acids, and Energy Biochemistry. 2016.
146. Wang, Y.P., et al., *Regulation of G6PD acetylation by SIRT2 and KAT9 modulates NADPH homeostasis and cell survival during oxidative stress.* EMBO J, 2014. **33**(12): p. 1304-20.
147. Ali, E.W. and E.E. Ahmed, *The role of erythrocyte enzyme glucose-6-phosphate dehydrogenase (G6PD) deficiency in the pathogenesis of anemia in patients on hemodialysis.* Saudi J Kidney Dis Transpl, 2013. **24**(6): p. 1153-6.
148. Jacobasch, G. and S.M. Rapoport, *Hemolytic anemias due to erythrocyte enzyme deficiencies.* Mol Aspects Med, 1996. **17**(2): p. 143-70.
149. Grace, R.F. and B. Glader, *Red Blood Cell Enzyme Disorders.* Pediatr Clin North Am, 2018. **65**(3): p. 579-595.
150. Vulliamy, T.J., et al., *Diverse point mutations in the human glucose-6-phosphate dehydrogenase gene cause enzyme deficiency and mild or severe hemolytic anemia.* Proc Natl Acad Sci U S A, 1988. **85**(14): p. 5171-5.

151. Peters, A.L. and C.J. Van Noorden, *Glucose-6-phosphate dehydrogenase deficiency and malaria: cytochemical detection of heterozygous G6PD deficiency in women.* J Histochem Cytochem, 2009. **57**(11): p. 1003-11.
152. van Wijk, R. and W.W. van Solinge, *The energy-less red blood cell is lost: erythrocyte enzyme abnormalities of glycolysis.* Blood, 2005. **106**(13): p. 4034-42.
153. Wiback, S.J. and B.O. Palsson, *Extreme pathway analysis of human red blood cell metabolism.* Biophys J, 2002. **83**(2): p. 808-18.
154. Suzuki, T., N.S. Agar, and M. Suzuki, *Red cell metabolism: a comparative study of some mammalian species.* Comp Biochem Physiol B, 1984. **79**(4): p. 515-20.
155. Rizvi, I., et al., *Acute life-threatening methaemoglobinaemia following ingestion of chloroquine.* BMJ Case Rep, 2012. **2012**.
156. Salvador, A., J. Sousa, and R.E. Pinto, *Hydroperoxyl, superoxide and pH gradients in the mitochondrial matrix: a theoretical assessment.* Free Radic Biol Med, 2001. **31**(10): p. 1208-15.
157. Kim, S.U. and F.A. Villamena, *Reactivities of superoxide and hydroperoxyl radicals with disubstituted cyclic nitrones: a DFT study.* J Phys Chem A, 2012. **116**(2): p. 886-98.
158. Ciana, A., et al., *On the association of lipid rafts to the spectrin skeleton in human erythrocytes.* Biochim Biophys Acta, 2011. **1808**(1): p. 183-90.
159. Dodge, J.T., C. Mitchell, and D.J. Hanahan, *The preparation and chemical characteristics of hemoglobin-free ghosts of human erythrocytes.* Arch Biochem Biophys, 1963. **100**: p. 119-30.
160. Laemmli, U.K., *Cleavage of structural proteins during the assembly of the head of bacteriophage T4.* Nature, 1970. **227**(5259): p. 680-5.
161. Ciana, A., C. Achilli, and G. Minetti, *Spectrin and Other Membrane-Skeletal Components in Human Red Blood Cells of Different Age.* Cell Physiol Biochem, 2017. **42**(3): p. 1139-1152.
162. Makhro, A., et al., *N-methyl-D-aspartate receptors in human erythroid precursor cells and in circulating red blood cells contribute to the intracellular calcium regulation.* Am J Physiol Cell Physiol, 2013. **305**(11): p. C1123-38.
163. Aitken A., L.M., *Estimation of Disulfide Bonds Using Ellman's Reagent*. 2009, Humana Press, Totowa, NJ.
164. Kaul, D.K., M.E. Fabry, and R.L. Nagel, *Microvascular sites and characteristics of sickle cell adhesion to vascular endothelium in shear flow conditions: pathophysiological implications.* Proc Natl Acad Sci U S A, 1989. **86**(9): p. 3356-60.

165. Froger, A. and J.E. Hall, *Transformation of plasmid DNA into E. coli using the heat shock method.* J Vis Exp, 2007(6): p. 253.
166. Scientific, T.F. *Pierce™ BCA Protein Assay Kit*. Available from: http://tools.thermofisher.com/content/sfs/manualsman0011430_pierce_bca_protein_asy_ug.pdf.
167. Mairbaurl, H., *Neocytolysis: How to Get Rid of the Extra Erythrocytes Formed by Stress Erythropoiesis Upon Descent From High Altitude.* Front Physiol, 2018. **9**: p. 345.
168. Snyder, L.M., et al., *Partition of catalase and its peroxidase activities in human red cell membrane: effect of ATP depletion.* Biochim Biophys Acta, 1977. **470**(2): p. 290-302.
169. Eshdat, Y. and A. Prujansky-Jakobovits, *Isolation of human erythrocyte membranes and their outer surface proteins by covalent fractionation on solid support.* FEBS Lett, 1979. **101**(1): p. 43-6.
170. Kampf, S., et al., *Aging Markers in Equine Red Blood Cells.* Front Physiol, 2019. **10**: p. 893.
171. Sheppard, C.W., W.R. Martin, and G. Beyl, *Cation exchange between cells and plasma of mammalian blood. II. Sodium and potassium exchange in the sheep, dog, cow, and man and the effect of varying the plasma potassium concentration.* J Gen Physiol, 1951. **34**(4): p. 411-29.
172. Fowler, M., *Medicine and Surgery of Camelids*. Wiley-Blackwell.
173. Riechers, A., et al., *Detection of protein phosphorylation on SDS-PAGE using probes with a phosphate-sensitive emission response.* Bioconjug Chem, 2009. **20**(4): p. 804-7.
174. Sodhi, K., et al., *The Na/K-ATPase Oxidant Amplification Loop Regulates Aging.* Sci Rep, 2018. **8**(1): p. 9721.
175. Parker, J.C., *Dog red blood cells. Adjustment of salt and water content in vitro.* J Gen Physiol, 1973. **62**(2): p. 147-56.
176. Shapiro, H.M., *Flow Cytometry: The Glass Is Half Full.* Methods Mol Biol, 2018. **1678**: p. 1-10.
177. Abraham, R.S. and G. Aubert, *Flow Cytometry, a Versatile Tool for Diagnosis and Monitoring of Primary Immunodeficiencies.* Clin Vaccine Immunol, 2016. **23**(4): p. 254-71.
178. Novelli, E.M. and M.T. Gladwin, *Crises in Sickle Cell Disease.* Chest, 2016. **149**(4): p. 1082-93.
179. Dong, J.F., *Cleavage of ultra-large von Willebrand factor by ADAMTS-13 under flow conditions.* J Thromb Haemost, 2005. **3**(8): p. 1710-6.

180. Bartolucci, P., et al., *Decreased sickle red blood cell adhesion to laminin by hydroxyurea is associated with inhibition of Lu/BCAM protein phosphorylation.* Blood, 2010. **116**(12): p. 2152-9.
181. Ford, K.G., et al., *Protein transduction: an alternative to genetic intervention?* Gene Ther, 2001. **8**(1): p. 1-4.
182. Jonges, G.N., et al., *Comparison between the chromate inhibition test and a cytochemical method for the determination of glucose-6-phosphate dehydrogenase deficiency in erythrocytes.* Clin Chim Acta, 1989. **181**(2): p. 135-41.
183. Cavana, P., et al., *Severe Heinz body anemia and methemoglobinemia in a kitten with chronic diarrhea.* Schweiz Arch Tierheilkd, 2018. **160**(4): p. 235-239.
184. Caprette, D.R. *Preparing Protein Samples for Electrophoresis*. [cited 1996 19 August]; Available from: https://www.ruf.rice.edu/~bioslabs/studies/sds-page/denature.html.
185. Cooper, C., W. Sears, and D. Bienzle, *Reticulocyte changes after experimental anemia and erythropoietin treatment of horses.* J Appl Physiol (1985), 2005. **99**(3): p. 915-21.
186. Parker, J.C., *Dog red blood cells. Adjustment of density in vivo.* J Gen Physiol, 1973. **61**(2): p. 146-57.
187. Mohanty, J.G., E. Nagababu, and J.M. Rifkind, *Red blood cell oxidative stress impairs oxygen delivery and induces red blood cell aging.* Front Physiol, 2014. **5**: p. 84.
188. Burton, G.J. and E. Jauniaux, *Oxidative stress.* Best Pract Res Clin Obstet Gynaecol, 2011. **25**(3): p. 287-99.
189. Hinrichs, G.R., et al., *Amiloride resolves resistant edema and hypertension in a patient with nephrotic syndrome; a case report.* Physiol Rep, 2018. **6**(12): p. e13743.
190. Tang, L., et al., *Bumetanide increases Cl--dependent short-circuit current in late distal colon: Evidence for the presence of active electrogenic Cl- absorption.* PLoS One, 2017. **12**(2): p. e0171045.
191. *Dog red blood cells. Adjustment of salt and water content in vitro.* 1973. **62**(2): p. 147-56.
192. Yoshida, K. and V.T. Nachmias, *Calcium sequestration in human platelets: is it stimulated by protein kinase C?* Cell Calcium, 1989. **10**(5): p. 299-307.
193. Low, P.S., et al., *The role of hemoglobin denaturation and band 3 clustering in red blood cell aging.* Science, 1985. **227**(4686): p. 531-3.
194. Giustarini, D., et al., *Age-related influence on thiol, disulfide, and protein-mixed disulfide levels in human plasma.* J Gerontol A Biol Sci Med Sci, 2006. **61**(10): p. 1030-8.
195. Bessman, J.D., *Reticulocytes*, in *Clinical Methods: The History, Physical, and Laboratory Examinations*, rd, et al., Editors. 1990: Boston.

196. Lew, V.L., et al., *Effects of age-dependent membrane transport changes on the homeostasis of senescent human red blood cells.* Blood, 2007. **110**(4): p. 1334-42.
197. Amiwero, C.E. and P.O. Olatunji, *Re-evaluation of methaemoglobin reduction as a screening procedure for glucose-6-phosphate dehydrogenase (G6PD).* Afr J Med Med Sci, 2007. **36**(2): p. 177-81.
198. Kirkwood, J., et al., *Using isoelectric point to determine the pH for initial protein crystallization trials.* Bioinformatics, 2015. **31**(9): p. 1444-51.
199. Kaestner, L. and G. Minetti, *The potential of erythrocytes as cellular aging models.* Cell Death Differ, 2017. **24**(9): p. 1475-1477.